Atmospheric-Wave Generation
An Exponential-Asymptotic Analysis

Elínborg Ingunn Ólafsdóttir

Doctor of Philosophy
University of Edinburgh
2006

For my family

Declaration

I declare that this thesis was composed by myself and that the work contained therein is my own, except where explicitly stated otherwise in the text.

Abstract

We use the tools of exponential-asymptotic analysis to describe the solutions of the three-dimensional Boussinesq equations and of Lorenz's five-component model that arise in geophysical fluid dynamics. In particular we use both of these models to study the generation of high-frequency motions known as inertia-gravity waves from slow balanced motion via the Stokes phenomenon. To start with we give an example demonstrating the Stokes phenomenon and to give an idea of the general approach of these techniques.

We derive a full asymptotic expansion of the solutions of the Scorer equation which is an inhomogeneous Airy equation. The Stokes phenomenon causes the particular integral to switch on solutions of the Airy equation as a Stokes line is crossed. We identify the Stokes lines and the anti-Stokes lines, and most importantly calculate the Stokes multipliers. We do this by studying the Borel-Laplace transform of the solutions of the homogeneous and inhomogeneous part together with examining the behaviour of late-terms in the asymptotic expansion of the particular integral.

We study homoclinic solutions of Lorenz's five-component model. We linearise the solution and hence we can use methods analogous to the ones mentioned above. Here the slow motion is represented by the first function in the linear expansion of the solution. It switches on the consequent term in the expansion representing the fast motion as a Stokes line is crossed.

By considering solutions to the Boussnesq equations that consist of a sheared flow and a perturbation we narrow our problem to a differential equation that governs the amplitude of the inertia-gravity waves. Analytically the particular integral represents the slow motion that switches on solutions of the homogeneous equations which represent the fast oscillation. It follows from this that we can derive a power series expansion of the Stokes multipliers where we derive an expression for the first terms. The other terms we calculate numerically.

We use the Fourier transform to reduce the Boussinesq equations to an ordinary differential equation. When we then carry out the inverse transform we use our previous result to replace the the integrand with its dominant behaviour. As the saddle point of the exponent governing the integrand collides with the endpoints for certain values we use Bleistein's method together with numerical integration to estimate the inverse.

Acknowledgements

First and foremost I want to thank my supervisors, Adri B. Olde Daalhuis and Jacques Vanneste, for their enthusiasm for my work, their illuminating and motivating conversations and the generous amount of time that they spent with me. Their temperaments was ideally suited for me.

I also want to thank my fellow students, in particular all my office mates at 6320 for their support during my PhD-studies. I want to thank Richard Hepworth for saving my thesis from burning and lastly but not least my husband Stefán Ingi for the good time we have had here in Edinburgh.

Table of Contents

Chapter 1

Introduction

The dynamics of the oceans and the atmosphere displays the simultaneous existence of various modes of motion which can be separated between high-energy slow motion and low-energy fast motion. The time-scale separation between the two types of modes is due to the fast rotation of the earth, and to the strong stratification of the fluids. The slow motion is often referred to as *balanced motion* and the fast motion as *inertia-gravity waves*. The aim of this thesis is to give an analytical description of the interactions between balanced motion and inertia-gravity waves, and more specifically of the spontaneous generation of these inertia-gravity waves by the balanced motion. We do this by studying two simple models, namely Lorenz's five-component model (Lorenz, 1986) and particular solutions of the Boussinesq equations describing rotating stratified fluid, see the book of Gill (1982) for details on the equations of motion. Our analysis is based on the theory of exponential asymptotics. In particular, we identify the mechanism of the generation of inertia-gravity waves as a Stokes phenomenon.

Generation of fast motion is not a phenomenon unique to geophysical-fluid dynamics. One of the simplest systems that shows such a generation is a pendulum with a stiff spring attached to its free end see figure 1.1. In this system the pendulum undergoes a slow motion and the spring the fast oscillations, and there is a small parameter, ε say, which represents the ratio of the typical frequency of the pendulum and that of the spring.

Our interest is in solutions of this system that have as little fast oscillations as possible. These are the so-called balanced solutions. The nature of the system is such that for any initial condition the pendulum will affect the evolution of the spring, so there cannot exist a solution completely free of fast oscillations. However, we can proceed asymptotically to define a state where the oscillations are reduced to some power of ε.

With appropriate oscillatory-free initial conditions, we represent a balanced solution of the pendulum equations via its perturbation series in the small param-

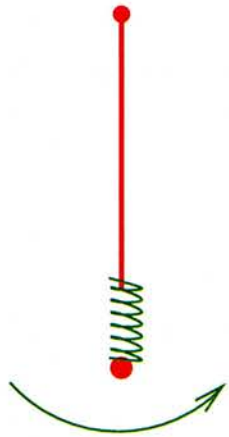

Figure 1.1: Pendulum with a stiff spring attached to its free end.

eter ε. The first term in this series represents a solution free of $O(1)$ oscillations. As time evolves the spring will affect the solution in the form of $O(\varepsilon)$ oscillations. To deal with this, we seek to find the second term in the asymptotic series that results in a solution free of $O(\varepsilon)$ oscillations for our initial conditions. In general we can keep on finding a balanced solution with oscillations limited to $O(\varepsilon^n)$ for all $n \in \mathbb{N}$. This solution seems to be independent of the spring, but we know that there is no such solution; the excitation of the spring cannot be eliminated although its amplitude is beyond all orders in ε; it is exponentially small. Using exponential asymptotics, we can include these exponentially small oscillatory terms and hence show how well-balanced a solution can be and describe the details of the oscillations that are generated.

This setup is related to the geophysical systems as, in fact, Lorenz's model is a pendulum spring system (cf. Bokhove and Shepherd, 1996; Camassa, 1995). Lorenz's model is composed of three nonlinear ordinary differential equations that describe the evolution of the slow motion, the pendulum, and a pair of linear ordinary differential equations describe the evolution of the fast motion, the spring.

The Boussinesq equations describe the generation of inertia-gravity waves in a more realistic setting. They are a set of nonlinear partial differential equations with special solutions that describe the spontaneous generation of inertia-gravity waves. By considering solutions that consist of a shear uniform flow and a perturbation represented by the Fourier transform we can reduce the system to an ordinary differential equation.

We describe the generation of inertia-gravity waves via the Stokes phenomenon. Hence, we start this thesis off with Chapter 2 that gives a detailed description of the technique of exponential asymptotics via a derivation of the asymptotic ex-

pansions of the Scorer functions and the Airy functions. We do this by studying the linear Scorer equation which is an inhomogeneous Airy equation. In Chapter 3 we look at the nonlinear Lorenz's model, for which we derive the leading order behaviour of the amplitude of the inertia gravity waves. Then we study the Boussinesq equations in Chapters 4–6. Chapter 4 is an introductory chapter to the following two chapters and is devoted to the reduction of the equations to an ordinary differential equation via the Fourier transform. In Chapter 5 we study the asympotics of this ordinary differential equation and in Chapter 6 we use the asymptotic behaviour that we obtained in the previous chapter to find an approximation to solutions of the full equations.

Chapter 2

Asymptotics of the Scorer function $-\mathrm{Gi}(z)$

2.1 The Stokes phenomenon

As paradoxical as it sounds, approximating finitely valued functions with divergent series is a very useful technique. A rigorous theory for this technique evolved following Poincaré's definition of an asymptotic expansion of a function in some sector in the complex plane, see for example Olver (1974, 16-19). However, there was no great interest shown in explaining the *Stokes phenomenon* first noticed by Stokes (1850). Considering large-$|\zeta|$ asymptotic expansion, this phenomenon is the sudden appearance of terms that are of order less than all powers of ζ and previously considered to be negligible. These terms are said to be *beyond all orders*. This sudden appearance happens as the ζ crosses a particular ray in the complex ζ-plane called the *Stokes line*.

To go into more detail of the technique of exponential asymptotics, let us assume that we have an inhomogeneous linear differential equation and that we have found the asymptotic expansion of its particular integral, say w_p. Let us also assume that this asymptotic expansion is divergent and that it is a valid approximation of w_p in some sector in the complex plane that is bounded by rays. These rays turn out to be the *anti-Stokes lines* defined in next paragraph. By an approximation we mean that the divergent series *optimally truncated*, that is truncated around its smallest term, gives an approximation of the function. Let us also assume that we know the asymptotic expansions of the solutions of the corresponding homogeneous equation.

Assuming that the behaviour of both the particular integral and the solutions of the corresponding homogeneous equations is governed by an exponential function, we find that the Stokes lines appear when one exponential maximally dominates another, that is when the imaginary part of the difference of the expo-

nents is zero. The anti-Stokes lines occur when the exponentials are comparable in size, that is when the real part of the difference of their exponents is zero.

We know that the asymptotic expansion of w_p is a solution of the differential equation before and after we pass the Stokes line. Thus, the additional exponentially small terms switched on as the Stokes line is passed have to be a solution of the homogeneous equation. Let us assume that $w_{p'}$ is another particular integral that has the same asymptotic expansion as w_p in a sector overlapping the sector of validity for the expansion of w_p. Because of the linearity of the differential equation, the difference of these two particular integrals is a solution, Kw say, of the homogeneous equation. That is the identity

$$w_p(\zeta) = w_{p'}(\zeta) + Kw(\zeta)$$

holds in the complex ζ-plane. The constant K is the *Stokes multiplier*. For a linear system this kind of identity can always be found but it is not always the case that we can do so with a known value of the Stokes multiplier. Hence we need an enhanced technique, the Borel-Laplace transform discussed in next section.

A new era in the study of the Stokes phenomenon started in the late eighties when Berry (1989) showed that the sudden change in the Stokes multipliers is continuous. This discovery of Berry had a huge impact in the field of asymptotics and was the starting point of today's flourishing field of exponential asymptotics.

2.1.1 The Borel-Laplace transform

Following Olde Daalhuis (1998) we give a description of the Borel-Laplace transform for solutions of an inhomogeneous linear problem. Here we consider the large parameter to be ε^{-1} where $|\varepsilon|$ is small.

Let us assume that $w_0(\varepsilon)$ is a particular integral of an inhomogeneous linear problem and $w_1(\varepsilon)$ is a solution to its homogeneous part. Assume that $w_0(\varepsilon)$ and $w_1(\varepsilon)$ have the asymptotic expansions

$$w_0(\varepsilon) \sim e^{-f_0/\varepsilon} \sum_{n=0}^{\infty} a_{0,n} \varepsilon^{n-\mu_0} \tag{2.1}$$

$$w_1(\varepsilon) \sim e^{-f_1/\varepsilon} \sum_{n=0}^{\infty} a_{1,n} \varepsilon^{n-\mu_1}. \tag{2.2}$$

These expansions are only valid in certain sectors in the complex ε-plane. Let us define two particular integrals w_{0_+} and w_{0_-} that have the same asymptotic expansion (2.2) in the overlapping sectors S_+ and S_- respectively. Then the difference $w_{0_+}(\varepsilon) - w_{0_-}(\varepsilon)$ is a solution to the homogeneous part of the system.

Hence, we get the connection relation

$$w_{0_+}(\varepsilon) = w_{0_-}(\varepsilon) + Kw_1(\varepsilon) \tag{2.3}$$

were K is the Stokes multiplier.

Let us define

$$y_0(t) = \sum_{n=0}^{\infty} \frac{a_{0,n}}{\Gamma(n-\mu_0)}(t-f_0)^{-(\mu_0+1-n)}$$
$$y_1(t) = \sum_{n=0}^{\infty} \frac{a_{1,n}}{\Gamma(n-\mu_1)}(t-f_1)^{-(\mu_1+1-n)}$$

where series on the right hand side are convergent for $|t-f_j| < |f_0-f_1|$, $j=0,1$. Then the functions $y_0(t)$ and $y_1(t)$ are the *Borel transforms* of the functions $w_0(\varepsilon)$ and $w_1(\varepsilon)$, that is they satisfy the Borel-Laplace integral representation

$$w_0(\varepsilon) = \int_{f_0}^{\infty e^{i\alpha}} e^{-t/\varepsilon} y_0(t)dt$$

and

$$w_1(\varepsilon) = \int_{f_1}^{\infty e^{i\alpha_1}} e^{-t/\varepsilon} y_1(t)dt$$

were α and α_1 are real numbers. The identity (2.3) implies the relation

$$y_0(t) = \frac{K}{e^{-2\pi i\mu_1}-1} y_1(t) + \mathrm{reg}(t-f_1) \tag{2.4}$$

between the functions y_0 and y_1, where the function $\mathrm{reg}(t-f_1)$ is analytic at the point $t=f_1$. This follows from (2.3) as

$$\begin{aligned} w_{0_+}(\varepsilon) - w_{0_-}(\varepsilon) &= \int_{f_0}^{\infty e^{i\alpha}+} e^{-t/\varepsilon} y_0(t)dt - \int_{f_0}^{\infty e^{i\alpha}-} e^{-t/\varepsilon} y_0(t)dt \\ &= \int_{\infty}^{(f_0)+} e^{-t/\varepsilon} y_0(t)dt = Kw_1(\varepsilon) \\ &= K\int_{f_1}^{\infty e^{i\alpha_1}} e^{-t/\varepsilon} y_1(t)dt \\ &= \frac{K}{e^{-2\pi i\mu_1}-1} \int_{\infty}^{(f_1)+} e^{-t/\varepsilon} y_1(t)dt \end{aligned} \tag{2.5}$$

where the contours in the second and the last integrals go from infinity around the points f_0 and f_1 respectively. The plus indicates that the contours are positively directed. Working backwards, we get the second last integral by collapsing the loop in the last integral, see figure 2.1 for the contours of integration.

Cauchy's integral formula of the coefficients in y_0 gives that

$$\frac{a_{0,n}}{\Gamma(n-\mu_0)} = \frac{1}{2\pi i} \oint \frac{y_0(t)}{(t-f_0)^{n-\mu_0}} dt$$

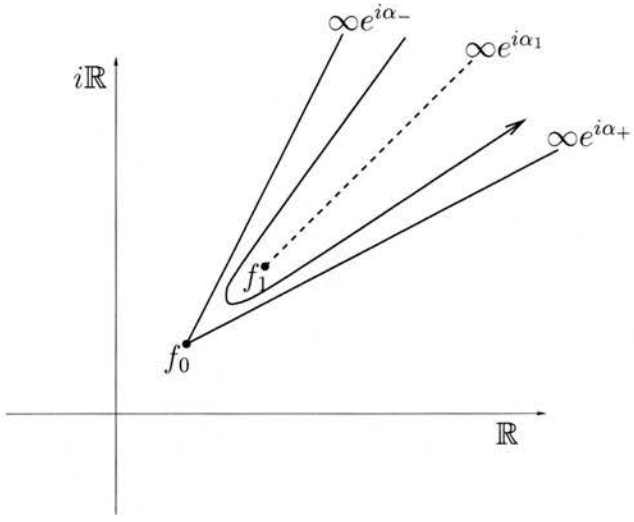

Figure 2.1: The contours of integration for the Borel-Laplace transform in (2.5). The loop around f_1 is collapsed to get the desired results.

where the contour encircles the point f_0. We blow up the contour of integration until we encounter the branch point at $t = f_1$; we adjust the contour of integration around it and hence, we get a contribution from a loop around f_1. This leads to a representation of the large n behaviour of the $a_{0,n}$-coefficients in terms of the $a_{1,n}$-coefficients. That is we get up to leading order that

$$a_{0,N} \sim \frac{K}{2\pi i} \frac{a_{1,0}\Gamma(N + \mu_1 - \mu_0)}{(f_1 - f_0)^{N+\mu_1-\mu_0}}, \quad \text{as} \quad N \to \infty$$

in some sector in the f-plane, or more generally

$$a_{0,N} \sim \frac{K}{2\pi i} \sum_{s=0}^{\infty} \frac{a_{1,s}\Gamma(N - s + \mu_1 - \mu_0)}{(f_1 - f_0)^{N-s+\mu_1-\mu_0}}, \quad \text{as} \quad N \to \infty. \tag{2.6}$$

In this thesis, when we encounter realtions like this there will be an extra variable t involved, hence, relations like this will only be valid in certain regions in the complex t-plane.

By substituting the asymptotic series (2.1) and (2.2) into the original inhomogeneous linear problem, we get a recurrence relation for the $a_{0,n}$-coefficients. It depends on the problem whether we can use this recurrence relation to get an analytical expression for the coefficients, but in all cases we can calculate the coefficients numerically. Hence, although (2.6) is a divergent series it can be used to evaluate the Stokes multiplier K. In this chapter we outline how to do this.

In most problems, there are more than one f_j, $j = 1, \ldots, k$, $k \in \mathbb{N}$ related to the homogeneous part of the problem. In the case $k = 2$, if $(f_2 - f_0) << (f_1 - f_0)$ we can not compute the relavant Stokes-multiplier K_2 with the method discussed

here. In such cases it is necessary to use hyperasymptotic procedures as outlined in (Olde Daalhuis, 1999).

This chapter is devoted to a rigorous description of this technique via the derivation of the full asymptotic expansion of the Scorer function $-\operatorname{Gi}(z)$, for large $|z|$. We also use this technique in Chapter 5 where we derive the full asymptotic expansions of the solutions of the equation

$$\varepsilon^2\left(\frac{\mathrm{d}^2\zeta}{\mathrm{d}t^2}-\frac{2t}{1+t^2}\frac{\mathrm{d}\zeta}{\mathrm{d}t}\right)+\left((1+\varepsilon)\left(1+\frac{2\varepsilon}{1+t^2}\right)+\frac{1+t^2}{\beta^2}\right)\zeta=\frac{1+t^2}{\beta^2}$$

in the limit of small ε. For these solutions we find that the Stokes multipliers are functions of ε that can be represented with their Taylor expansions. We also discuss the Stokes phenomenon for a nonlinear problem in Chapter 3, see also the discussion in Section 3.2.1, where we derive the leading behaviour of exponentially small terms switched on by solutions of the five-component Lorenz equations.

2.2 The asymptotics of the Scorer function $-\operatorname{Gi}(z)$

The inhomogeneous Airy equation

$$\frac{d^2w(z)}{dz^2}-zw(z)=\frac{1}{\pi}, \tag{2.7}$$

known as the Scorer equation, has the special functions, the Scorer functions, $-\operatorname{Gi}(z)$ and $\operatorname{Hi}(z)$ as particular integrals. These functions are named after Scorer (1950) who tabulated their numerical values via the integral representations

$$\operatorname{Gi}(z)=\frac{1}{\pi}\int_0^\infty \sin(zu+\frac{1}{3}u^3)du \tag{2.8}$$

and

$$\operatorname{Hi}(z)=\frac{1}{\pi}\int_0^\infty e^{zu-\frac{1}{3}u^3}du. \tag{2.9}$$

In this chapter we will derive the full asymptotic expansion for the function $-\operatorname{Gi}(z)$ for large z using the technique of exponential asymptotics. It is possible to derive all that follows from the integral representations (2.8) and (2.9), however we do not use such techniques as we want to illustrate how to proceed in the absence of such exact representations.

In this derivation we need to know the asymptotic nature of the solutions to the Airy equation which is the homogeneous part of equation (2.7). One of its solutions is the Airy function, $\operatorname{Ai}(z)$, also known via the Airy integral

$$\operatorname{Ai}(z)=\frac{1}{\pi}\int_0^\infty \cos\left(zu+\frac{u^3}{3}\right)du,$$

see for example Olver (1974, 53). This equation and function are named after Airy (1838) who was the first to tabulate the values of the Airy integral for certain real values of z. It was then Stokes who carried on with this work, specifically for large values of real z. This he does first in (Stokes, 1850) where he for the first time encounters the phenomenon later named after him. In this paper he realises that there is a discontinuity in the multipliers in the asymptotic expansion of the Airy function. He evaluates the multipliers but in that paper he cannot explain why the Stokes phenomenon takes place. In a later paper (Stokes, 1857) he revisits the problem and identifies the Stokes lines via the optimal truncation of the asymptotic series. Let us finish what these two great minds started.

2.2.1 Asymptotic expansion of the Airy function

To find the leading behaviour of the solutions of the Airy equation

$$\frac{d^2w(z)}{dz^2} - zw(z) = 0 \tag{2.10}$$

for large z, we introduce the function $V(z) = w'(z)/w(z)$. Insertion into equation (2.10) gives the Riccati equation

$$V'(z) + V^2(z) = z. \tag{2.11}$$

There are three possible dominant balances for this equation for large z. They are the following:

1. $V'(z) \sim -V^2(z)$ which implies that $V(z) \sim z^{-1}$, but then z is not negligible as we have assumed,

2. $V'(z) \sim z$ which implies that $V(z) \sim z^2/2$, but then $V^2(z)$ is not negligible as we have assumed,

3. $V^2(z) \sim z$ implies that $2V(z)V'(z) \sim 1$ or $V'(z) \sim 1/(2V(z))$ meaning that $V'(z)$ is negligible as z tends to infinity.

Thus, only the last dominant balance is possible implying that $V(z) \sim \pm\sqrt{z}$.

Considering the dominant balance, we assume that $V(z) \sim \sum_{n=0}^{\infty} v_n z^{-(n-1)/2}$. Substitution of this series into (2.11) gives

$$v_0^2 = 1$$

$$\sum_{k=0}^{n} v_k v_{n-k} + \left(2 - \frac{n}{2}\right) v_{n-3} = 0, \qquad n = 1, 2, 3, \ldots$$

where we define $v_{-2} = v_{-1} = 0$. It follows from this that

$$v_{3n+1} = v_{3n+2} = 0$$

for all $n = 0, 1, 2, \ldots$. Also, we get $v_3 = -1/4$ so

$$\int V(z)dz \sim \int (v_0\sqrt{z} + v_3 z^{-1} + \ldots)dz \sim \pm\frac{2}{3}z^{3/2} - \frac{1}{4}\ln z + \ldots .$$

Then as $w(z) \sim \exp\left(\int V(z)dz\right)$ we get that

$$w(z) \sim C_1 \frac{e^{-\frac{2}{3}z^{3/2}}}{z^{1/4}} \sum_{k=0}^{\infty} a_k z^{-k/2} + C_2 \frac{e^{\frac{2}{3}z^{3/2}}}{z^{1/4}} \sum_{k=0}^{\infty} \tilde{a}_k z^{-k/2} \tag{2.12}$$

for some coefficients a_k and $\tilde{a}_k$ and some constants C_1 and C_2. We could have obtained the same result by by considering a WKB ansatz.

We know that the Airy function, $\mathrm{Ai}(z)$, is a solution to (2.10). According to (Olver, 1974, 116) the Airy function can be represented via the integral

$$\mathrm{Ai}(z) = \frac{e^{-\frac{2}{3}z^{3/2}}}{2\pi} \int_0^{\infty} e^{-z^{1/2}t} \cos\left(\frac{t^{3/2}}{3}\right) t^{-1/2} dt \quad \text{if } |\operatorname{ph}(z)| < \pi.$$

Using Watson's Lemma on the integral we get

$$\mathrm{Ai}(z) \sim \frac{e^{-\frac{2}{3}z^{3/2}}}{2\sqrt{\pi}z^{1/4}}, \qquad |\operatorname{ph}(z)| < \pi.$$

This implies that the Airy function has an asymptotic expansion of the form (2.12) with $C_1 = 1/(2\sqrt{\pi})$ and $C_2 = 0$ if we choose $a_0 = 1$. From now on let us focus on the asymptotics of the Airy function.

Inserting (2.12) into (2.10) gives $a_1 = a_2 = 0$ resulting in $a_{3k+1} = a_{3k+2} = 0$ for all $k = 0, 1, 2, \ldots$. Let $a_{3k} = (-1)^k (3/2)^k b_k$. Then $b_0 = 1$ and

$$\begin{aligned} b_k &= \frac{1}{72k}(6k-5)(6k-1)b_{k-1} \\ &= \frac{1}{72^k k!} \frac{\prod_{m=0}^{3k-1}(2m+1)}{3^k \prod_{m=1}^{k}(2m-1)} \\ &= \frac{(2k+1)(2k+3)\ldots(6k-1)}{(216)^k k!} \\ &= \frac{2^k}{3^{3k}(2k)!} \frac{\Gamma(3k+1/2)}{\Gamma(1/2)}. \end{aligned} \tag{2.13}$$

Thus

$$\mathrm{Ai}(z) \sim \frac{e^{-\frac{2}{3}z^{3/2}}}{2\sqrt{\pi}z^{1/4}} \sum_{k=0}^{\infty} (-1)^k b_k \left(3/2\right)^k z^{-3k/2}, \qquad |\operatorname{ph}(z)| < \pi. \tag{2.14}$$

The function $\mathrm{Ai}(ze^{2\pi i/3})$ is another solution of (2.10). As $\mathrm{Ai}(z)$ is an entire function and takes real values for $z \in \mathbb{R}$, $\mathrm{Ai}(ze^{-2\pi i/3})$, the conjugate of $\mathrm{Ai}(ze^{2\pi i/3})$, is also a solution. Let us now define, following Olver (1974, 413) the functions

$$\begin{aligned} \mathrm{Ai}_0(z) &= \mathrm{Ai}(z), \\ \mathrm{Ai}_{-1}(z) &= \mathrm{Ai}(ze^{2\pi i/3}) \quad \text{and} \\ \mathrm{Ai}_1(z) &= \mathrm{Ai}(ze^{-2\pi i/3}). \end{aligned}$$

Then $\mathrm{Ai}_0(z)$ has the asymptotic expansion (2.14) and

$$\mathrm{Ai}_{-1}(z) \sim e^{-\frac{\pi i}{6}} \frac{e^{\frac{2}{3}z^{3/2}}}{2\sqrt{\pi} z^{1/4}} \sum_{k=0}^{\infty} b_k \, (3/2)^k \, z^{-3k/2}, \qquad -\frac{5\pi}{3} < \mathrm{ph}(z) < \frac{\pi}{3}, \tag{2.15}$$

$$\mathrm{Ai}_{1}(z) \sim e^{\frac{\pi i}{6}} \frac{e^{\frac{2}{3}z^{3/2}}}{2\sqrt{\pi} z^{1/4}} \sum_{k=0}^{\infty} b_k \, (3/2)^k \, z^{-3k/2}, \qquad -\frac{\pi}{3} < \mathrm{ph}(z) < \frac{5\pi}{3}. \tag{2.16}$$

Let us derive a connection relation between these functions.

2.2.2 Connection relation

As equation (2.10) is linear and of second order we know there exist constants α, β and γ such that

$$\alpha \, \mathrm{Ai}_0(z) + \beta \, \mathrm{Ai}_1(z) + \gamma \, \mathrm{Ai}_{-1}(z) = 0.$$

Let us write $z = re^{\theta i}$ where $r, \theta \in \mathbb{R}$. For the value $\theta = 0$, $\mathrm{Ai}_0(z)$ is recessive to $\mathrm{Ai}_j(z)$, $j = -1, 1$, giving

$$\beta e^{\pi i/6} + \gamma e^{-\pi i/6} = 0.$$

On the ray $\theta = -2\pi/3$ the function $\mathrm{Ai}_{-1}(z)$ is recessive to $\mathrm{Ai}_j(z)$, $j = 0, 1$. The asymptotic expansion of $\mathrm{Ai}_1(z)$, (2.16), is not defined for $\theta = -2\pi/3$ but as $\mathrm{Ai}_1(z)$ is an entire function we have $\mathrm{Ai}_1(ze^{-2\pi/3}) = \mathrm{Ai}_1(ze^{4\pi/3})$. Thus we get in the same way as before

$$\alpha e^{\pi i/6} + \beta e^{-\pi i/6} = 0.$$

Now if we fix $\alpha = 1$, solving the last two equations together gives $\beta = e^{-2\pi i/3}$ and $\gamma = e^{2\pi i/3}$. Hence we get the identity

$$\mathrm{Ai}_0(z) = e^{\pi i/3} \, \mathrm{Ai}_1(z) + e^{-\pi i/3} \, \mathrm{Ai}_{-1}(z). \tag{2.17}$$

This identity gives very useful information on what is switched on via the Stokes phenomenon. We will see in the next section that the factors $e^{\pm \pi i/3}$ are the Stokes multipliers.

2.2.3 The Stokes phenomenon

Let us consider the asymptotic expansions of the functions $\mathrm{Ai}_j(z)$, $j = -1, 0, 1$. Recall that the large-z behaviour of these three functions is governed by exponential functions. An anti-Stokes line is defined as a ray, here in the complex z-plane, on which two asymptotic expansions are comparable in size. Hence, on an anti-Stokes line the difference of the corresponding exponents is purely imaginary. The anti-Stokes lines for the Airy functions are given by

$$\Re\left\{\frac{2}{3}z^{\frac{3}{2}} - \left(\frac{2}{3}z^{\frac{3}{2}}\right)\right\} = \Re\left\{\frac{4}{3}z^{\frac{3}{2}}\right\} = 0.$$

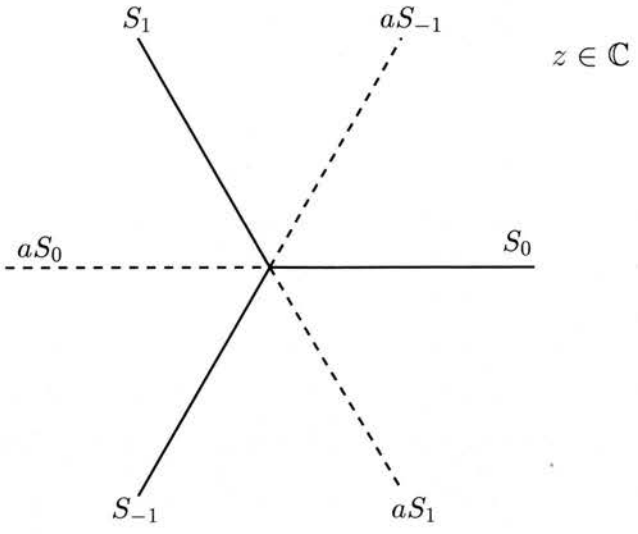

Figure 2.2: The Stokes lines S_j and the anti-Stokes lines aS_j, $j = -1, 0, 1$, in the complex z-plane.

These are the rays aS_1, aS_{-1} and aS_0 on which $\mathrm{ph}(z) = -\pi/3$, $\mathrm{ph}(z) = \pi/3$ and $\mathrm{ph}(z) = \pi$ respectively, see figure 2.2. Comparing to the expansions (2.14)–(2.16), we note that the anti-Stokes lines are the rays which define the sectors of validity of the expansions.

A Stokes line is a ray in the complex z-plane where one solution maximally dominates another. Hence, this is where the difference of the exponents governing the asymptotic expansions of the functions is purely real. The Stokes lines for the Airy functions are given by

$$\Im\left\{\frac{2}{3}z^{\frac{3}{2}} - \left(\frac{2}{3}z^{\frac{3}{2}}\right)\right\} = \Im\left\{\frac{4}{3}z^{\frac{3}{2}}\right\} = 0.$$

These are the rays S_{-1}, S_0 and S_1 with $\mathrm{ph}(z) = -2\pi/3$, $\mathrm{ph}(z) = 0$ and $\mathrm{ph}(z) = 2\pi/3$ respectively, see figure 2.2.

Let us consider the function $\mathrm{Ai}_0(z)$ in a neighbourhood of the Stokes line S_1. As we rotate z counterclockwise across the Stokes line, a multiple of the function $\mathrm{Ai}_1(z)$ is switched on as it is the relevant recessive function. That is, we get that

$$\mathrm{Ai}_0(z) \sim \begin{cases} \dfrac{e^{-\frac{2}{3}z^{3/2}}}{2\sqrt{\pi}z^{1/4}} + 0 \cdot e^{\frac{\pi i}{6}} \dfrac{e^{\frac{2}{3}z^{3/2}}}{2\sqrt{\pi}z^{1/4}} & \text{for } \mathrm{ph}(z) = \frac{2\pi}{3} - \varepsilon \\ \dfrac{e^{-\frac{2}{3}z^{3/2}}}{2\sqrt{\pi}z^{1/4}} + K_1 e^{\frac{\pi i}{6}} \dfrac{e^{\frac{2}{3}z^{3/2}}}{2\sqrt{\pi}z^{1/4}} & \text{for } \mathrm{ph}(z) = \frac{2\pi}{3} + \varepsilon \end{cases}$$

where K_1 is the Stokes multiplier and $\varepsilon > 0$ is small. Now, we compare this asymptotic behaviour of the function $\mathrm{Ai}_0(z)$ to the identity

$$\mathrm{Ai}_0(z) = e^{\pi i/3}\,\mathrm{Ai}_1(z) + e^{-\pi i/3}\,\mathrm{Ai}_{-1}(z)$$

where we replace the functions on the right hand side with their asymptotic expansion (2.15) and (2.16). Noting that $e^{-\pi i/3}\,\mathrm{Ai}_{-1}(z)$ has the same asymptotic expansion as $\mathrm{Ai}_0(z)$ near the Stokes line we get that

$$K_1 = e^{\pi i/3}.$$

In the same way, we get that as z crosses the Stokes line S_{-1} clockwise, a K_{-1}-multiple of $\mathrm{Ai}_{-1}(z)$ is switched on where

$$K_{-1} = e^{-\pi i/3}.$$

Similarly, we can find the Stokes multiplier for any of the functions $\mathrm{Ai}_j(z)$ crossing a Stokes line where the function is maximally dominant and switches on a multiple of the relevant recessive function by comparing to the identity (2.17). That is, the identity (2.17) together with the knowledge of the dominance between the functions and the position of the Stokes lines gives all the information needed to determine the values of the Stokes multipliers.

In general, for linear differential equations, a connection relation such as (2.17) can always be found. However, unlike this case, exact values of the Stokes multipliers are not always known. Hence, in cases where we are not as fortunate as here, other methods are needed. For this purpose we introduce the Borel-Laplace transform in Section 2.2.10 but first, let us confirm that the asymptotic expansion of the function $\mathrm{Ai}_0(z)$, (2.14), and thus the expansions (2.15)–(2.16) for the other $\mathrm{Ai}_j(z)$ functions, is indeed an asymptotic expansion.

To be specific, we have not yet shown that the error terms in the expansions are of order not exceeding the order of the next term in the expansions after truncation. We do this by introducing a Stieltjes integral representation of the Airy functions. Before that, we introduce a scaling of the variables.

2.2.4 Rescaling of variables

To simplify our calculations, let us define $\zeta = \frac{2}{3}z^{3/2}$ and the function $W_0(\zeta)$ such that

$$\mathrm{Ai}_0(z) = z^{-1/4}W_0(\zeta).$$

Similarly to before, we define

$$W_{-1}(\zeta) = W_0(\zeta e^{\pi i}) \quad \text{and} \quad W_1(\zeta) = W_0(\zeta e^{-\pi i}).$$

Then all the $W_j(\zeta)$ functions, $j = -1, 0, 1$, are solutions of

$$\frac{d^2W(\zeta)}{d\zeta^2} - \left(1 - \frac{5}{36}\zeta^{-2}\right)W(\zeta) = 0. \tag{2.18}$$

As

$$\mathrm{Ai}_{-1}(z) = e^{-\pi i/6} z^{-1/4} W_{-1}(\zeta) \quad \text{and} \quad \mathrm{Ai}_1(z) = e^{\pi i/6} z^{-1/4} W_1(\zeta),$$

we get that the asymptotic expansions of $W_j(\zeta)$, $j = -1, 0, 1$, are

$$W_0(\zeta) \sim \frac{e^{-\zeta}}{2\sqrt{\pi}} \sum_{k=0}^{\infty} (-1)^k b_k \zeta^{-k}, \qquad |\operatorname{ph}(\zeta)| < \frac{3\pi}{2}, \tag{2.19}$$

$$W_1(\zeta) \sim \frac{e^{\zeta}}{2\sqrt{\pi}} \sum_{k=0}^{\infty} b_k \zeta^{-k}, \qquad -\frac{\pi}{2} < \operatorname{ph}(\zeta) < \frac{5\pi}{2}, \tag{2.20}$$

$$W_{-1}(\zeta) \sim \frac{e^{\zeta}}{2\sqrt{\pi}} \sum_{k=0}^{\infty} b_k \zeta^{-k}, \qquad -\frac{5\pi}{2} < \operatorname{ph}(\zeta) < \frac{\pi}{2}. \tag{2.21}$$

Compare (2.14). Then identity (2.17) gives

$$iW_0(\zeta) = W_{-1}(\zeta) - W_1(\zeta). \tag{2.22}$$

2.2.5 Stieltjes integral representation of the function $W_1(\zeta)$

In the manner of (Olde Daalhuis and Olver, 1994) let us define $v_0(\zeta) = \zeta^{-1} e^{-\zeta} W_0(\zeta)$ and $v_1(\zeta) = \zeta^{-1} e^{-\zeta} W_1(\zeta)$. Then according to (2.19) and (2.20)

$$v_0(\zeta) \sim \zeta^{-1} \frac{e^{-2\zeta}}{2\sqrt{\pi}} \sum_{k=0}^{\infty} (-1)^k b_k \zeta^{-k}, \qquad |\operatorname{ph}(\zeta)| < \frac{3\pi}{2}, \tag{2.23}$$

$$v_1(\zeta) \sim \frac{\zeta^{-1}}{2\sqrt{\pi}} \sum_{k=0}^{\infty} b_k \zeta^{-k}, \qquad -\frac{\pi}{2} < \operatorname{ph}(\zeta) < \frac{5\pi}{2}. \tag{2.24}$$

As $W_{-1}(\zeta) = W_1(\zeta e^{2\pi i})$ we can write the identity (2.22) as

$$iW_0(\zeta) = W_1(\zeta e^{2\pi i}) - W_1(\zeta).$$

This becomes

$$iv_0(\zeta) = v_1(\zeta e^{2\pi i}) - v_1(\zeta) \tag{2.25}$$

after multiplying both sides by $\zeta^{-1} e^{-\zeta}$.

According to Cauchy's integral formula we have that

$$v_1(\zeta) = \frac{1}{2\pi i} \oint_{\mathcal{C}} \frac{v_1(t)}{\zeta - t} dt \tag{2.26}$$

where ζ with $\operatorname{ph}(\zeta) \in (0, 2\pi)$ is in the interior of the clockwise orientated contour $\mathcal{C}$ composed of the following paths:

$$\begin{aligned} A &= Re^{i\theta}, & \theta &\in (0, 2\pi), \\ B &= re^{i\theta}, & \theta &\in (0, 2\pi), \\ C &= s, & s &\in [r, R], \\ D &= se^{i2\pi}, & s &\in [r, R]. \end{aligned}$$

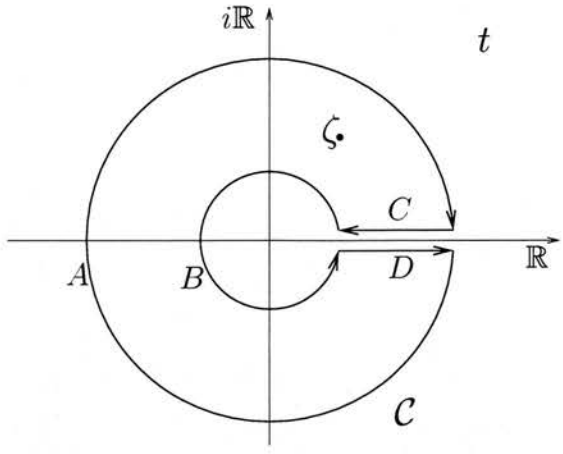

Figure 2.3: The contour, $\mathcal{C}$, of integration in (2.26).

Figure 2.3 displays the contour of integration $\mathcal{C}$. The point of choosing this contour is firstly that we want the contribution from the part A and B to be negligible by using the asymptotic behaviour of $v_1(t)$ and secondly that we want to be able to simplify the contribution from the contours C and D by using the identity (2.25). Let us show this.

On the contour A, the expansion (2.24) implies that $v_1(t) = O(1/R)$ as R tends to infinity. Hence

$$\lim_{R\to\infty} \frac{1}{2\pi i} \int_A \frac{v_1(t)}{\zeta - t} dt = 0.$$

On the contour B we have for small $|t|$ that

$$\frac{v_1(t)}{\zeta - t} = \frac{t^{-1}e^{-t}W_1(t)}{\zeta - t} = \frac{t^{-1}e^{-t}e^{\frac{\pi i}{6}}\left(\frac{3t}{2}\right)^{\frac{1}{6}} \mathrm{Ai}_1((\frac{3t}{2})^{2/3})}{\zeta - t} = t^{-5/6}O(1)$$

as $\mathrm{Ai}_1(t)$ is an entire function. Thus

$$\frac{1}{2\pi i} \int_B \frac{v_1(t)}{t - \zeta} dt = O(r^{1/6}) \qquad \text{as } |r| \to 0.$$

Therefore in the limit $R \to \infty$ and $r \to 0$ the contours C and D are the only ones that contribute, so

$$v_1(\zeta) = \lim_{\substack{R\to\infty \\ r\to 0}} \frac{1}{2\pi i} \left(\int_{re^{2\pi i}}^{Re^{2\pi i}} + \int_R^r \right) \frac{v_1(t)}{\zeta - t} dt.$$

Now let $t = te^{2\pi i}$ in the first integral. Then

$$\begin{aligned} v_1(\zeta) &= \lim_{\substack{R\to\infty \\ r\to 0}} \frac{1}{2\pi i} \int_r^R \frac{(v_1(te^{2\pi i}) - v_1(t))}{\zeta - t} dt \\ &= \frac{1}{2\pi} \int_0^\infty \frac{v_0(t)}{\zeta - t} dt \end{aligned} \tag{2.27}$$

by using the identity (2.25).

The representation (2.27) is an improvement of (2.26) since in (2.27) we integrate a function that is $O(e^{-2t})$ for large $|t|$ over the positive real axis. Thus, the integrand is exponentially small and hence we gain an integral representation which we know quite well how to manipulate.

In terms of the functions $W_j(\zeta)$, $j = 0, 1$, (2.27) becomes

$$\zeta^{-1}e^{-\zeta}W_1(\zeta) = \frac{1}{2\pi}\int_0^\infty \frac{e^{-t}W_0(t)}{t(\zeta - t)}dt \quad \text{if} \quad 0 < \text{ph}(\zeta) < 2\pi. \tag{2.28}$$

Thus we have found an integral representation of $W_1(\zeta)$ in terms of the function $W_0(\zeta)$. Let us now use this to get a representation of the error term in the asymptotic expansion of $W_1(\zeta)$.

2.2.6 The error term for $W_1(\zeta)$

In order to find an integral representation of the error term in the asymptotic expansion of the function $W_1(\zeta)$, let us start by focusing on the integral in the equation (2.28).

We define

$$I(\zeta) = \frac{1}{2\pi}\int_0^\infty \frac{e^{-t}W_0(t)}{t(\zeta - t)}dt$$

in the sector $0 < \text{ph}(\zeta) < 2\pi$. As

$$\frac{1}{\zeta - t} = \frac{1}{\zeta}\frac{1}{(1 - t/\zeta)} = \frac{1}{\zeta}\left(1 + \frac{t}{\zeta} + \left(\frac{t}{\zeta}\right)^2 + \cdots + \left(\frac{t}{\zeta}\right)^{n-1} + \frac{(t/\zeta)^n}{(1 - t/\zeta)}\right)$$

we get that

$$\begin{aligned} I(\zeta) &= \frac{1}{2\pi}\int_0^\infty \frac{e^{-t}W_0(t)}{\zeta t}\sum_{k=0}^{n-1}\left(\frac{t}{\zeta}\right)^k dt + \frac{1}{2\pi}\int_0^\infty \frac{e^{-t}W_0(t)}{\zeta t}\frac{(t/\zeta)^n}{(1 - t/\zeta)}dt \\ &= \sum_{k=0}^{n-1}\zeta^{-(k+1)}\frac{1}{2\pi}\int_0^\infty e^{-t}W_0(t)t^{k-1}dt + \zeta^{-n}\frac{1}{2\pi}\int_0^\infty e^{-t}W_0(t)\frac{t^{n-1}}{\zeta - t}dt \\ &= \frac{1}{2\sqrt{\pi}}\sum_{k=0}^{n-1} b_k\zeta^{-(k+1)} + E_n(\zeta) \end{aligned} \tag{2.29}$$

where we will see that $\sum_{k=1}^\infty b_k\zeta^{-(k+1)}$ is the asymptotic expansion of $I(\zeta)$. For this to hold the error term

$$E_n(\zeta) = \zeta^{-n}\frac{1}{2\pi}\int_0^\infty e^{-t}W_0(t)\frac{t^{n-1}}{\zeta - t}dt \tag{2.30}$$

must be of order not exceeding $\zeta^{-(n+1)}$. We will show this in next section.

As $I(\zeta) = \zeta^{-1}e^{-\zeta}W_1(\zeta)$, for $\zeta \in (0, 2\pi)$, and $W_1(\zeta)$ has only one asymptotic expansion in that sector for ζ, the b_k coefficients in the asymptotic expansions of $I(\zeta)$ and $W_1(\zeta)$, given by (2.20), are the same. Thus, for the b_k-coefficients we have the integral representation

$$b_k = \frac{1}{\sqrt{\pi}} \int_0^\infty e^{-t} W_0(t) t^{k-1} dt \tag{2.31}$$

in terms of the function $W_0(t)$. Thus, the integral representation introduced to find the order of the error terms gives this nice integral representation of the b_k-coefficients.

Let us now find the order of the error term.

2.2.7 The order of the error term for $W_1(\zeta)$

Let us show that the error in the asymptotic expansion, $\sum_{k=1}^{\infty} b_k \zeta^{-(k+1)}$, of $I(\zeta)$, is of order not exceeding $\zeta^{-(n+1)}$ if the series is truncated after $n-1$ terms. To start with, let $\zeta = u + iv$ with $0 < \mathrm{ph}(\zeta) < 2\pi$. Then we need to consider the two cases, $u \leq 0$ and $u > 0$.

If $u \leq 0$, then

$$|\zeta - t|^2 = u^2 + v^2 + (t^2 - 2ut) \geq u^2 + v^2 = |\zeta|^2,$$

as $t \in \mathbb{R}_+$, so $|\zeta - t|^{-1} \leq |\zeta|^{-1}$. As $W_0(t)$ is an entire function and $W_0(t)$ is governed by e^{-t} for $t \in \mathbb{R}_+$

$$\sup_{t \in [0,\infty)} |W_0(t)| < \infty.$$

Hence

$$\begin{aligned} |E_n(\zeta)| &= \left| \zeta^{-n} \frac{1}{2\pi} \int_0^\infty e^{-t} W_0(t) \frac{t^{n-1}}{\zeta - t} dt \right| \\ &\leq \left| \zeta^{-(n+1)} \right| \frac{1}{2\pi} \int_0^\infty e^{-t} |W_0(t)| t^{n-1} dt \leq C_1(n) \left| \zeta^{-(n+1)} \right| \end{aligned}$$

where $C_1(n) = O(1)$ is defined by

$$C_1(n) = \sup_{t \in [0,\infty)} |W_0(t)| \frac{\Gamma(n)}{2\pi}.$$

Thus in this case we have $E_n(\zeta) = O(\zeta^{-(n+1)})$.

If $u > 0$ we need to change the contour of integration in (2.30). As the behaviour of $W_0(t)$ is governed by e^{-t} for large $|t|$ in the sector $|\mathrm{ph}(t)| < \pi/2$ we can rotate the contour of integration up or down in the plane as the contribution

from the arc linking the rotated contour to the original one is negligible. The direction in which we rotate the contour depends on the sign of v.

If $v > 0$ we rotate the contour of integration by $-\pi/4$ and if $v < 0$ we rotate the contour by $\pi/4$, see figure 2.4. In both cases

$$|\zeta - t| \geq \frac{1}{\sqrt{2}}|\zeta|.$$

If we join the two cases, we get

$$\begin{aligned}
|E_n(\zeta)| &= \left| \zeta^{-n} \frac{1}{2\pi} \int_0^{\infty e^{\pm\frac{\pi i}{4}}} e^{-t} W_0(t) \frac{t^{n-1}}{t-\zeta} dt \right| \\
&\leq |\zeta|^{-(n+1)} \frac{1}{\sqrt{2}\pi} \int_0^{\infty e^{\pm\frac{\pi i}{4}}} \left| e^{-t} W_0(t) t^{n-1} \right| |dt| \\
&\leq |\zeta|^{-(n+1)} \frac{1}{\sqrt{2}\pi} \sup_{t \in [0, \infty e^{\pm\frac{\pi i}{4}})} |W_0(t)| \int_0^{\infty e^{\pm\frac{\pi i}{4}}} \left| e^{-t} t^{n-1} \right| |dt| .
\end{aligned}$$

For values of $t \in [0, \infty e^{\pm\frac{\pi i}{4}})$, the behaviour of the entire function $W_0(t)$ is governed by e^{-t}, thus

$$\sup_{t \in [0, \infty e^{\pm\frac{\pi i}{4}})} |W_0(t)| < \infty.$$

Now let $t = \tau e^{\pm\frac{\pi i}{4}}$ in the last integral above. As $\tau \in \mathbb{R}_+$ we get

$$\begin{aligned}
|E_n(\zeta)| &\leq |\zeta|^{-(n+1)} \frac{1}{\sqrt{2}\pi} \sup_{t \in [0, \infty e^{\pm\frac{\pi i}{4}})} |W_0(t)| \int_0^{\infty} \left| e^{-\tau e^{\pm\frac{\pi i}{4}}} \right| \left| \tau e^{\pm\frac{\pi i}{4}} \right|^{n-1} d\tau \\
&= |\zeta|^{-(n+1)} \frac{1}{\sqrt{2}\pi} \sup_{t \in [0, \infty e^{\pm\frac{\pi i}{4}})} |W_0(t)| \int_0^{\infty} e^{-\frac{\tau}{\sqrt{2}}} \tau^{n-1} d\tau \\
&= C_2(n) |\zeta|^{-(n+1)}
\end{aligned}$$

where $C_2(n) = O(1)$ is defined by

$$C_2(n) = \sup_{t \in [0, \infty e^{\pm\frac{\pi i}{4}})} |W_0(t)| \frac{\Gamma(n)}{\pi} 2^{\frac{(n-1)}{2}}.$$

We have shown that $E_n(\zeta) = O(\zeta^{-(n+1)})$ for all values of $\zeta \in \mathbb{C}$, $0 < \mathrm{ph}(\zeta) < 2\pi$, and hence we get that the the series (2.19)–(2.21) are the asymptotic expansions of the functions $W_j(\zeta)$, $j = 0, 1, -1$ respectively. Let us summarise.

2.2.8 The asymptotic expansion of $W_j(\zeta)$

Let us summarise the information we have on the asymptotic expansions of $W_j(\zeta)$, $j = 0, 1$. According to (2.28) and (2.29) we have

$$\zeta^{-1} e^{-\zeta} W_1(\zeta) = \frac{1}{2\sqrt{\pi}} \sum_{k=0}^{n} b_k \zeta^{-(k+1)} + E_n(\zeta) \quad \text{if} \quad 0 < \mathrm{ph}(\zeta) < 2\pi.$$

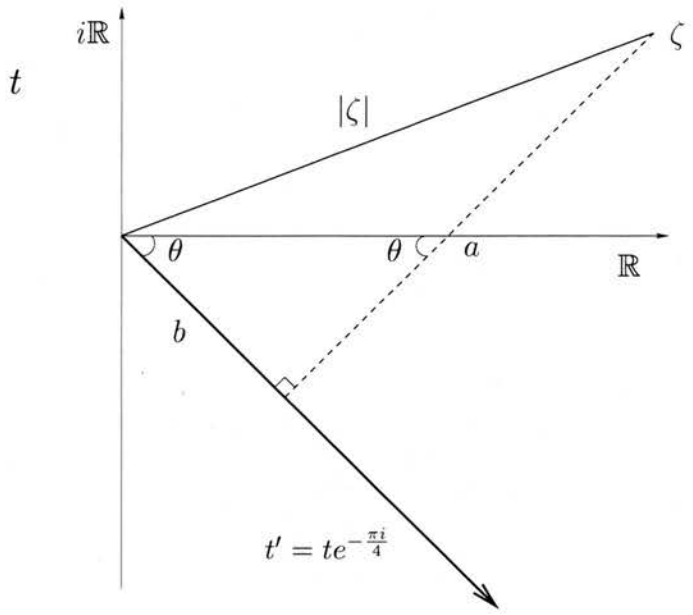

Figure 2.4: The integration contour for the error term $E_n(\zeta)$ when ζ has positive real and imaginary part. As a is the shortest distance from ζ to the rotated contour and $\theta = \pi/4$ we have that $a \geq b$ and $|\zeta - t| \geq a$ for any t on the contour. Now $|\zeta|^2 = a^2 + b^2 \leq 2a^2$, thus $|\zeta| \leq \sqrt{2}a$. When the imaginary part of ζ is negative we rotate the contour of integration up in the plane and obtain the same result in the same way.

This simplifies to

$$W_1(\zeta) = \frac{e^{\zeta}}{2\sqrt{\pi}} \left[\sum_{k=0}^{n} b_k \zeta^{-k} + R_{1n}(\zeta) \right] \quad \text{if} \quad 0 < \operatorname{ph}(\zeta) < 2\pi \tag{2.32}$$

where

$$\begin{aligned} b_k &= \frac{2^k}{3^{3k}(2k)!} \frac{\Gamma(3k + 1/2)}{\Gamma(1/2)} \\ &= \frac{1}{\sqrt{\pi}} \int_0^{\infty} e^{-t} W_0(t) t^{k-1} dt \end{aligned}$$

and

$$R_{1n}(\zeta) = 2\sqrt{\pi}\zeta E_n(\zeta) = \frac{\zeta^{-(n-1)}}{\sqrt{\pi}} \int_0^{\infty} e^{-t} W_0(t) \frac{t^{n-1}}{\zeta - t} dt = O(\zeta^{-n})$$

for large $|\zeta|$ with $0 < \operatorname{ph}(\zeta) < 2\pi$.

Remember that $W_1(\zeta) = W_0(\zeta e^{-\pi i})$. Thus, we know that

$$W_0(\zeta) = \frac{\zeta e^{-\zeta}}{2\pi} \int_0^{\infty} \frac{e^{-t} W_0(t)}{t(\zeta + t)} dt = \frac{e^{-\zeta}}{2\sqrt{\pi}} \left[\sum_{k=0}^{n-1} (-1)^k b_k \zeta^{-k} + R_{0n}(\zeta) \right] \tag{2.33}$$

for $|\operatorname{ph}(\zeta)| < \pi$. The remainder $R_{0n}(\zeta)$ of the asymptotic expansion of $W_0(\zeta)$ is

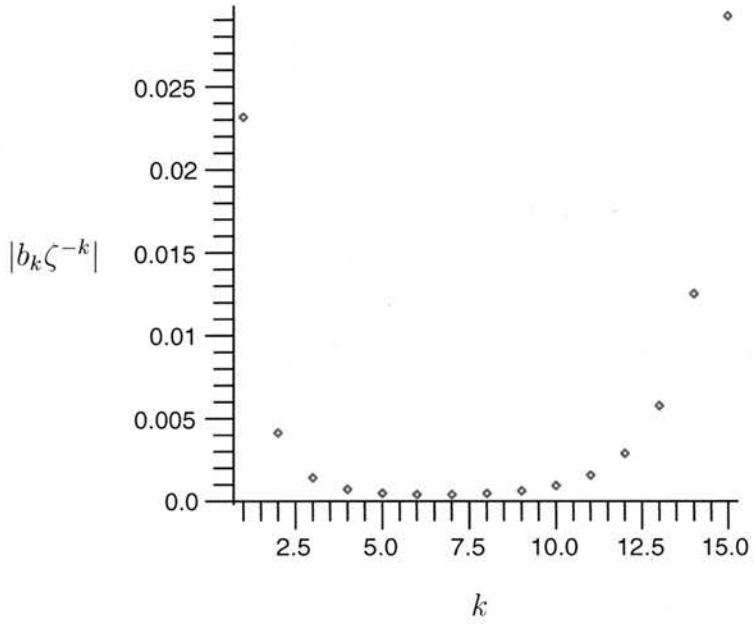

Figure 2.5: The value of the term $|b_k\zeta^{-k}|$ against k for $z = 3$ and $k = 1 \ldots 15$. Here we see how the terms in the series $\{|b_k\zeta^{-k}|\}_k$ decrease in size to start with but then they become larger in size. Remember that $b_0 = 1$.

given by

$$R_{0n}(\zeta) = \frac{(-1)^n \zeta^{-(n-1)}}{\sqrt{\pi}} \int_0^\infty e^{-t} W_0(t) \frac{t^{n-1}}{\zeta + t} dt = O(\zeta^{-n}),$$

for large $|\zeta|$ with $|\operatorname{ph}(\zeta)| < \pi$. The integral representation (2.28) provides the general asymptotic expansion of the $W_j(\zeta)$ functions. The difference from (2.19)–(2.21) is that now the b_k-coefficients are represented via an integral where the function $W_0(\zeta)$ is a factor of the integrand.

As the asymptotic expansions of the functions $W_j(\zeta)$ are divergent we want to truncate them optimally as we use them to approximate the functions. Thus the associated error can then be estimated via its integral representation.

2.2.9 Optimal number of terms and the optimal error

In practice, for a fixed value of large ζ we have to truncate the series (2.19)–(2.21) to approximate the value of $W_j(\zeta)$. As the series are divergent we will use a truncation that will give us the best approximation. In order to do this we notice that there exists some $N \in \mathbb{N}$ such that the sequence $\{|b_k\zeta^{-k}|\}_{k>N}$ is non decreasing, see figure 2.5. Truncating the series at the point when the sequence of absolute values of the terms stops decreasing, that is truncating after

n terms where the $(n-1)$th term is asymptotic to the nth term, should give the best approximation of the functions $W_j(\zeta)$. Note that in Poincaré's approach to asymptotics, he requires a fixed N for all ζ in a sector, on the other hand, optimal truncation allows N to vary as a function of $|\zeta|$.

We use the integral representation (2.31) of the b_k-coefficients. The large t-behaviour of $W_0(t)$ is governed by e^{-t} for $t \in \mathbb{R}_+$ so

$$\int_0^\infty e^{-t} W_0(t) t^{k-1} dt \sim \frac{1}{2\sqrt{\pi}} \int_0^\infty e^{-2t} t^{k-1} dt = \frac{\Gamma(k)}{2^{k+1}\sqrt{\pi}}$$

Therefore

$$\left| \frac{b_k \zeta^{-k}}{b_{k+1}\zeta^{-(k+1)}} \right| = |\zeta| \left| \frac{\int_0^\infty e^{-t} W_0(t) t^{k-1} dt}{\int_0^\infty e^{-t} W_0(t) t^k dt} \right| \sim |\zeta| \frac{2\Gamma(k)}{\Gamma(k+1)} = \frac{2\,|\zeta|}{k}.$$

Then the kth and the $(k+1)$th terms in (2.19)–(2.21) are of similar size when $2|\zeta|/k \approx 1$, that is when $k = 2[|\zeta|]$, where $[\cdot]$ is the function which rounds a number to the next integer.

Now, as we know the number of terms which give the best approximation of the W_j functions, we would like to know the error in that approximation.

If we truncate the series after the optimal number, $n = 2|\zeta| + \gamma$, of terms, where $\zeta = |\zeta| e^{i\theta_\zeta}$ with $\zeta \in (0, 2\pi)$ and $\gamma \in (-\frac{1}{2}, \frac{1}{2}]$, assuming that the function $[\cdot]$ rounds $1/2$ up to 1, the error is

$$\begin{aligned} E_{n+1}(\zeta) &= \zeta^{-(n+1)} \frac{1}{2\pi} \int_0^\infty e^{-t} W_0(t) \frac{t^n}{\zeta - t} dt \\ &= \zeta^{-(2|\zeta|+\gamma+1)} \frac{1}{2\pi} \int_0^\infty e^{-t} W_0(t) \frac{t^{2|\zeta|+\gamma}}{\zeta - t} dt. \end{aligned}$$

For large values of n the main contribution of the integrand comes from a neighbourhood of infinity. We therefore replace $W_0(t)$ by its asymptotic behaviour for large t. This gives

$$E_{n+1}(\zeta) \sim \zeta^{-(2|\zeta|+\gamma+1)} \frac{1}{4\pi^{3/2}} \int_0^\infty e^{-2t} \frac{t^{2|\zeta|+\gamma}}{\zeta - t} dt.$$

Now let $t = |\zeta|\tau$ in the last integral. Then

$$\begin{aligned} E_{n+1}(\zeta) &\sim \frac{1}{4\pi^{3/2}} \frac{|\zeta|^{2|\zeta|+\gamma}}{\zeta^{2|\zeta|+\gamma+1}} \int_0^\infty e^{-2|\zeta|\tau} \frac{\tau^{2|\zeta|+\gamma}}{\zeta/|\zeta| - \tau} dt \\ &= \frac{1}{4\pi^{3/2}} \frac{|\zeta|^{2|\zeta|+\gamma}}{\zeta^{2|\zeta|+\gamma+1}} \int_0^\infty e^{-2|\zeta|(\tau - \ln(\tau))} \frac{\tau^\gamma}{\zeta/|\zeta| - \tau} dt. \end{aligned}$$

Applying Laplace's method to the last integral then gives

$$E_{n+1}(\zeta) \sim \frac{1}{4\pi} \frac{|\zeta|^{2|\zeta|+\gamma-1/2}}{\zeta^{2|\zeta|+\gamma+1}} \frac{e^{-2|\zeta|}}{e^{i\theta_\zeta} - 1}.$$

In terms of this, the errors in the expansions (2.32) and (2.33) become

$$R_{0,n+1}(\zeta) \sim \frac{(-1)^{2|\zeta|+\gamma+1}}{2\sqrt{\pi}} \frac{|\zeta|^{2|\zeta|+\gamma-1/2}}{\zeta^{2|\zeta|+\gamma}} \frac{e^{-2|\zeta|}}{e^{i\theta_\zeta}+1}, \qquad |\operatorname{ph}(\zeta)| < \pi,$$

$$R_{1,n+1}(\zeta) \sim \frac{1}{2\sqrt{\pi}} \frac{|\zeta|^{2|\zeta|+\gamma-1/2}}{\zeta^{2|\zeta|+\gamma}} \frac{e^{-2|\zeta|}}{e^{i\theta_\zeta}-1}, \qquad 0 < \operatorname{ph}(\zeta) < 2\pi.$$

From these representations we see that the errors are governed by the exponential function $e^{-2|\zeta|}$, that is, they decay exponentially as $|\zeta|$ becomes large. Also, we note that the error is exponentially smaller that the governing term in the asymptotic expansion.

By changing back from ζ to $\frac{2}{3}z^{3/2}$ we can write out the full asymptotic expansion of the functions $\mathrm{Ai}_j(z)$ and the leading behaviour of the error term. However, there is a way to derive the same results using the somewhat sophisticated technique of the Borel-Laplace transform. To demonstrate this technique we derive the asymptotic expansion of the function $W_0(\zeta)$ and the identity (2.22) again.

2.2.10 Borel-Laplace transform

Let us derive the asymptotic expansion of the function $W_0(\zeta)$ again.

We represent $W_0(\zeta)$ with the Laplace type integral

$$W_0(\zeta) = \zeta \int_1^\infty e^{-\zeta t} y(t) dt. \tag{2.34}$$

Integration by parts gives

$$\begin{aligned} W_0(\zeta) &= -e^{-\zeta t} y(t)\big|_1^\infty + \int_1^\infty e^{-\zeta t} y'(t) dt \\ &= e^{-\zeta} y(1) + \int_1^\infty e^{-\zeta t} y'(t) dt \end{aligned}$$

implying that the behaviour of $W_0(\zeta)$ is dominated by $e^{-\zeta}$ as we knew from (2.19).

Let us now find an equation for the function $y(t)$. We can obtain one by inserting (2.34) into

$$\frac{d^2 W_0(\zeta)}{d\zeta^2} - \left(1 - \frac{5}{36}\zeta^{-2}\right) W_0(\zeta) = 0. \tag{2.35}$$

Further integration by parts gives

$$\zeta^{-2} W_0(\zeta) = \int_1^\infty \frac{e^{-\zeta t}}{\zeta} y(t) dt = \int_1^\infty e^{-\zeta t} \left(\int_1^t y(\tau) d\tau \right) dt \quad \text{and}$$

$$W_0''(\zeta) = \int_1^\infty e^{-\zeta t} \left(\zeta t^2 - 2t\right) y(t) dt = e^{-\zeta} y(1) + \int_1^\infty e^{-\zeta t} t^2 y'(t) dt$$

so equation (2.35) becomes

$$\int_1^\infty e^{-\zeta t}\left[(t^2-1)y'(t)+\frac{5}{36}\int_1^t y(\tau)d\tau\right]dt=0.$$

As this integral is a Laplace transform, we can deduce that

$$(t^2-1)y'(t)+\frac{5}{36}\int_1^t y(\tau)d\tau=0.$$

Differentiating this equation once gives

$$(t^2-1)y''(t)+2ty'(t)+\frac{5}{36}y(t)=0. \tag{2.36}$$

This equation has regular singular points at $t=\pm 1$ and at $t=\infty$, hence it is of hypergeometric type and we can rescale the variables so that the equation has the appearance of a hypergeometric differential equation.

By letting $z=(1-t)/2$ in (2.36) we map the singular points $t=-1$ to $z=1$ and $t=1$ to $z=0$. Then equation (2.36) in terms of z becomes

$$z(1-z)Y''(z)+(1-2z)Y'(z)-\frac{5}{36}Y(z)=0 \tag{2.37}$$

where $Y(z)=y((1-t)/2)$.

The nature of the asymptotic expansion of $W_0(\zeta)$ implies that $y(t)$ is analytic in a neighbourhood of $t=1$. This means that we want to look at solutions of (2.37) which are analytic in a neighbourhood of $z=0$. Thus we look at solutions of the form

$$Y(z)=C\,{}_2F_1\left(\begin{matrix}\frac{1}{6}&\frac{5}{6}\\1\end{matrix};z\right)$$

where ${}_2F_1$ is the hypergeometric function and C is some constant, see Temme (1996, 107-114). Since $W_0(\zeta)\sim\frac{1}{2\sqrt{\pi}}e^{-\zeta}$ and ${}_2F_1\left(\begin{matrix}\frac{1}{6}&\frac{5}{6}\\1\end{matrix};0\right)=1$ it follows that $C=\frac{1}{2\sqrt{\pi}}$. Thus

$$W_0(\zeta)=\frac{\zeta}{2\sqrt{\pi}}\int_1^\infty e^{-\zeta t}\,{}_2F_1\left(\begin{matrix}\frac{1}{6}&\frac{5}{6}\\1\end{matrix};\frac{1-t}{2}\right)dt. \tag{2.38}$$

The function ${}_2F_1\left(\begin{matrix}\frac{1}{6}&\frac{5}{6}\\1\end{matrix};\frac{1-t}{2}\right)$ has a regular singularity at infinity, thus its growth for large t is algebraic. Hence, the exponential function dominates the behaviour of the integrand for real values of t and the integrand contributes mainly to the integral from a region around 1. To evaluate the asymptotic behaviour of the integral we therefore insert the Taylor expansion

$${}_2F_1\left(\begin{matrix}\frac{1}{6}&\frac{5}{6}\\1\end{matrix};\frac{1-t}{2}\right)=\frac{1}{2\pi}\sum_{n=0}^\infty\frac{\Gamma(n+1/6)\Gamma(n+5/6)}{(n!)^2}\left(\frac{1-t}{2}\right)^n$$

into (2.38). Then

$$\begin{aligned} W_0(\zeta) &\sim \frac{\zeta}{4\sqrt{\pi}^{3/2}} \int_1^\infty e^{-\zeta t} \sum_{n=0}^\infty \frac{\Gamma(n+1/6)\Gamma(n+5/6)}{(n!)^2} \left(\frac{1-t}{2}\right)^n dt \\ &\sim \frac{\zeta}{4\sqrt{\pi}^{3/2}} \sum_{n=0}^\infty \frac{\Gamma(n+1/6)\Gamma(n+5/6)}{2^n (n!)^2} \int_1^\infty e^{-\zeta t} (1-t)^n \, dt \\ &\sim \frac{e^{-\zeta}}{4\sqrt{\pi}^{3/2}} \sum_{n=0}^\infty \frac{(-1)^n \Gamma(n+1/6)\Gamma(n+5/6)}{2^n n!} \zeta^{-n}. \end{aligned}$$

For $|\operatorname{ph}(\zeta)| < \frac{3\pi}{2}$ we have that $W_0(\zeta) \sim \frac{e^{-\zeta}}{2\sqrt{\pi}} \sum_{n=0}^\infty (-1)^n b_n \zeta^{-n}$ so we find again the value of the b_n-coefficients, (2.13), but with a new presentation, the third so far. That is we find

$$\begin{aligned} b_0 &= 1, \\ b_n &= \frac{\Gamma(n+1/6)\Gamma(n+5/6)}{2^{n+1}\pi n!} \qquad \text{if } n \geq 0. \end{aligned}$$

Let us now explore what information the function $y(t)$ gives about the asymptotic expansion of $W_0(\zeta)$.

2.2.11 The asymptotic expansion of $W_0(\zeta)$ for different values of $\operatorname{ph}(\zeta)$

Let us derive the identity (2.22) again by varying the values of ζ.

The integral representation

$$W_0(\zeta) = \frac{\zeta}{2\sqrt{\pi}} \int_1^\infty e^{-\zeta t} {}_2F_1\left(\begin{matrix} \frac{1}{6} & \frac{5}{6} \\ 1 \end{matrix} ; \frac{1-t}{2} \right) dt \tag{2.39}$$

is only valid for $|\operatorname{ph}(\zeta)| < \pi/2$, otherwise the integral on the right hand side does not converge.

Before we go any further, to simplify things, let us write $\zeta = r_\zeta e^{\theta_\zeta i}$ and define the path

$$l_t = 1 + re^{\theta_t i} \quad \text{where} \quad \begin{cases} 0 \leq r < \infty & \\ \theta_t = -\theta_\zeta & \text{if } \theta_\zeta \neq \pi \\ \theta_t \in (-\pi, -\pi/2) & \text{if } \theta_\zeta = \pi. \end{cases}$$

Rotating the contour of integration from the real axis to the contour l_t gives us the analytic continuation of (2.39) to other values of $\operatorname{ph}(\zeta)$. The integrand is dominated by $e^{-\zeta t}$ as the hypergeometric functions have a regular singularity at infinity, thus the growth of the integrand at infinity is algebraic and the contribution is zero from arcs linking the rotated contour and the original one.

We can rotate the contour of integration until we encounter the regular singularity $t = -1$ of the hypergeometric function. In a neighbourhood of $t = -1$ we have

$$ {}_2F_1\left(\begin{matrix}\frac{1}{6} & \frac{5}{6}\\ 1\end{matrix};\frac{1-t}{2}\right) = -\frac{1}{2\pi}\left[\ln\left(\frac{1+t}{2}\right){}_2F_1\left(\begin{matrix}\frac{1}{6} & \frac{5}{6}\\ 1\end{matrix};\frac{1+t}{2}\right) + H(t)\right] $$

where $H(t)$ is analytic at $t = -1$, see Temme (1996, 114). Thus as the angle of ζ becomes larger than π, the angle of the rotated contour l_t is less than $-\pi$ and we get an extra contribution from a loop around $t = -1$, say l_{-1}, see figure 2.6. That is

$$ \begin{aligned} W_0(\zeta) \sim & -\frac{\zeta}{4\pi^{3/2}}\int_{l_{-1}} e^{-\zeta t}\left[\ln\left(\frac{1+t}{2}\right){}_2F_1\left(\begin{matrix}\frac{1}{6} & \frac{5}{6}\\ 1\end{matrix};\frac{1+t}{2}\right) + H(t)\right]dt \\ & + \frac{\zeta}{2\sqrt{\pi}}\int_{l_t} e^{-\zeta t}{}_2F_1\left(\begin{matrix}\frac{1}{6} & \frac{5}{6}\\ 1\end{matrix};\frac{1-t}{2}\right)dt. \end{aligned} $$

Now, let us collapse the loop in the first integral. Then

$$ \begin{aligned} W_0(\zeta) &= -\frac{i\zeta}{2\sqrt{\pi}}\int_{-\infty}^{-1} e^{-\zeta t}{}_2F_1\left(\begin{matrix}\frac{1}{6} & \frac{5}{6}\\ 1\end{matrix};\frac{1+t}{2}\right)dt + \frac{\zeta}{2\sqrt{\pi}}\int_{l_t} e^{-t\zeta}{}_2F_1\left(\begin{matrix}\frac{1}{6} & \frac{5}{6}\\ 1\end{matrix};\frac{1-t}{2}\right)dt \\ &= -\frac{i\zeta}{2\sqrt{\pi}}\int_{1}^{\infty} e^{\zeta t}{}_2F_1\left(\begin{matrix}\frac{1}{6} & \frac{5}{6}\\ 1\end{matrix};\frac{1-t}{2}\right)dt + \frac{\zeta}{2\sqrt{\pi}}\int_{l_t} e^{-t\zeta}{}_2F_1\left(\begin{matrix}\frac{1}{6} & \frac{5}{6}\\ 1\end{matrix};\frac{1-t}{2}\right)dt \\ &= -iW_0(\zeta e^{\pi i}) + W_0(\zeta e^{2\pi i}). \end{aligned} $$

For the last equality we have used the definition (2.39) for the first integral. For the second integral in the last equality, we consider the angles θ_t of l_t and θ_ζ to belong to one Riemann sheet below. That is we think of the angles as $\theta_t + 2\pi$ and $\theta_\zeta - 2\pi$ respectively and thus $\theta_\zeta - 2\pi$ is in the interval $(-\pi, \pi)$ and (2.39) holds.

Now, let $\zeta = \zeta e^{\pi i}$. Then the identity

$$ iW_0(\zeta e^{\pi i}) = W_0(\zeta e^{2\pi i}) - W_0(\zeta) $$

becomes

$$ iW_0(\zeta) = W_{-1}(\zeta) - W_1(\zeta) $$

which we know as equation (2.22).

Having looked at the asymptotics of the solutions of the Airy equation it is time to look at the Scorer equation.

2.3 The Scorer equation

Let us explore the large z-asymptotics of the particular integral of the Scorer equation

$$ \frac{d^2w(z)}{dz^2} - zw(z) = \frac{1}{\pi}. \tag{2.40} $$

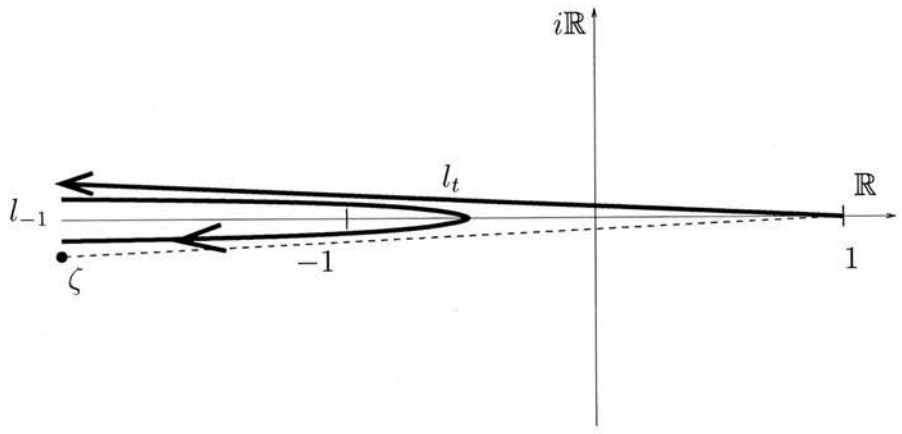

Figure 2.6: The integration path for the Borel transform of W_0

Let us assume that $w_p(z)$ is a particular integral of (2.40) and that $w_p(z) \sim \sum_{n=0}^{\infty} a_n z^{-n}$. This is a formal series representation of the function w_p, its sector of validity will be determined later on in this section. Substitution into (2.40) then gives that

$$\begin{aligned} a_0 &= a_2 = 0, \\ a_1 &= -1/\pi, \\ a_n &= (n-2)(n-3)a_{n-3} \quad \text{for } n \geq 3. \end{aligned}$$

From this we see that $a_{3n} = a_{3n+2} = 0$ for $n = 0, 1, 2, \ldots$. Recall that the shifted factorial is defined by

$$\begin{aligned} (a)_0 &= 1, \\ (a)_n &= a(a+1)(a+2)\cdots(a+n-1), \qquad n > 0. \end{aligned}$$

That is

$$(a)_n = \frac{\Gamma(a+n)}{\Gamma(a)} \qquad n \geq 0.$$

Using this, we can solve the recurrence relation as follows

$$\begin{aligned} a_{3n+1} &= (3n-1)(3n-2)a_{3n-2} \\ &= (n-1/3)\,(n-2/3)\,3^2 a_{3n-2} \\ &= (1/3)_n\,(2/3)_n\,3^{2n} a_1 \end{aligned}$$

Thus

$$w_p(z) \sim -\frac{1}{\pi} \sum_{n=0}^{\infty} 3^{2n} (1/3)_n (2/3)_n z^{-(3n+1)}. \tag{2.41}$$

The existence of the Stokes phenomenon, discussed in Section 2.1, leads to a switching on of one of the $\mathrm{Ai}_j(z)$ functions, $j = -1, 0, 1$, as one of the Stokes lines is crossed. Assume that the exponential function e^0 is the one that multipliers

the asymptotic expansion of the particular integral. Then the Stokes lines may occur, as mentioned before, when the ratio of the governing exponents is purely real and the anti-Stokes lines occur when this ratio is purely imaginary. Thus, as the exponent for the particular integral is zero, the Stokes lines and the anti-Stokes lines are the same as before, see figure 2.2. On an anti-Stokes line the particular integral and the relevant $\mathrm{Ai}_j(z)$ functions are comparable in size, thus the asymptotic expansion (2.41) holds in a sector bounded by two anti-Stokes lines.

If we translate this in terms of the phase of z, we get that the asymptotic expansion (2.41) is valid in three intervals of $\mathrm{ph}(z)$. That is, for $-\pi < \mathrm{ph}(z) < \pi/3$, $-\pi/3 < \mathrm{ph}(z) < \pi$ and $-5\pi/3 < \mathrm{ph}(z) < -\pi/3$. If we look at figure 2.2 we see that these sectors are bounded by anti-Stokes lines. Also, each of these sectors contains Stokes lines and an anti-Stokes line. Thus, we might think these sectors are too big. This is not the case as what is switched on at a Stokes line depends on in which direction we rotate the value of z. Let us define the functions w_{pj}, $j = 1, 2, 3$ such that

the series (2.41) is asymptotic to $w_{p1}(z)$ for $\mathrm{ph}(z) \in (-\pi, \pi/3)$,
the series (2.41) is asymptotic to $w_{p2}(z)$ for $\mathrm{ph}(z) \in (-\pi/3, \pi)$,
the series (2.41) is asymptotic to $w_{p3}(z)$ for $\mathrm{ph}(z) \in (-5\pi/3, -\pi/3)$.

As these sectors are of maximal size these functions are well defined.

Considering the asymptotic expansions of these three solutions and the integral representation (2.9), we see that

$$\begin{aligned} w_{p1}(z) &= e^{-\frac{2\pi i}{3}} \mathrm{Hi}(ze^{-\frac{2\pi i}{3}}) \\ w_{p2}(z) &= e^{\frac{2\pi i}{3}} \mathrm{Hi}(ze^{\frac{2\pi i}{3}}) \\ w_{p3}(z) &= \mathrm{Hi}(z) \end{aligned}$$

as the asymptotic expansions of the Hi-Scorer functions are the same as for the w_p-functions and the sectors of validity have the maximum size. Also the function $w_{p1}(z)$ has the same asymptotic expansion as the Scorer function $-\mathrm{Gi}(z)$ for $\mathrm{ph}(z) \in (-\pi/3, \pi/3)$, see Olver (1974, 432). That is, the difference of $w_{p1}(z)$ and $-\mathrm{Gi}(z)$ is a solution of the Airy equation and is exponentially small for large z. Hence, as we want to derive the full asymptotic expansion of the Scorer function $-\mathrm{Gi}(z)$, we focus our analysis on the function $w_{p1}(z)$.

2.3.1 Connection relation for the particular integrals

As (2.40) is a linear ordinary differential equation, the differences $w_{p1}(z) - w_{p2}(z)$ and $w_{p1}(z) - w_{p3}(z)$ are solutions of the Airy equation, the homogeneous part

of equation (2.40). Thus, these solutions can be written as linear combinations of the Ai_j functions, $j = -1, 0, 1$. The particular integrals are defined via their asymptotic expansion in certain sectors. As only one of the Airy functions is recessive in each of the sectors we get the following relation

$$w_{p1}(z) = w_{p2}(z) + K_{12}\,\mathrm{Ai}_0(z), \tag{2.42}$$

$$w_{p1}(z) = w_{p3}(z) + K_{13}\,\mathrm{Ai}_{-1}(z). \tag{2.43}$$

The coefficients K_{1i}, $i = 2, 3$, are the Stokes multipliers and their values can be found by an examination of the large-n behaviour of the late coefficients in the asymptotic expansion of $w_{p1}(z)$. First we do some rescaling to ease our calculations.

2.3.2 Rescaling

As before, let $\zeta = \frac{2}{3}z^{3/2}$. We define the function $W_p(\zeta)$ such that

$$W_p(\zeta) = w_p((3\zeta/2)^{2/3}) = w_p(z).$$

Then $W_p(\zeta)$ is a solution of

$$\frac{d^2W_p(\zeta)}{d\zeta^2} + \frac{1}{3\zeta}\frac{dW_p(\zeta)}{d\zeta} - W_p(\zeta) = \frac{1}{\pi(3\zeta/2)^{2/3}} \tag{2.44}$$

and

$$W_p(\zeta) \sim -\frac{(2/3)^{2/3}}{\pi\zeta^{2/3}}\sum_{n=0}^{\infty} 2^{2n}(1/3)_n(2/3)_n\zeta^{-2n}. \tag{2.45}$$

Then in the same way as with $w_p(z)$ we define the functions $W_{pj}(\zeta)$, $j = 1, 2, 3$ such that the

the series (2.45) is asymptotic to $W_{p1}(\zeta)$ for $\mathrm{ph}(\zeta) \in (-3\pi/2, \pi/2)$,
the series (2.45) is asymptotic to $W_{p2}(\zeta)$ for $\mathrm{ph}(\zeta) \in (-\pi/2, 3\pi/2)$,
the series (2.45) is asymptotic to $W_{p3}(\zeta)$ for $\mathrm{ph}(\zeta) \in (-5\pi/2, -\pi/2)$.

Thus, these functions satisfy the relations

$$W_{p1}(\zeta) = W_{p2}(\zeta) + K_{12}z^{-1/4}W_0(\zeta), \tag{2.46}$$

$$W_{p1}(\zeta) = W_{p3}(\zeta) + K_{13}e^{-\pi i/6}z^{-1/4}W_{-1}(\zeta). \tag{2.47}$$

Let us now examine the asymptotic expansion of the function $W_p(\zeta)$ via the Borel-Laplace transform.

2.3.3 Borel transform

In the same manner as with the solution to the homogeneous equation (2.10), we represent $W_p(\zeta)$ via the integral

$$W_p(\zeta) = \zeta \int_0^{\infty e^{\alpha i}} e^{-\zeta t} y_p(t) dt \tag{2.48}$$

where $\alpha \in \mathbb{R}$ is some constant chosen such that the real part of ζt is positive and that all other conditions for the integral on the right hand side to exist are satisfied. Let us now find a differential equation for $y_p(t)$ by substituting (2.48) into (2.44).

After substituting the integral representation of $W_p(\zeta)$ we simplify the outcome by using partial integration. Now,

$$W_p(\zeta) = y_p(0) + \int_0^{\infty e^{\alpha i}} e^{-\zeta t} y_p'(t) dt.$$

From previous results we know that $W_p(\zeta) \sim -\pi^{-1}(3\zeta/2)^{-2/3}$ and thus we find that $y_p(t) \approx -(\pi\Gamma(5/3))^{-1}(2t/3)^{2/3}$, as it can been shown from the formal integral representation of the Γ function that, with our condition on α,

$$\zeta \int_0^{\infty e^{\alpha i}} e^{-\zeta t} t^k dt = \frac{\Gamma(k+1)}{\zeta^k}.$$

Thus, we take as an initial condition that $y_p(0) = 0$. Hence,

$$W_p(\zeta) = \int_0^{\infty e^{\alpha i}} e^{-\zeta t} y_p'(t) dt.$$

and

$$\begin{aligned} \zeta^{-1} \frac{dW_p(\zeta)}{d\zeta} &= \int_0^{\infty e^{\alpha i}} e^{-\zeta t} \left(\int_0^t y_p(\tau) d\tau - t y_p(t) \right) dt, \\ \frac{d^2 W_p(\zeta)}{d\zeta^2} &= \int_0^{\infty e^{\alpha i}} e^{-\zeta t} t^2 y_p'(t) dt. \end{aligned}$$

Furthermore we write

$$\frac{(2/3)^{2/3}}{\pi \zeta^{2/3}} = \frac{(2/3)^{2/3}}{\pi \Gamma(2/3)} \int_0^{\infty e^{\alpha i}} e^{-\zeta t} t^{-1/3} dt.$$

Then equation (2.44) gives the following equation for $y_p(t)$:

$$(t^2 - 1) y_p'(t) - \frac{t}{3} y_p(t) + \frac{1}{3} \int_0^t y_p(\tau) d\tau = \frac{(2/3)^{2/3}}{\pi \Gamma(2/3)} t^{-1/3}.$$

By differentiating this equation we get the second order differential equation

$$(t^2 - 1) y_p''(t) + \frac{5t}{3} y_p'(t) = -\frac{(2/3)^{2/3}}{3\pi \Gamma(2/3)} t^{-4/3} \tag{2.49}$$

which has regular singularities at the points $t = \pm 1$, $t = 0$ and $t = \infty$.

Local analysis of this equation shows that in a neighbourhood of the regular singularity zero we have $y_p(t) = \sum_{n=0}^{\infty} y_n^{(0)} t^{n+2/3}$. Substitution of this series into (2.49) gives

$$y_0^{(0)} = -\frac{(2/3)^{2/3}}{\pi\Gamma(5/3)} \quad \text{and} \quad y_1^{(0)} = 0.$$

Thus, $y_{2n+1}^{(0)} = 0$ for all $n \geq 0$. For the rest of the coefficients we get the following recurrence relation

$$\begin{aligned} y_{2n}^{(0)} &= \frac{(2n-4/3)(2n-2/3)}{(2n+2/3)(2n-1/3)} y_{2(n-1)}^{(0)} \\ &= \frac{2^{2n}(1/3)_n(2/3)_n}{(5/3)_{2n}} y_0^{(0)} \qquad\qquad n = 0, 1, 2, \ldots . \end{aligned}$$

Notice how these coefficients look similar to the ones in the asymptotic expansion of $W_p(\zeta)$, (2.45). Let us see how this is not a coincidence.

To start with, let us simplify the representation of the asymptotic expansion, (2.45), of $W_p(\zeta)$. That is, let us write

$$W_p(\zeta) \sim \zeta^{-2/3} \sum_{n=0}^{\infty} c_n \zeta^{-n} \tag{2.50}$$

where

$$c_0 = -\frac{(2/3)^{2/3}}{\pi}$$

and for $n \geq 1$

$$\begin{aligned} c_{2n} &= 2^{2n}(1/3)_n(2/3)_n c_0, \\ c_{2n-1} &= 0. \end{aligned}$$

The main contribution of the integrand to the integral in the right hand side of (2.48) comes from a neighbourhood of zero. We therefore substitute for $y_p(t)$ with its expansion around zero. Thus,

$$\begin{aligned} W_p(\zeta) &= \zeta \int_0^{\infty e^{\alpha i}} e^{-\zeta t} y_p(t) dt \\ &\sim \sum_{n=0}^{\infty} y_n^{(0)} \zeta \int_0^{\infty e^{\alpha i}} e^{-\zeta t} t^{n+2/3} dt \\ &\sim \sum_{n=0}^{\infty} y_n^{(0)} \Gamma(n + 5/3) \zeta^{-(n+2/3)}. \end{aligned} \tag{2.51}$$

Here we assume $t^{2/3}$ takes its principal value.

As $W_p(\zeta)$ has only one asymptotic expansion, $\zeta^{-2/3}\sum_{n=0}^{\infty} c_n\zeta^{-n}$, we get that

$$\begin{aligned} c_0 &= y_0^{(0)}\Gamma(5/3) = -\frac{(2/3)^{2/3}}{\pi}, \\ c_{2n} &= y_{2n}^{(0)}\Gamma(2n+5/3) = 2^{2n}(1/3)_n(2/3)_n c_0, \qquad \text{and} \\ c_{2m+1} &= y_{2m+1}^{(0)}\Gamma(2m+8/3) = 0 \end{aligned}$$

where $n > 0$ and $m \geq 0$. That is, the behaviour of the function $y_p(t)$ around its regular singular point zero has given us enough information to construct the asymptotic expansion of $W_p(\zeta)$ again without having any additional information.

Let us now see how the behaviour of c_n for large n can give us the full asymptotic behaviour of $W_p(\zeta)$.

2.3.4 Late coefficients

We look at the behaviour of the late c_n-coefficients in the asymptotic expansion (2.50) of $W_p(\zeta)$, that is the behaviour of c_n as n tends to infinity.

Remember that according to Cauchy's integral formula

$$y_n^{(0)} = \frac{c_n}{\Gamma(n+5/3)} = \frac{1}{2\pi i}\oint_{\mathcal{C}} \frac{t^{-2/3}y_p(t)}{t^{n+1}}dt = \frac{1}{2\pi i}\oint_{\mathcal{C}} \frac{y_p(t)}{t^{n+5/3}}dt \tag{2.52}$$

where $\mathcal{C}$ is a closed counterclockwise directed contour surrounding zero.

The differential equation, (2.49), for $y_p(t)$ implies that $y_p(t)$ is an analytic function in all $\mathbb{C}$ except at the points $t = \pm 1$ and $t = 0$. The singularity $t = 0$ is not relevant here as the factor $t^{-2/3}$ in (2.52) removes the singularity. Therefore we will choose $\mathcal{C}$ as the closed contour around zero which consists of loops around ± 1 and arcs, of radius R from the origin, linking the loops together, see figure 2.7.

The growth of $y_p(t)$ for large t is algebraic as $t = \infty$ is a regular singularity. Thus, we get that the contributions from the arcs tend to zero as we let R tend to infinity. Hence, we only have to consider the loops around $t = \pm 1$, say $l_\pm$ respectively. From now on we focus on the interval $0 < \mathrm{ph}(t) < \pi$. Hence, $1 = e^{0\pi i}$ and $-1 = e^{\pi i}$.

Local analysis at the points $t = \pm 1$ gives that

$$y_p(t) = C_\pm \sum_{n=0}^{\infty} y_n^{(\pm 1)}(t \mp 1)^{n+1/6} + f_\pm(t \mp 1) \tag{2.53}$$

where $C_\pm$ are some constants and the functions $f_\pm(t \mp 1)$ are analytic in a neighbourhood of $t = \pm 1$ respectively. Here we assume $(\cdot)^{1/6}$ to take its principal value, that is considering $y_p(t)$ in a neighbourhood of $t = -1$ we have $t \notin (-\infty, -1]$ and considering $y_p(t)$ in a neighbourhood of $t = 1$ we have $t \notin [1, \infty)$. Thus, in a

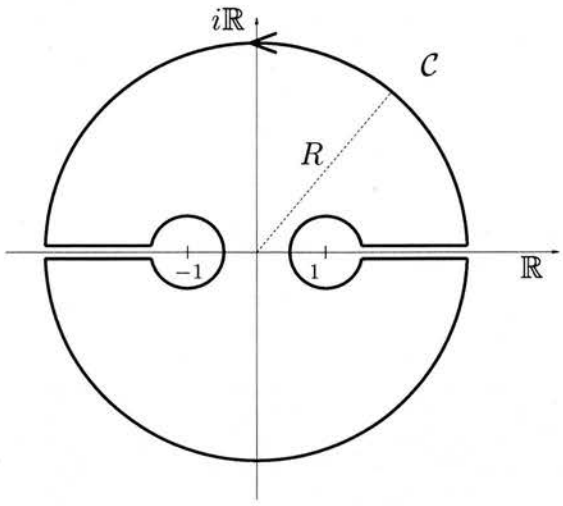

Figure 2.7: The contour $\mathcal{C}$ of integration in Cauchy's integral formula.

neighbourhood of the points $t = \pm 1$, $y_p(t)$ consists of a multivalued part, which is a solution of the homogeneous part of (2.49), and an analytic part, $f_\pm(t \mp 1)$, which contains the particular integral. Let us choose $y_0^{(\pm 1)} = 1$, then for $n \geq 0$ we have

$$\begin{aligned} y_n^{(1)} &= (-1)^n \frac{(1/6)_n (5/6)_n}{2^n (7/6)_n n!}, \\ y_n^{(-1)} &= (-1)^n y_n^{(1)}. \end{aligned} \tag{2.54}$$

The analytic functions $f_\pm(t \mp 1)$ do not contribute to the integral (2.52), thus for large n we have

$$\begin{aligned} y_n^{(0)} &= \frac{c_n}{\Gamma(n + 5/3)} \\ &= \frac{1}{2\pi i} \left(\int_{l_+} + \int_{l_-} \right) \left(\frac{y_p(t)}{t^{n+5/3}} \right) dt \\ &\sim \frac{C_+}{2\pi i} \int_{l_+} \frac{\sum_{k=0}^{\infty} y_k^{(1)} (t-1)^{k+1/6}}{t^{n+5/3}} dt + \frac{C_-}{2\pi i} \int_{l_-} \frac{\sum_{k=0}^{\infty} y_k^{(-1)} (t+1)^{k+1/6}}{t^{n+5/3}} dt. \end{aligned}$$

Hence

$$\begin{aligned}\frac{c_n}{\Gamma(n+5/3)} &\sim \frac{C_+}{2\pi i}\sum_{k=0}^{\infty} y_k^{(1)} \int_{l_+} \frac{(t-1)^{k+1/6}}{t^{n+5/3}}dt + \frac{C_-}{2\pi i}\sum_{k=0}^{\infty} y_k^{(-1)} \int_{l_-} \frac{(t+1)^{k+1/6}}{t^{n+5/3}}dt \\ &\sim \frac{C_+}{2\pi i}\sum_{k=0}^{\infty} y_k^{(1)} \left(1-e^{\frac{\pi i}{3}}\right) \mathrm{B}(k+7/6, n-k+1/2) \\ &\qquad + \frac{C_-}{2\pi i}\sum_{k=0}^{\infty} (-1)^{n-k} y_k^{(-1)} e^{\frac{\pi i}{2}} \left(1-e^{\frac{\pi i}{3}}\right) \mathrm{B}(k+7/6, n-k+1/2) \\ &\sim \frac{e^{-\frac{\pi i}{3}} C_+}{2\pi i}\sum_{k=0}^{\infty} y_k^{(1)} \frac{\Gamma(k+7/6)\Gamma(n-k+1/2)}{\Gamma(n+5/3)} \\ &\qquad + \frac{e^{\frac{\pi i}{6}} C_-}{2\pi i}\sum_{k=0}^{\infty} (-1)^{n-k} y_k^{(-1)} \frac{\Gamma(k+7/6)\Gamma(n-k+1/2)}{\Gamma(n+5/3)}\end{aligned}$$

where we have used the not so common representation of the Beta integral

$$B(\alpha,\beta) = \frac{\Gamma(\alpha)\Gamma(\beta)}{\Gamma(\alpha+\beta)} = \frac{1}{e^{2\pi i\alpha}-1}\int_{\infty}^{(0+)} w^{\alpha-1}(w+1)^{-(\alpha+\beta)}dw,$$

where we integrate from infinity and back counterclockwise around zero, and that $(1-e^{\pi i/3}) = e^{-\pi i/3}$. This means that for large n

$$\begin{aligned}c_n \sim{}& \frac{e^{-\frac{\pi i}{3}} C_+}{2\pi i}\sum_{k=0}^{\infty} y_k^{(1)} \Gamma(k+7/6)\Gamma(n-k+1/2) \\ &+ \frac{e^{\frac{\pi i}{6}} C_-}{2\pi i}\sum_{k=0}^{\infty} (-1)^{n-k} y_k^{(-1)} \Gamma(k+7/6)\Gamma(n-k+1/2).\end{aligned} \tag{2.55}$$

We know that $c_{2m+1} = 0$ for all $m = 0, 1, 2, \ldots$, thus

$$y_0^{(1)} C_+ - y_0^{(-1)} e^{\frac{\pi i}{2}} C_- = 0.$$

Then, using (2.54), we get

$$C_- = e^{-\frac{\pi i}{2}} C_+.$$

Hence

$$c_{2n} \sim \frac{e^{-\frac{5\pi i}{6}} C_+}{\pi}\sum_{k=0}^{\infty} y_k^{(1)} \Gamma(k+7/6)\Gamma(2n-k+1/2).$$

We obtain

$$C_+ = \frac{(2/3)^{1/6} e^{-\frac{\pi i}{6}}}{\sqrt{\pi}\Gamma(7/6)}$$

by comparing the leading order term of this expansion to the dominant behaviour of the exact representation given by

$$\begin{aligned}c_{2n} &= -\frac{(2/3)^{2/3}}{\pi}\frac{\sqrt{3}}{2\pi} 2^{2n}\Gamma(n+1/3)\Gamma(n+2/3) \\ &\sim -\frac{2^{2/3}}{3^{1/6}\pi^2} 2^{2n} e^{-(2n+1)} (n+1/3)^{n-1/6}(n+2/3)^{n+1/6} \qquad \text{as } n\to\infty,\end{aligned}$$

where we have used Stirling's formula

$$\Gamma(x) \sim e^{-x}x^x \left(\frac{2\pi}{x}\right)^{1/2} \qquad \text{as } x \to \infty$$

to find the large-n asymptotic behaviour of the Γ-function. Hence,

$$c_{2n} \sim \frac{(2/3)^{1/6}}{\pi^{3/2}\Gamma(7/6)} \sum_{k=0}^{\infty} y_k^{(1)} \Gamma(k+7/6)\Gamma(2n-k+1/2). \tag{2.56}$$

Here we have derived the full large-n asymptotic expansion for all of the c_n coefficients in terms of the behaviour of $y_p(t)$ around $t = \pm 1$. Let us see if we can stretch this further.

2.3.5 The Stokes phenomenon, computation of the Stokes multipliers

Let us now look at the integral representation

$$W_{p1}(\zeta) = \zeta \int_0^{\infty e^{\alpha i}} e^{-\zeta t} y_p(t) dt$$

where the $\alpha \in \mathbb{R}$ is fixed. The function $W_{p1}(\zeta)$ exists for all values of $\zeta \in \mathbb{C}$ but the integral on the right hand side does not. In this section we will extend this integral representation to all values of $\mathrm{ph}(\zeta)$.

We define $\theta_\zeta = \mathrm{ph}(\zeta)$ and $\theta_t = \mathrm{ph}(t)$ and let

$$l_t = re^{\theta i} \text{ where } \begin{cases} 0 \le t \le \infty \\ \theta = -\theta_\zeta. \end{cases}$$

The growth of $y_p(t)$ is algebraic for large t so the behaviour of the integrand is dominated by $e^{-\zeta t}$ for large values of t. Thus we can rotate the contour of integration, that is

$$W_{p1}(\zeta) = \zeta \int_{l_t} e^{-\zeta t} y_p(t) dt \tag{2.57}$$

as long as we do not rotate ζ over the real axis as we know from (2.49) that the function $y_p(t)$ has regular singularities at $t = \pm 1$.

Rotating ζ over the real axis gives two kind of extra contributions to $W_{p1}(\zeta)$ in addition with (2.57), depending on whether we passed the positive real axis or the negative. We restrict our analysis to the singularity $t = 1 = e^{0\pi i}$.

When we rotate ζ over the positive real axis, let us assume that the value of α is fixed in the interval $(0, \pi)$ and that $\theta_\zeta = -\alpha$. Then if we let $\mathrm{ph}(\zeta)$ travel from $-\alpha$ to α we rotate the phase of the contour of integration from α to $-\alpha$ such that $\mathrm{ph}(\zeta t) = 0$. As ζ passes the real axis we have to take in account that the function

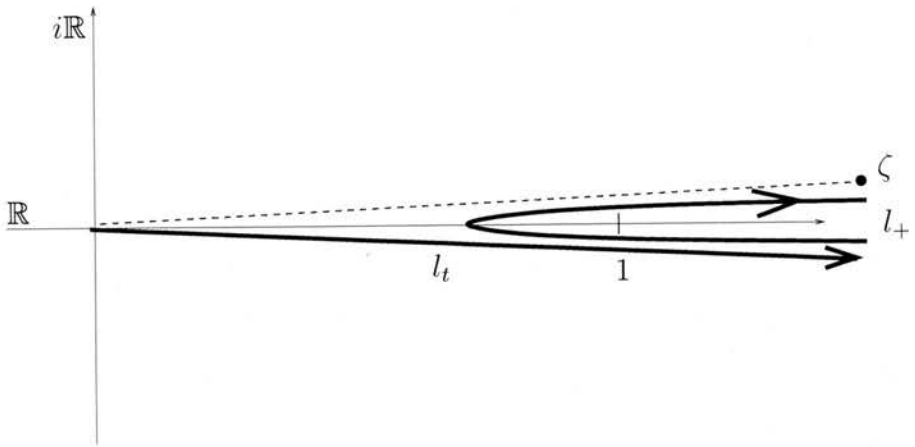

Figure 2.8: The contour of integration for the integrals in (2.58).

$y_p(t)$ has a regular singularity at $t = 1$. Hence, we get an additional contribution to the integral representation of the function $W_{p1}(\zeta)$ from a loop around $t = 1$, say l_+ as before. This gives

$$W_{p1}(\zeta) = \zeta \left(\int_{l_t} + \int_{l_+} \right) e^{-\zeta t} y_p(t) dt \quad \text{for} \quad \text{ph}(\zeta) \in (0, \pi), \tag{2.58}$$

see figure 2.8 Let us use this integral representation to find the large-ζ asymptotic expansion of $W_{p1}(\zeta)$.

The integrals in (2.58) are dominated by the exponential function in the integrand. Hence, we can substitute for the function $y_p(t)$ with its expansion around $t = 0$ in the first integral and around $t = 1$ in the latter one. Then

$$W_{p1}(\zeta) \sim \sum_{n=0}^{\infty} y_n^{(0)} \Gamma(n + 5/3) \zeta^{-(n+2/3)} + C_+ e^{-\frac{\pi i}{3}} e^{-\zeta} \sum_{n=0}^{\infty} y_n^{(1)} \Gamma(n + 7/6) \zeta^{-(n+1/6)}$$

where the first sum with terms that are $O(\zeta^{-n})$ comes from the integral over l_t and the latter sum with terms that are exponentially small come from the integral over l_+. For $\text{ph}(\zeta) \in (-\pi, \pi/2)$ we see that the first expansion agrees with the expansion (2.51). But what about the latter sum?

We recall the identity

$$W_{p1}(\zeta) = W_{p2}(\zeta) + K_{12} z^{-1/4} W_0(\zeta)$$

from Section 2.3.2. This identity holds for all values of ζ, so in particular for large values of $|\zeta|$. We also recollect from same section that for $\text{ph}(\zeta) \in (-\pi/2, \pi/2)$ the functions $W_{p1}(\zeta)$ and $W_{p2}(\zeta)$ have the same asymptotic expansion (2.45), or equivalently (2.51). Hence, if we substitute for the particular integrals on both

sides of the identity with their asymptotic expansion we get by comparison that

$$K_{12}z^{-1/4}W_0(\zeta) \sim C_+e^{-\frac{\pi i}{3}}e^{-\zeta}\sum_{n=0}^{\infty} y_n^{(1)}\Gamma(n+7/6)\zeta^{-(n+1/6)}$$
$$\sim -\frac{i(2/3)^{1/6}}{\sqrt{\pi}}e^{-\zeta}\sum_{n=0}^{\infty} y_n^{(1)}\frac{\Gamma(n+7/6)}{\Gamma(7/6)}\zeta^{-(n+1/6)} \quad \text{for} \quad |\operatorname{ph}(\zeta)| < \frac{3\pi}{2}.$$

Comparing the dominant behaviours of both sides we obtain that

$$K_{12} = -2i.$$

In a similar way we obtain that

$$K_{13} = -2.$$

Furthermore, comparing the coefficients we see that

$$y_n^{(1)} = \frac{(-1)^n b_n \Gamma(7/6)}{\Gamma(n+7/6)}.$$

Hence, we can write

$$c_{2n} \sim \frac{(2/3)^{1/6}}{\pi^{3/2}}\sum_{k=0}^{\infty}(-1)^k b_k \Gamma(2n-k+1/2).$$

This result is very nice as we can write the late c_n-term behaviour as an expansion with the same coefficients as the asymptotic expansions of the functions W_j, $j = -1, 0, 1$, which form a solution basis for the rescaled Airy equation.

Let us now summarise what we have done in the asymptotic expansion of the Scorer function $-\operatorname{Gi}(z)$.

2.4 The asymptotic expansion of $-\operatorname{Gi}(z)$

We have now gained enough information to derive the asymptotic expansion of the Scorer function $-\operatorname{Gi}(z)$. The function $w_{p1}(z)$ and the Scorer function $-\operatorname{Gi}(z)$ have the same asymptotic expansion (2.41) in the sector $|\operatorname{ph}(z)| < \pi/3$. With the value of the Stokes multiplier $K_{12} = -2i$ the connection relation (2.42) becomes

$$w_{p1}(z) = w_{p2}(z) - 2i\operatorname{Ai}_0(z). \tag{2.59}$$

It follows from the integral representations (2.8) and (2.9) that

$$-\operatorname{Gi}(z) = \frac{1}{2}e^{-\frac{2\pi i}{3}}\operatorname{Hi}(ze^{-\frac{2\pi i}{3}}) + \frac{1}{2}e^{\frac{2\pi i}{3}}\operatorname{Hi}(ze^{\frac{2\pi i}{3}})$$

and, as mentioned before, that $\mathrm{Hi}(z) = w_{p3}(z)$. Hence

$$-\mathrm{Gi}(z) = \frac{1}{2}w_{p1}(z) + \frac{1}{2}w_{p2}(z). \tag{2.60}$$

If we use the relation (2.59) to replace the function $w_{p2}(z)$ on the right hand side, we get that

$$-\mathrm{Gi}(z) = w_{p1}(z) + i\,\mathrm{Ai}_0(z), \tag{2.61}$$

and if we use the relation (2.59) to replace the function $w_{p1}(z)$ on the right hand side of (2.60) we get that

$$-\mathrm{Gi}(z) = w_{p2}(z) - i\,\mathrm{Ai}_0(z). \tag{2.62}$$

We use the relation (2.61) to find the asymptotic expansion of the function $-\mathrm{Gi}(z)$ for large $|z|$ in the sector $-\pi < \mathrm{ph}(z) < \pi/3$. We know that if we consider the asymptotic expansion of the function $w_{p1}(z)$ as z crosses the positive real axis clockwise the Stokes phenomenon occurs and a $-2i$-multiple of the function $\mathrm{Ai}_0(z)$ is switched on. With this addition, the asymptotic expansion of the function $-\mathrm{Gi}(z)$ in the section $0 \le \mathrm{ph}(z) < \pi$ is the same as the right hand side of (2.62). To summarise, the asymptotic expansion of the function $-\mathrm{Gi}(z)$ for large $|z|$ in the sector $|\mathrm{ph}(z)| < \pi$ is given by

$$-\mathrm{Gi}(z) \sim -\frac{1}{\pi}\sum_{n=0}^{\infty} 3^{2n}(1/3)_n(2/3)_n z^{-(3n+1)} + \begin{cases} -\dfrac{e^{-\frac{2}{3}z^{3/2}}}{2\sqrt{\pi}iz^{1/4}}\displaystyle\sum_{k=0}^{\infty}(-1)^k b_k\,(3/2)^k\,z^{-3k/2} & \text{if } \mathrm{ph}(z) \in \left(-\pi, \dfrac{\pi}{3}\right) \\ \dfrac{e^{-\frac{2}{3}z^{3/2}}}{2\sqrt{\pi}iz^{1/4}}\displaystyle\sum_{k=0}^{\infty}(-1)^k b_k\,(3/2)^k\,z^{-3k/2} & \text{if } \mathrm{ph}(z) \in \left(-\dfrac{\pi}{3}, \pi\right) \end{cases}$$

where the discontinuity in the latter term is explained by the Stokes phenomenon. The two possibilities for the latter term are exponentially smaller than the first one in the sector $|\mathrm{ph}(z)| < \pi/3$. As the switching on happens as z crosses the positive real axis, the best choice of the latter term is to take the upper one for $\mathrm{ph}(z) < 0$ and the other for $\mathrm{ph}(z) > 0$.

2.5 Summary

We have derived the full asymptotic expansion of the Scorer function $-\mathrm{Gi}(z)$ by using the technique of exponential asymptotics. We did this by representing a particular integral of the Scorer equation in terms of the rescaled variable $\zeta = \frac{2}{3}z^{3/2}$ as the Borel-Laplace transform, (2.48), of the function $y_p(t)$. The evaluation

of the Stokes multipliers then followed from an examination of the integral and the function $y_p(t)$.

The Stokes phenomenon for the particular integral $w_p(z)$ appears in the switching on of one of the Airy functions $\mathrm{Ai}_j(z)$, $j = -1, 0, 1$ as a Stokes line is crossed in the complex z-plane. We calculated the Stokes multipliers multiplying the Airy functions $\mathrm{Ai}_0(z)$ and $\mathrm{Ai}_{-1}(z)$ that are switched on as the Stokes lines S_0 and S_{-1} are crossed, see figure 2.2. We did these calculations by comparing the two pieces of information that we gained from the singular points of the function $y_p(t)$ which appears in the Borel-Laplace transform of the particular integral.

We gain information from the singular points in two ways: firstly, by using the singular behaviour close to zero to find the asymptotic expansion of the particular integral. This gives a relation between the coefficients in the asymptotic expansion and the coefficients in the Laurent-series of $y_p(t)$ around $t = 0$. Then we used the Cauchy formula to find the late term behaviour of the coefficients in the asymptotic expansion of the particular integral in terms of the coefficients in the Laurent series of $y_p(t)$ close to the singular points $t = \pm 1$.

Secondly, we rotated the contour of integration in the Borel-Laplace transform of $y_p(t)$. The singular points $t = \pm 1$ of $y_p(t)$ in the complex t-plane introduced a restriction for how far we could rotate the contour of integration. That is, as the contour of integration crosses the real axis we get an additional contribution from a loop around the singular points. These loops represent the exponentially small terms that are being switched on as the Stokes lines are crossed. Comparison to a connection relation that exists because of the linearity of the Scorer equation gives a relation between the coefficients in the asymptotic expansion of the Airy functions and the coefficients in the Laurent series of y_p around the singular points $t = \pm 1$.

The two relations between the coefficients in the Laurent series for $y_p(t)$ close to the singular points $t = \pm 1$ give a relation between the coefficients in the asymptotic expansion of the particular integral and the asymptotic expansion of the Airy functions that are switched on. In other words, we can say that the particular integral $-\mathrm{Gi}(z)$ of the Scorer equation knows about the corresponding Airy functions but the reverse cannot be true since $-\mathrm{Gi}(z)$ is the solution of only one inhomogeneous Airy equation. As we have obtained exact expressions for both Laurent-coefficients we can evaluate the Stokes multipliers by comparison.

Looking back over our calculations, one could argue that we could have reduced our calculations significantly without any loss of information. However, the purpose of this work is to give a demonstration of the technique of exponential asymptotics, in particular the role of the Borel-Laplace transform. It is my hope

that this chapter gives an understanding of the calculations done in Chapters 3 and 5.

There are some more things to be done, such as to estimate the error and find the optimal number of terms for the asymptotic expansion of Scorer's functions. If desired, we would do this in the same manner as for the Airy function.

Chapter 3

Exponential asymptotics for Lorenz's model

3.1 Introduction

The main characteristics of the dynamics of the atmosphere and the oceans are high-energy slow balanced modes and low-energy fast modes. Among the latter are the fast time-scale gravity waves that are generated in a spontaneous manner by the slow balanced motion. In numerical weather forecasts that are based on solving primitive-equation models this generation of gravity waves is not realistic; because of erroneous initial conditions, spuriously large inertia-gravity wave amplitudes are predicted. To handle this problem, initialisation procedures were introduced that replaced the observed initial conditions by ones that eliminated the inertia-gravity wave components as much as possible. Concerned with these procedures and the existence of the so called *slow manifold*, Lorenz (1986) introduced a simple model to study the generation of gravity waves and hence to study the existence of the slow manifold. This is a system of five ordinary differential equations that is basically a truncation of the shallow-water equations.

The idea of the slow manifold is the following (MacKay, 2004). In the state space of the primitive equations there exists a lower dimensional manifold, the slow manifold, such that the full dynamics of the system remains confined to a neighbourhood of this manifold if the initial conditions lie in that neighbourhood. The balancing initialisation procedures previously mentioned can be thought of as projections from the initial conditions onto the slow manifold. Balanced models which describe an approximate dynamics entirely free of oscillations are obtained by constraining the motion to the slow manifold. In other words, the phase paths of the balanced models lie in the slow manifold.

Slow manifolds can be defined using iterative procedures that improve the slowness of the manifold order by order in a small parameter ε at each iteration.

This can not be done to an order beyond all orders because of the spontaneous generation of the fast oscillations which takes place at an exponentially small level.

In this chapter, we want to give an analytical description of the spontaneous generation of inertia-gravity waves in a simple system. Hence, we revisit Lorenz's five-component model that features this spontaneous generation in an idealised setting. The basis for our analysis is identifying the generation of fast oscillation as the Stokes phenomenon in a nonlinear setting. We then use the techniques of exponential asymptotics and derive the first two order terms in the asymptotic expansion of the fast oscillation for all five components in the model. This work extends the one done by Vanneste (2004) who derives the first order terms for the fast variables using a different method.

Our work gives a bound on how well we can define the slow manifold. That is, it implies that we can define the slow manifold to an arbitrary order of ε using the iterative procedure mentioned above, but we cannot do it to an order beyond all orders as we show that the amplitude of the inertia-gravity waves is non-zero but exponentially small.

3.2 Lorenz's five-component model

We study Lorenz's five-component model, also known as the Lorenz–Krishnamurty model (Lorenz and Krishnamurthy, 1987), which consists of

$$\begin{aligned} \dot{u} &= -vw + \varepsilon\beta vy, \\ \dot{v} &= uw - \varepsilon\beta uy, \\ \dot{w} &= -uv \end{aligned} \tag{3.1}$$

and

$$\begin{aligned} \varepsilon\dot{x} &= -y, \\ \varepsilon\dot{y} &= x + \beta uv. \end{aligned} \tag{3.2}$$

This model is a very simple nonlinear system with which the idea of fast-slow interactions can be studied. Here

$$\varepsilon = \frac{\beta R}{\sqrt{1+\beta^2}} \tag{3.3}$$

is defined in terms of the rotational Froude number β and the Rossby number R, see Vanneste (2004). In the limit $0 < \varepsilon \ll 1$, that is $\beta = O(1)$ and $0 < R \ll 1$, this model describes the slow motion with frequency $O(1)$ represented by u, v and w and its interaction with the fast inertia-gravity waves of frequency $O(1/\varepsilon)$ in the pair x and y.

As mentioned in the previous section, Lorenz's model is obtained by truncating and simplifying the shallow water equations. The functions u, v, w, x and y are composed of the coefficients accompanying the first three Fourier modes in the expressions of the velocity potential, the stream function and the height of the free surface. In the simplification process the variables u, v, w, x and y have lost an exact physical meaning, though with the restriction that all but one of the functions are set to be the constant function zero, the nonzero one corresponds to a certain pattern of the velocity field for the original model. Also, as mentioned in Chapter 1 this model is a pendulum spring model (Camassa, 1995). In this case we note that $u^2 + v^2 = R^2$ where $R \in \mathbb{R}$ is a constant. Hence, we can represent u and v with the polar coordinates $u = R\cos(\theta/2)$ and $v = R\sin(\theta/2)$. With this representation the first three equations (3.1) reduce to a pendulum equation for the angle θ. The second two equations (3.2) are a system describing a spring. However, these systems are coupled together in a way which is complicated to give a physical meaning.

We interpret the generation of the fast inertia-gravity waves as a Stokes phenomenon. Thus, we can use the tools of exponential asymptotics to derive an expression for the leading order behaviour of the exponentially small fast motion that is generated by the slow motion.

3.2.1 The Stokes phenomenon

We are revisiting the work of Vanneste (2004) with a different approach. In that paper he calculates the exponentially small terms switched on for the functions $x(t)$ and $y(t)$. His approach to evaluating these small terms is to use matched asymptotics in a neighbourhood of a singularity, t_j, of the slow motion, see Section 3.3.2. An expression for the outer expansion, assuming $|t-t_j| = O(1)$, is found by considering a dominant balance for the second two equations for $x(t)$ and $y(t)$ of Lorenz's equations. The inner expansion, assuming $|t-t_j|$ is close to zero, is found by Borel-Laplace transforming the solutions of a system obtained by rescaling the time accordingly. All of these calculations are done up to leading order and he only provides estimate of the leading order terms of the fast oscillation, that is for the functions $x(t)$ and $y(t)$.

We take these calculations further by examining the late terms in the perturbation series, (3.5) below, representing the slow motion that generates the fast oscillations in the same manner as we do in Chapter 2, with the additions that are needed because of the nonlinearity of Lorenz's model.

To explain the technique of exponential asymptotics for a general nonlinear problem, we assume that U_0 is a solution of the nonlinear problem. To determine

what can be switched on via a Stokes phenomenon we try a solution of the form

$$U_0 + CU_1$$

where C is some constant and with U_1 being exponentially small compared with U_0. However in a nonlinear problem with only one exponential scale we automatically get a trans-series expansion, that is a series of the form

$$\sum_{n=0}^{\infty} C^n U_n$$

where U_{n+1} is exponentially small compared with U_n and all the U_n, $n \geq 1$, satisfy linear equations. If there were another exponential scale the trans-series would take on more complicated from with additional cross terms arising from products.

The Stokes phenomenon appears in such a way that when a Stokes line is crossed, a function in the trans-series switches on the function next to it. The Stokes line and the anti-Stokes lines are defined as in the linear case; they occur when the difference of the exponents is purely real or purely imaginary respectively. In general, with the notation above, the Stokes phenomenon is the discontinuous change of the constant C to $C + K$ when a Stokes line is crossed.

In this setting, the technique for finding the Stokes multipliers is no different to the linear case; we find them by exploring the nature of the late terms in the asymptotic expansion of the function that switches on the exponentially small terms.

The first function in the series has the largest magnitude. Hence, to find the leading behaviour of the solution we look at the asymptotic behaviour of the first function and how it switches on the exponentially small second term in the trans-series. Notably, the function U_1 is a solution of a homogeneous equation. IIence, the constant C is a free variable.

To return to our analysis of Lorenz's model, the balanced solution, that is the first function in the trans-series (3.28) below, is represented by a general perturbation series (3.5) below; in other words we re-expand the first functions in the trans-series. As in Chapter 2, the value of the Stokes multipliers can be derived through a resurgence relation of the late coefficients in the perturbation series. We establish this relation and the value of the Stokes multipliers by comparison to the singular behaviour of the coefficients. In our derivation we proceed as follows. We start by establishing the series expansion of the balanced motion. Then we examine the singular nature of the coefficients in this expansion, we establish a resurgence relation for the late coefficients and find the values of the Stokes multipliers. Finally, we derive an expression for the leading order terms of the exponentially small terms that are switched on as a Stokes line is crossed.

Let us start with a derivation of a perturbation series that represents the slow balanced motion.

3.3 A slow balanced solution

Let us consider the equations (3.1) in the case $\varepsilon = 0$. Then the triplet (u,v,w) becomes independent of the pair (x,y) and an exact solution of the system can be found. One set of solutions is

$$\begin{array}{lll} u_0(t) &= \operatorname{sech} t, & \\ v_0(t) &= -\tanh t, & x_0(t) = -\beta u_0(t) v_0(t), \\ w_0(t) &= -\operatorname{sech} t, & y_0(t) = 0 \end{array} \tag{3.4}$$

found by considering the initial condition that $u_0(t) = w_0(t) = 0$ and $v_0(t) = 1$ as $t \to -\infty$. These solutions where previously considered by Lorenz and Krishnamurthy (1987) who examined a forced-dissipative version of Lorenz's model. These solutions are obviously free of fast oscillations and hence truly represent the slow motion for $\varepsilon = 0$. For $\varepsilon \neq 0$, slow, balanced solutions can be represented by their perturbation series

$$u_b(t) = \sum_{n=0}^{\infty} u_n(t)\varepsilon^n, \quad \ldots \quad , y_b(t) = \sum_{n=0}^{\infty} y_n(t)\varepsilon^n. \tag{3.5}$$

We find the coefficients in the series (3.5) by substituting into (3.1) and (3.2). This gives

$$\begin{array}{lll} \dot{u}_0 &= -v_0 w_0, & \dot{x}_0 = -\beta u_0 v_0, \\ \dot{v}_0 &= u_0 w_0, & \dot{y}_0 = 0, \\ \dot{w}_0 &= -u_0 v_0, & \end{array} \tag{3.6}$$

and for $n > 0$ the recurrence relation

$$\begin{aligned} \dot{u}_n + v_0 w_n + v_n w_0 &= -\sum_{k=1}^{n-1} v_k [w_{n-k} - \beta y_{n-1-k}] + \beta v_0 y_{n-1}, \\ \dot{v}_n - u_0 w_n - u_n w_0 &= \sum_{k=1}^{n-1} u_k [w_{n-k} - \beta y_{n-1-k}] - \beta u_0 y_{n-1}, \\ \dot{w}_n + u_0 v_n + u_n v_0 &= -\sum_{k=1}^{n-1} u_k v_{n-k}, \\ x_n &= -\ddot{x}_{n-2} - \beta \sum_{k=0}^{n} u_k v_{n-k}, \\ y_n &= -\dot{x}_{n-1} \end{aligned} \tag{3.7}$$

where we define $x_{-1} = 0$.

We consider slow solutions of (3.6)–(3.7) that reduce to (3.4) as $\varepsilon = 0$, that is, we take

$$\begin{array}{lll} u_0(t) &= \operatorname{sech} t, & x_0(t) = \beta \sinh t / \cosh^2 t, \\ v_0(t) &= -\tanh t, & y_0(t) = 0. \\ w_0(t) &= -\operatorname{sech} t, & \end{array} \tag{3.8}$$

It follows directly from this and (3.7) that

$$y_1(t) = \frac{\beta(\cosh^2 t - 2)}{\cosh^3 t}$$

and that in general the symmetries

$$\begin{array}{ll} u_b(-t) = u_b(t), & x_b(-t) = -x_b(t), \\ v_b(-t) = -v_b(t), & y_b(-t) = y_b(t), \\ w_b(-t) = w_b(t) & \end{array} \tag{3.9}$$

hold.

Our derivation of the asymptotic behaviour of the fast oscillation generated by the balanced solutions (3.5) depends on the large-n behaviour of the coefficients in (3.5). Hence, we need to calculate more terms.

Since $y_0 = 0$ we get for all n that the coefficients u_{2n+1}, v_{2n+1}, w_{2n+1}, x_{2n+1} and y_{2n} solve the homogeneous part of (3.7). Because of the symmetries (3.9) these coefficients are all zero. Finding the values of the other coefficients for $n > 0$ is difficult, and general expressions do not seem to exist. For a fixed value of n, the equations for the nth coefficients in the expansion (3.5) for $u_b(t)$, $v_b(t)$ and $w_b(t)$ decouple from the equations for the nth coefficient in the expansion of $x_b(t)$ and coefficient number $(n+1)$ in the expansion of $y_b(t)$. Hence, for a fixed n even, we only need to solve the part of (3.7) for $u_n(t)$, $v_n(t)$ and $w_n(t)$. The values of $x_n(t)$ and $y_{n+1}(t)$ then follow. Let us give a procedure to solve the recurrence (3.7) for $u_n(t)$, $v_n(t)$ and $w_n(t)$ for n even.

3.3.1 Procedure to calculate the coefficients in the perturbation series

We can write the first three equations in (3.7) as

$$\begin{aligned} \dot{\bar{u}}_n = \begin{bmatrix} \dot{u}_n \\ \dot{v}_n \\ \dot{w}_n \end{bmatrix} &= \begin{bmatrix} 0 & -w_0 & -v_0 \\ w_0 & 0 & u_0 \\ -v_0 & -u_0 & 0 \end{bmatrix} \begin{bmatrix} u_n \\ v_n \\ w_n \end{bmatrix} + \bar{h} \\ &= B\bar{u}_n + \bar{h} \end{aligned}$$

where $\bar{h}$ is the right hand side of the relevant equations in (3.7). We solve this in the following way. Let A be a matrix solution of the homogeneous system. It

satisfies $\dot{A} = BA$ and $\det(A) \neq 0$. A can be verified to be the matrix

$$A = \begin{bmatrix} \frac{\sinh t}{\cosh^2 t} & \cosh t & \frac{t\sinh t - \cosh t}{\cosh^2 t} \\ \frac{1}{\cosh^2 t} & 0 & \frac{\cosh t}{\sinh t} + \frac{(t\sinh t - \cosh t)}{\cosh^2 t \sinh t} \\ -\frac{\sinh t}{\cosh^2 t} & \cosh t & -\frac{(t\sinh t - \cosh t)}{\cosh^2 t} \end{bmatrix}.$$

Let

$$\bar{u}_n = A\bar{\alpha}$$

where $\bar{\alpha}$ is some vector. Then

$$\dot{\bar{u}}_n = \dot{A}\bar{\alpha} + A\dot{\bar{\alpha}} = BA\bar{\alpha} + \bar{h}.$$

It follows that

$$A\dot{\bar{\alpha}} = \bar{h},$$

and hence

$$\dot{\bar{\alpha}} = A^{-1}\bar{h}$$

where

$$A^{-1} = \begin{bmatrix} \frac{t+\cosh t \sinh t}{2\cosh t} & -\frac{(t\sinh t - \cosh t)}{\cosh t} & -\frac{(t+\cosh t \sinh t)}{2\cosh t} \\ \frac{1}{2\cosh t} & 0 & \frac{1}{2\cosh t} \\ -\frac{1}{2\cosh t} & \frac{\sinh t}{\cosh t} & \frac{1}{2\cosh t} \end{bmatrix}.$$

We then find the elements of the vector $\bar{\alpha}$ by integration and hence the elements of $\bar{u}_n$, and finally the coefficients $x_n(t)$ and $y_{n+1}(t)$.

Using this method we were able to calculate the coefficients successfully up to $n = 4$ using MAPLE. In principle, we can find as many coefficients as we need by using this procedure.

3.3.2 Singular nature of the coefficients

To be able to calculate the asymptotic behaviour of the exponentially small terms switched on, we need to know the singular behaviour of the balanced solutions (3.5) of Lorenz's equations (3.1). The first nonzero coefficients in the perturbation series (3.5) imply that the functions $u_b(t)$, $v_b(t)$, $w_b(t)$, $x_b(t)$ and $y_b(t)$ are all singular at the points $t = i(\pi/2 + k\pi)$ for all $k \in \mathbb{Z}$. The contribution from the singular points closest to the real axis, $t = \pm i\pi/2$, dominates the asymptotic behaviour for real t.

The singular points $t_j = (-1)^j \pi i/2$, $j = 0, 1$, are poles of order one for the triplet $(u_b(t), v_b(t), w_b(t))$ and poles of order two for the pair $(x_b(t), y_b(t))$. Thus, in a neighbourhood of the singular points t_j we represent the nth coefficient in

(3.5) with its Laurent series:

$$\begin{aligned} u_n(t) &= a_{n,0}(t-t_j)^{-(n+1)} + a_{n,1}(t-t_j)^{-n} + \dots , \\ v_n(t) &= b_{n,0}(t-t_j)^{-(n+1)} + b_{n,1}(t-t_j)^{-n} + \dots , \\ w_n(t) &= c_{n,0}(t-t_j)^{-(n+1)} + c_{n,1}(t-t_j)^{-n} + \dots , \\ x_n(t) &= d_{n,0}(t-t_j)^{-(n+2)} + d_{n,1}(t-t_j)^{-(n+1)} + \dots , \\ y_n(t) &= e_{n,0}(t-t_j)^{-(n+2)} + e_{n,1}(t-t_j)^{-(n+1)} + \dots . \end{aligned} \tag{3.10}$$

We obtain recurrence relations for the coefficients in the Laurent series by inserting (3.10) into (3.7). This gives that the ith coefficients in the Laurent series for the nth coefficient in the perturbation series can be found by solving

$$\begin{aligned} &(n+1-i)\, a_{n,i} - \sum_{j=0}^{i} b_{0,j} c_{n,i-j} - \sum_{j=0}^{i} b_{n,j} c_{0,i-j} = \\ &\qquad \sum_{k=1}^{n-1} \sum_{j=0}^{i} b_{k,j} \left(c_{n-k,i-j} - \beta e_{n-1-k,i-j} \right) - \beta \sum_{j=0}^{i} b_{0,j} e_{n-1,i-j}, \\ &(n+1-i)\, b_{n,i} + \sum_{j=0}^{i} a_{0,j} c_{n,i-j} + \sum_{j=0}^{i} a_{n,j} c_{0,i-j} = \\ &\qquad - \sum_{k=1}^{n-1} \sum_{j=0}^{i} a_{k,j} \left(c_{n-k,i-j} - \beta e_{n-1-k,i-j} \right) + \beta \sum_{j=0}^{i} a_{0,j} e_{n-1,i-j}, \\ &(n+1-i)\, c_{n,i} - \sum_{j=0}^{i} a_{0,j} b_{n,i-j} - \sum_{j=0}^{i} a_{n,j} b_{0,i-j} = \sum_{k=1}^{n-1} \sum_{j=0}^{i} a_{k,j} b_{n-k,i-j} \end{aligned} \tag{3.11}$$

and

$$\begin{aligned} d_{n,i} &= -(n-i)(n+1-i)\, d_{n-2,i} - \beta \sum_{k=0}^{n} \sum_{j=0}^{i} a_{k,j} b_{n-k,i-j}, \\ e_{n,i} &= (n+1-i)\, d_{n-1,i}. \end{aligned} \tag{3.12}$$

Here we define $d_{-2,n}$ and $d_{-1,n}$ to be zero for $n = 0, 1, 2, \dots$. The first coefficients (3.8) in the perturbation series (3.5) give us initial conditions for these recurrence relations. We solve them numerically to find the large-n behaviour of the late coefficients in the expansions (3.5).

We know that the solution of (3.1) is real so the contribution from t_1 must be the complex conjugate of the contribution from t_0. Therefore we need only solve the recurrence for $t = t_0$. Similarily to the nth coefficient in the perturbation series (3.5), the nth coefficients in the Laurent series for the pair $(x_n(t), y_n(t))$ can be deduced from the nth coefficients in the Laurent series for the triplet $(u_n(t), v_n(t), w_n(t))$. Hence we only need initial conditions for the latter ones.

We use coefficients number $n = 0$ and $n = 2$ in the series (3.5) calculated with the technique described in Section 3.3.1 to provide initial conditions to solve the

recurrence relations (3.11). These initial conditions are

$$\begin{array}{llll} a_{0,0}=-i, & a_{0,1}=0, & a_{2,1}=-\beta^2\pi/4, & a_{0,2}=i/6, \\ b_{0,0}=-1, & b_{0,1}=0, & b_{2,1}=\beta^2 i\pi/4, & b_{0,2}=-i/3, \\ c_{0,0}=i, & c_{0,1}=0, & c_{2,1}=\beta^2\pi/4, & c_{0,2}=-i/6. \end{array} \tag{3.13}$$

We note that these initial conditions for the recurrence relations (3.11) have the interesting properties

$$a_{n,k} = ib_{n,k}, \qquad k = 0, 1 \tag{3.14}$$

for all $n \geq 0$ and

$$\begin{aligned} a_{n+2,1} &= -\frac{i\pi(n+1)\beta^2}{4} a_{n,0}, \\ b_{n+2,1} &= -\frac{i\pi(n+1)\beta^2}{4} b_{n,0}, \\ c_{n+2,1} &= -\frac{i\pi(n+1)\beta^2}{4} c_{n,0}, \\ d_{n+2,1} &= -\frac{i\pi(n+2)\beta^2}{4} d_{n,0}, \\ e_{n+2,1} &= -\frac{i\pi(n+2)\beta^2}{4} e_{n,0} \end{aligned} \tag{3.15}$$

for all $n \geq 0$. This can be proved by insertion into the relation (3.11). There is no evidence that analogous relations hold for $j > 1$.

With this knowledge of the singular behaviour of the coefficients in the perturbation series for a slow solution of Lorenz's equations, we can establish an asymptotic expansion of the late coefficients in the same series.

3.3.3 Late term behaviour

To evaluate the Stokes multipliers we need to know the large-n asymptotic behaviour of the coefficients in the perturbation series (3.5). We consider a simple ansatz for the late coefficients. There turns out to be a connection between the components of the ansatz for the x_n coefficient and the ansatz for the others coefficients such that the late-term behaviour of the $u_n(t)$, $v_n(t)$, $w_n(t)$ and $y_n(t)$ follows from the late behaviour of the x_n-coefficients. Let us establish this.

We find the late term behaviour of the x_n-coefficients by inserting the ansatz

$$x_n(t) \sim \frac{g_x(t)\Gamma(n+\alpha)}{(-f(t))^{n+\alpha}} \tag{3.16}$$

into the relevant recurrence relation in (3.7). Observing the dominant large-n terms

$$\frac{g_x(t)\Gamma(n+\alpha)}{(-f(t))^{n+\alpha}} = -\frac{g_x(t)(f'(t))^2}{(-f(t))^{n+\alpha}}\Gamma(n+\alpha)$$

implies that

$$(f'(t))^2 = -1 \text{ or } f(t) = \pm it + C_\pm, \tag{3.17}$$

where $C_\pm$ are two constants, one for each sign of $f'(t)$. In a neighbourhood of the dominant singularities t_j, $j = 0, 1$, (3.16) and (3.10) are comparable in size. Hence, the comparison gives $\alpha = 2$ and $C_\pm = \mp it_j$. We note that there are four choices here, two for plus and minus and further two for the choice of the singular points t_j. It is worth mentioning that the ability to determine the Stokes multipliers using a factorial-over-power ansatz depends on the distribution of the singularities in the Borel plane and in some cases it is necessary to use hyperasyptotic procedures, see Section **??**.

We find the late-term behaviour of the other coefficients in terms of the functions $f(t)$ and $g_x(t)$. The equation for the y_n-coefficients in (3.7) obviously gives that

$$\begin{aligned} y_n(t) &\sim -\frac{g_x(t)f'(t)\Gamma(n+2)}{(-f(t))^{n+2}} \\ &\sim \frac{g_y(t)\Gamma(n+2)}{(-f(t))^{n+2}}, \end{aligned}$$

where

$$g_y(t) = -g_x(t)f'(t). \tag{3.18}$$

Similarly if we assume that

$$u_n(t) \sim \frac{g_u(t)\Gamma(n)}{(-f(t))^n} \text{ and } v_n(t) \sim \frac{g_v(t)\Gamma(n)}{(-f(t))^n}$$

insertion into (3.7) gives

$$\begin{aligned} g_u(t) &= -\beta v_0 g_x(t), \\ g_v(t) &= \beta u_0 g_x(t). \end{aligned} \tag{3.19}$$

Finally, we assume that

$$w_n(t) \sim \frac{g_w(t)\Gamma(n-1)}{(-f(t))^{n-1}}$$

to find

$$g_w(t)f'(t) = -\beta[u_0^2 - v_0^2]g_x(t). \tag{3.20}$$

These relations are the leading-order terms in the large-n asymptotic expansions of the perturbation coefficients. That is, we have found relations between

the first terms in expansions of the form

$$
\begin{aligned}
u_n(t) &\sim \frac{1}{2\pi i}\sum_{j=0}^{1}\sum_{k=0}^{1}\sum_{s=0}^{\infty}\frac{g_{u,j,k,s}(t)\Gamma(n-s)}{(-f_{jk}(t))^{n-s}},\\
v_n(t) &\sim \frac{1}{2\pi i}\sum_{j=0}^{1}\sum_{k=0}^{1}\sum_{s=0}^{\infty}\frac{g_{v,j,k,s}(t)\Gamma(n-s)}{(-f_{jk}(t))^{n-s}},\\
w_n(t) &\sim \frac{1}{2\pi i}\sum_{j=0}^{1}\sum_{k=0}^{1}\sum_{s=0}^{\infty}\frac{g_{w,j,k,s}(t)\Gamma(n-s-1)}{(-f_{jk}(t))^{n-s-1}},\\
x_n(t) &\sim \frac{1}{2\pi i}\sum_{j=0}^{1}\sum_{k=0}^{1}\sum_{s=0}^{\infty}\frac{g_{x,j,k,s}(t)\Gamma(n-s+2)}{(-f_{jk}(t))^{n-s+2}},\\
y_n(t) &\sim \frac{1}{2\pi i}\sum_{j=0}^{1}\sum_{k=0}^{1}\sum_{s=0}^{\infty}\frac{g_{y,j,k,s}(t)\Gamma(n-s+2)}{(-f_{jk}(t))^{n-s+2}}.
\end{aligned}
\tag{3.21}
$$

as $n \in \mathbb{N}$ tends to infinity. We introduce the factor $(2\pi i)^{-1}$ in line with standard notation; it does not affect the relation we have established between the first g-coefficients. Here we have defined

$$
f_{jk}(t) = i(-1)^k(t - t_j), \qquad j = 0, 1, \quad k = 0, 1. \tag{3.22}
$$

These functions satisfy the relation $f_{j1}(t) = -f_{j0}(t)$, and they come in pairs of complex conjugates for real values of t, that is

$$
f_{00}(t) = \bar{f}_{11}(t) \quad \text{and} \quad f_{01}(t) = \bar{f}_{10}(t)
$$

for $t \in \mathbb{R}$.

We note that for $s > n$, the point $n - s$ is a singular point of the function $\Gamma(n-s)$ in the first expansion in 3.21. A rigorous way to represent this would be to write

$$
u_n(t) = \frac{1}{2\pi i}\sum_{j=0}^{1}\sum_{k=0}^{1}\sum_{s=0}^{S}\frac{g_{u,j,k,s}(t)\Gamma(n-s)}{(-f_{jk}(t))^{n-s}} + \Gamma(n)O(n^{-S})
$$

where $S < n$. As the expansion is an asymptotic series, meaning that we would always only use a few of the first terms to approximate the function on the left hand side we choose to ignore these singularities and use the notation above. Similar argument hold for v, w, x and y and the same is relevant to the asymptotic expansions in next paragraph.

Using the functional relations $f_{j1}(t) = -f_{j0}(t)$ we can simplify (3.21) to

$$u_n(t) \sim \frac{1}{2\pi i} \sum_{j=0}^{1} \sum_{s=0}^{\infty} \left[\frac{g_{u,j,1,s}(t) + (-1)^{n-s} g_{u,j,0,s}(t)}{(-f_{j1}(t))^{n-s}} \right] \Gamma(n-s),$$

$$v_n(t) \sim \frac{1}{2\pi i} \sum_{j=0}^{1} \sum_{s=0}^{\infty} \left[\frac{g_{v,j,1,s}(t) + (-1)^{n-s} g_{v,j,0,s}(t)}{(-f_{j1}(t))^{n-s}} \right] \Gamma(n-s),$$

$$w_n(t) \sim \frac{1}{2\pi i} \sum_{j=0}^{1} \sum_{s=0}^{\infty} \left[\frac{g_{w,j,1,s}(t) + (-1)^{n-s-1} g_{w,j,0,s}(t)}{(-f_{j1}(t))^{n-s-1}} \right] \Gamma(n-s-1),$$

$$x_n(t) \sim \frac{1}{2\pi i} \sum_{j=0}^{1} \sum_{s=0}^{\infty} \left[\frac{g_{x,j,1,s}(t) + (-1)^{n-s+2} g_{x,j,0,s}(t)}{(-f_{j1}(t))^{n-s+2}} \right] \Gamma(n-s+2),$$

$$y_n(t) \sim \frac{1}{2\pi i} \sum_{j=0}^{1} \sum_{s=0}^{\infty} \left[\frac{g_{y,j,1,s}(t) + (-1)^{n-s+2} g_{y,j,0,s}(t)}{(-f_{j1}(t))^{n-s+2}} \right] \Gamma(n-s+2).$$

Because every odd coefficient in the perturbation series (3.5) for $u_b(t)$, $v_b(t)$, $w_b(t)$ and $x_b(t)$ is zero and every even term in the perturbation series for $y_b(t)$ is zero the terms in these asymptotic expansions have to cancel each other completely. This fact provides the very useful coefficient relations

$$\begin{aligned} g_{u,j,1,s}(t) &= (-1)^s g_{u,j,0,s}(t), \\ g_{v,j,1,s}(t) &= (-1)^s g_{v,j,0,s}(t), \\ g_{w,j,1,s}(t) &= (-1)^{s+1} g_{w,j,0,s}(t), \\ g_{x,j,1,s}(t) &= (-1)^s g_{x,j,0,s}(t), \\ g_{y,j,1,s}(t) &= (-1)^s g_{y,j,0,s}(t) \end{aligned} \tag{3.23}$$

for $j = 0, 1$.

Let us now find expressions for the g-coefficients.

3.3.3.1 Expressions for g-coefficients

To evaluate the g_x-coefficients and the other g-coefficients we derive a recurrence relation by substituting the full ansatz (3.21) into (3.7). For our analysis we only need the first two g-coefficients, hence in this section we concentrate on finding their values. The full recurrence relation is given in Appendix A.

For fixed j and k the main relations are

$$\begin{aligned} g'_{x,j,k,0}(t) &= 0, \\ g'_{x,j,k,1}(t) f'_{jk}(t) &= -\tfrac{\beta^2}{2}(u_0^2(t) - v_0^2(t)) g_{x,j,k,0}(t), \\ 2g'_{x,j,k,2}(t) f'_{jk}(t) &= -g''_{x,j,k,1}(t) - \beta^2(u_0^2(t) - v_0^2(t)) g_{x,j,k,1}(t), \end{aligned}$$

implying that $g_{x,j,k,0}(t)$ are constants, say C_{jk0}, in terms of t, and that $g_{x,j,k,1}(t)$ and $g_{x,j,k,2}(t)$ are the non-constant functions

$$\begin{aligned} g_{x,j,k,1}(t) &= \frac{(-1)^k i\beta^2 g_{x,j,k,0}}{2}\int \frac{(1-\sinh^2 t)}{\cosh^2 t}dt \\ &= \frac{(-1)^k i\beta^2 C_{jk0}}{2}(2\tanh t - t) + C_{jk1}, \quad \text{and} \\ g_{x,j,k,2}(t) &= -\frac{\beta^2 C_{jk0}}{2}\left[\frac{-\beta^2 t\sinh t\cosh t + (1-\beta^2)}{\cosh^2 t} + \frac{\beta^2 t^2}{4}\right] \\ &\quad +(-1)^{k+1} i\beta^2\left[-\tanh t + \frac{(t+2)}{2}\right] C_{jk1} + C_{jk2} \end{aligned} \tag{3.24}$$

where C_{jk1} and C_{jk2} are constants of integration. Note that $g_{x,j,k,1}(t)$ and $g_{x,j,k,2}(t)$ are singular at the points $t = i(\pi/2 + k\pi)$, $k \in \mathbb{Z}$, and so is $x_b(t)$.

The g-coefficients of the first terms in the expansion of $u_n(t)$, $v_n(t)$, $w_n(t)$ and $y_n(t)$ are related to $g_{k,j,l,0}$ as given in (3.18)–(3.20)

$$\begin{aligned} g_{u,j,k,0}(t) &= -\beta v_0(t) g_{x,j,k,0}, \\ g_{v,j,k,0}(t) &= \beta u_0(t) g_{x,j,k,0}, \\ f'_{kj}(t) g_{w,j,k,0}(t) &= -\beta(u_0^2(t) - v_0^2(t)) g_{x,j,k,0}, \\ g_{y,j,k,0}(t) &= -f'_{jk}(t) g_{x,j,k,0}. \end{aligned}$$

For the second terms, we find

$$\begin{aligned} g_{u,j,k,1}(t) &= -\beta v_0(t) g_{x,j,k,1}(t), \\ g_{v,j,k,1}(t) &= \beta u_0(t) g_{x,j,k,1}(t), \\ f'_{kj}(t) g_{w,j,k,1}(t) &= 2\beta(u'_0(t)u_0(t) - v'_0(t)v_0(t)) g_{x,j,k,0} - \beta(u_0^2(t) - v_0^2(t)) g_{x,j,k,1}(t), \\ g_{y,j,k,1}(t) &= -f'_{jk}(t) g_{x,j,k,1}(t). \end{aligned}$$

As the derivatives of the f_{jk} functions are constants, it follows from this that $g_{y,j,k,0}(t)$ is also a constant, whereas the zero terms corresponding to the u, v and w-functions are non constant functions of t which are singular at the points $t = i(\pi/2 + k\pi)$, $k \in \mathbb{Z}$. The functions $u_b(t)$, $v_b(t)$, $w_b(t)$ and $y_b(t)$ are also singular at these points.

3.3.3.2 Constants of integration in the g-coefficients

We find the constants of integration in (3.24) by comparing the coefficients in the Laurent series around the singular points t_j and the resurgence relation (3.21).

Observing the solutions of (3.12) for large n with the initial conditions (3.13), we find for n even that

$$\begin{aligned} d_{n,0} &\sim -i^{(n+1)}\Gamma(n+2)\kappa_0, \\ d_{n,1} &\sim \frac{i^n \pi}{4}\Gamma(n+1)\kappa_1 \end{aligned} \tag{3.25}$$

where κ_0 and κ_1 are real constants defined as the limits

$$\kappa_0 = \lim_{n\to\infty} \frac{i^{(n+1)}(-1)^n d_{n,0}}{\Gamma(n+2)} = \lim_{n\to\infty} \frac{i^{(n+1)} d_{n,0}}{\Gamma(n+2)},$$
$$\kappa_1 = \lim_{n\to\infty} \frac{4i^n(-1)^n d_{n,1}}{\pi\Gamma(n+1)} = \lim_{n\to\infty} \frac{4i^n d_{n,1}}{\pi\Gamma(n+1)}.$$

The factor $\pi/4$ is introduced for convenience. Then the d-relation in (3.15) gives that $\kappa_1 = \beta^2\kappa_0$. We confirm this numerically, see figure 3.1 which displays κ_0 and κ_1 as a function of β. Note, that because of this relation between the limits they

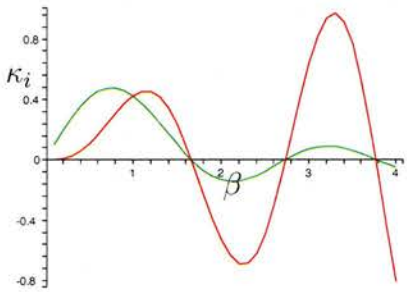

Figure 3.1: The value of κ_i, $i = 0, 1$, as a function of β. The green graph is κ_0 and the red one is κ_1. We know that $\kappa_1 = \beta^2\kappa_0$, hence κ_0 and κ_1 have the same zeros as functions of β.

both vanish for same values of β. We will see in Section 3.3.4 that the κ-constants are the Stokes multipliers.

In the numerical evaluation of κ_0 and κ_1 we use Richardson type extrapolation as Vanneste (2004) to speed up the convergence. Specifically, we let

$$\kappa_{n,0} = \frac{i^{(n+1)} d_{n,0}}{\Gamma(n+2)},$$
$$\kappa_{n,1} = \frac{4i^n d_{n,1}}{\pi\Gamma(n+1)}$$

and we assume for $i = 0, 1$ that

$$\kappa_{n,i} = \kappa_i + \frac{l_{1i}}{n} + \frac{l_{2i}}{n^2} + \ldots$$

for some real coefficients l_{si} where i and s are positive integers. Then we use that

$$n\kappa_{n,i} - (n-1)\kappa_{(n-1),i} = \kappa_i + O\left(\frac{1}{n^2}\right).$$

The following tables show the rate of convergence for κ_0 and κ_1 for a few values of β. The tables indicate the number n of iterations, the values of β and the numerical estimates for κ_0 and κ_1 respectively.

κ_0						
β	0.25	0.5	0.75	1.	1.5	2.
$n=4$	0.23727	0.40495	0.46765	0.45833	0.90234	4.66667
$n=6$	0.23757	0.40619	0.46231	0.40056	-0.02039	-1.66222
$n=8$	0.23768	0.40680	0.46349	0.40344	0.10151	0.15182
$n=10$	0.23772	0.40708	0.46421	0.40443	0.09369	-0.13329
$n=12$	0.23774	0.40726	0.46467	0.40521	0.09455	-0.10779
$n=16$	0.23775	0.40737	0.46500	0.40577	0.09492	-0.11089
$n=18$	0.23777	0.40751	0.46522	0.40616	0.09527	-0.11182
$n=20$	0.23778	0.40747	0.46540	0.40644	0.09563	-0.11258

κ_1						
β	0.25	0.5	0.75	1.	1.5	2.
$n=4$	0.0087348	0.048191	0.040666	-0.30843	-4.94441	-24.6740
$n=6$	0.0090837	0.060776	0.15400	0.27416	1.75658	16.9976
$n=8$	0.0091305	0.061848	0.15582	0.23390	-0.096341	-5.26378
$n=10$	0.0091471	0.062278	0.15815	0.24130	0.13391	0.57233
$n=12$	0.0091536	0.062484	0.15934	0.24453	0.12355	-0.31429
$n=16$	0.0091583	0.062599	0.16003	0.24650	0.12683	-0.24657
$n=18$	0.0091612	0.062671	0.16044	0.24775	0.12845	-0.26002
$n=20$	0.0091628	0.062710	0.16074	0.24858	0.12979	-0.26559

For large n and t close to t_0 we can compare (3.10) and (3.21) in size to determine the values of the constants of integration in the g-coefficients. For t in a neighbourhood of t_0, the terms including the functions $f_{00}(t)$ and $f_{01}(t)$ in the expansions (3.21) dominate the large-n behaviour of the late coefficients. Hence we want to compare $d_{n,0}$ to the constants multiplying $(t-t_0)^{-(n+2)}$ in

$$\frac{1}{2\pi i}\sum_{k=0}^{1}\sum_{s=0}^{\infty}\frac{g_{x,0,k,s}(t)}{(-f_{0k}(t))^{(n-s+2)}}\Gamma(n-s+2)$$

and we want to compare $d_{n,1}$ to the constants multiplying $(t-t_0)^{-(n+1)}$ in the same expression. We know that the f_{0k}-functions are multiples of $(t-t_0)$ so it is clear that we want to compare the constant coefficients $g_{x,0,k,0}=C_{0k0}$ to $d_{n,0}$. It is not so clear what to compare to $d_{n,1}$. Thus let us look at the Laurent series of the coefficients $g_{x,0,k,1}(t)/(-f_{0k}(t))^{(n+1)}$ close to the singular point $t=t_0$. We assume that n is even because otherwise the d-coefficients are zero.

For t in a neighbourhood of t_0 we have

$$\begin{aligned}\frac{g_{x,0,k,1}(t)}{(-f_{0k}(t))^{(n+1)}} &= \frac{g_{x,0,k,1}(t)}{((-1)^{k+1}i(t-t_0))^{(n+1)}}\\ &= \frac{(-1)^{k+1}}{i^{(n+1)}}\left[i\beta^2(-1)^kC_{0k0}(t-t_0)^{-(n+2)}\right.\\ &\qquad\left.+\left(C_{0k1}+\frac{\pi\beta^2(-1)^kC_{0k0}}{4}\right)(t-t_0)^{-(n+1)}+\dots\right].\end{aligned}$$

The first coefficient in this series contributes to the value of $d_{n,0}$ implying that the d-coefficients are functions of n and thus can be represented by their large-n expansion. We expand the coefficient $g_{x,0,k,2}(t)$ to gain more information of the value of $d_{n,1}$. For t close to t_0 we have

$$\begin{aligned}\frac{g_{x,0,k,2}(t)}{(-f_{0k}(t))^n} &= \frac{g_{x,0,k,2}(t)}{((-1)^{k+1}i(t-t_0))^n} \\ &= \frac{\beta^2}{i^n}\left[\frac{(1-\beta^2)C_{0k0}}{2}(t-t_0)^{-(n+2)}\right. \\ &\qquad \left. + \left((-1)^k C_{0k1} + \frac{i\beta^2\pi C_{0k0}}{4}\right)(t-t_0)^{-(n+1)} + \dots\right].\end{aligned}$$

Hence using the coefficient relation

$$\begin{aligned} g_{x,0,1,0}(t) &= g_{x,0,0,0}(t), \\ g_{x,0,1,1}(t) &= -g_{x,0,0,1}(t) \end{aligned}$$

from (3.23) we obtain the first terms in the large-n expansions

$$d_{n,0} = \frac{\Gamma(n+2)}{i^{(n+2)}}\frac{C_{000}}{\pi i}\left(1 + \frac{\beta^2}{(n+1)} - \frac{(1-\beta^2)}{2(n+1)n} + \dots\right)$$

and

$$d_{n,1} = \frac{\Gamma(n+1)}{i^{(n+1)}}\frac{1}{\pi i}\left(-\left(C_{001} + \frac{\pi\beta^2 C_{000}}{4}\right) + \frac{i\beta^2\left(C_{001} + \frac{i\beta^2\pi C_{000}}{4}\right)}{n} + \dots\right).$$

We can now calculate the value of the first two constants of integration by comparing the large-n expansions of $d_{n,0}$ and $d_{n,1}$ to their large-n behaviour (3.25). This comparison, the relation $\kappa_1 = \beta^2\kappa_0$ and the relation (3.23) give

$$\begin{aligned} C_{000} &= C_{010} = -\pi\kappa_0 \\ C_{001} &= -C_{011} = \frac{\pi^2}{2}\kappa_1. \end{aligned}$$

We will see in the next section that we only need information on the coefficients $g_{x,0,1,s}(t)$ and $g_{x,1,0,s}(t)$ to be able to find an expression for the leading order behaviour of the exponentially small terms being switched on. We note that with our knowledge of the constants of integration it follows from this that

$$g_{x,0,k,1}(t) = \frac{(-1)^k\pi}{2}\left(-i(2\tanh t - t) + \pi\right)\kappa_1 \quad k = 0, 1.$$

Hence

$$\begin{aligned} g_{u,0,k,0}(t) &= -\pi\kappa_0\beta\tanh t, \\ g_{v,0,k,0}(t) &= -\pi\kappa_0\beta\,\mathrm{sech}\,t, \\ g_{w,0,k,0}(t) &= (-1)^{k+1}i\pi\kappa_0\beta\left(\frac{1-\sinh^2 t}{\cosh^2 t}\right), \\ g_{y,0,k,0}(t) &= (-1)^k i\pi\kappa_0 \end{aligned} \tag{3.26}$$

and

$$
\begin{aligned}
g_{u,0,k,1}(t) &= \frac{(-1)^k \beta\pi \tanh t}{2} \left(-i(2\tanh t - t) + \pi\right) \kappa_1 \\
g_{v,0,k,1}(t) &= \frac{(-1)^k \beta\pi}{2\cosh t} \left(-i(2\tanh t - t) + \pi\right) \kappa_1 \\
g_{w,0,k,1}(t) &= i\pi \left[\frac{4(-1)^{k+1}}{\beta} \frac{\sinh t}{\cosh^3 t} + \frac{\beta}{2} \left(\frac{1-\sinh^2 t}{\cosh^2 t}\right) \left(-i(2\tanh t - t) + \pi\right)\right] \kappa_1 \\
g_{y,0,k,1}(t) &= -\frac{\pi i}{2} \left(-i(2\tanh t - t) + \pi\right) \kappa_1
\end{aligned}
\tag{3.27}
$$

We note that κ_0 and κ_1 are the Stokes multipliers. As mentioned above, κ_0 and κ_1 vanish for the same values of β, see figure 3.1. Therefore the large-n asymptotic behavior for $d_{n,i}$, $i = 0, 1$, given by (3.25) does not hold at all, or at least not up to leading order for all values of β. For the latter case, it is difficult to say which is the first nonzero g-coefficient in the expansion of the late-term expansions (3.21). These zeros of the coefficients in the expansion of the Stokes multipliers will not be discussed any further here.

Let us now find the asymptotic behaviour of the exponentially small terms that are switched on.

3.3.4 Exponential asymptotics

To find the exponentially small terms switched on, we follow the technique discussed in Section 3.2.1 and linearise the solution to the system of differential equations (3.1). That is, we let

$$
\begin{aligned}
u(t) &= \sum_{n=0}^{\infty} U_n(t), \\
v(t) &= \sum_{n=0}^{\infty} V_n(t), \\
w(t) &= \sum_{n=0}^{\infty} W_n(t), \\
x(t) &= \sum_{n=0}^{\infty} X_n(t), \\
y(t) &= \sum_{n=0}^{\infty} Y_n(t)
\end{aligned}
\tag{3.28}
$$

where we assume that the $(n+1)$th coefficients are exponentially smaller than the nth coefficients. Here we are going to find the leading order term of the second $(n = 1)$ coefficients in these expansions as they are switched on via the Stokes

phenomenon by the first coefficients. Compared to Section 3.2.1, the constant C is a free constant and here it is same for all of the functions u, v, w, x and y. Here we make the choice to normalise $C = 1$ and put the additional freedom of choice into the second functions in (3.28), that is the functions U_1, V_1, W_1, X_1 and Y_1.

By inserting (3.28) into the equation (3.1), and by considering the dominant balance, we get the relations

$$\begin{aligned}
\dot{U}_n &= -\sum_{k=0}^{n} V_k[W_{n-k} - \varepsilon\beta Y_{n-k}], \\
\dot{V}_n &= \sum_{k=0}^{n} U_n[W_{n-k} - \varepsilon\beta Y_{n-k}], \\
\dot{W}_n &= -\sum_{k=0}^{n} U_k V_{n-k}, \\
\varepsilon\dot{X}_n &= -Y_n, \\
\varepsilon\dot{Y}_n &= X_n + \beta\sum_{k=0}^{n} U_k V_{n-k}.
\end{aligned} \tag{3.29}$$

Hence, the first terms in the series (3.28) are solutions of the original system (3.1); they represent the slow balanced motion and have the asymptotic expansions (3.5).

Let us assume that the second coefficients in (3.28) have the asymptotic expansions

$$\begin{aligned}
U_1(t) &\sim e^{f_{jk}(t)/\varepsilon}\sum_{n=0}^{\infty} g_{u,j,k,n}(t)\varepsilon^n, \\
V_1(t) &\sim e^{f_{jk}(t)/\varepsilon}\sum_{n=0}^{\infty} g_{v,j,k,n}(t)\varepsilon^n, \\
W_1(t) &\sim e^{f_{jk}(t)/\varepsilon}\sum_{n=0}^{\infty} g_{w,j,k,n}(t)\varepsilon^{n+1}, \\
X_1(t) &\sim e^{f_{jk}(t)/\varepsilon}\sum_{n=0}^{\infty} g_{x,j,k,n}(t)\varepsilon^{n-2}, \\
Y_1(t) &\sim e^{f_{jk}(t)/\varepsilon}\sum_{n=0}^{\infty} g_{y,j,k,n}(t)\varepsilon^{n-2}.
\end{aligned} \tag{3.30}$$

These functions satisfy the system

$$\begin{aligned}
\dot{U}_1 &= -\left[V_0(t)W_1(t) + V_1(t)W_0(t)\right] + \varepsilon\beta\left(V_0Y_1 + V_1Y_0\right), \\
\dot{V}_1 &= \left[U_0(t)W_1(t) + U_1(t)W_0(t)\right] - \varepsilon\beta\left(U_0Y_1 + U_1Y_0\right), \\
\dot{W}_1 &= -\left[U_0(t)V_1(t) + U_1(t)V_0(t)\right], \\
\varepsilon\dot{X}_1 &= -Y_1, \\
\varepsilon\dot{Y}_1 &= X_1 + \beta\left[U_0(t)V_1(t) + U_1(t)V_0(t)\right].
\end{aligned} \tag{3.31}$$

We observe the resurgence property by substituting the series (3.30) into these equations. That is, we find that the function $f_{jk}(t)$ satisfies (3.17) and the g-coefficients satisfy the same recurrence relations as the g-coefficients in (3.21), see Appendix A. Hence, choosing the function $f_{jk}(t)$ here to be one of the functions f_{jk} in (3.22) and the constants of integration for the g-coefficients to be the same as for the g-coefficients in previous sections leads to the correct evaluation of the Stokes multipliers. Let us define the functions $U_{1,jk}(t)$, $V_{1,jk}(t)$, $W_{1,jk}(t)$, $X_{1,jk}(t)$ and $Y_{1,jk}(t)$ via their asympotic expansions (3.30).

For positive real values of t the functions $e^{f_{01}(t)/\varepsilon}$ and $e^{f_{10}(t)/\varepsilon}$ are recessive to the functions $e^{f_{00}(t)/\varepsilon}$ and $e^{f_{11}(t)/\varepsilon}$ and hence they are uniquely determined via their expansions (3.30). The exponent, e^0, multiplying the first term in the series (3.28) is maximally dominating the functions $e^{f_{01}(t)/\varepsilon}$ and $e^{f_{10}}$ when $\Im f_{01}(t) = \Im f_{10}(t) = 0$. Hence, there are two Stokes lines that we have to consider which are given by

$$\{t \in \mathbb{C} \mid \Im(0 - f_{01}(t)) = 0\} = \{t \in \mathbb{C}, \Re t = 0\}$$

and

$$\{t \in \mathbb{C} \mid \Im(0 - f_{10}(t)) = 0\} = \{t \in \mathbb{C}, \Re t = 0\}.$$

Thus, the Stokes lines both lie along the imaginary axis in the complex t-plane, see figure 3.2. We note that the singular points t_j, $j = 0, 1$ lie on the Stokes line. As this double Stokes line is crossed the first functions in the expansion (3.28) switch on a sum of the functions $U_{1,01}(t)$, $V_{1,01}(t)$, $W_{1,01}(t)$, $X_{1,01}(t)$ and $Y_{1,01}(t)$, and $U_{1,10}(t)$, $V_{1,10}(t)$, $W_{1,10}(t)$, $X_{1,10}(t)$ and $Y_{1,10}(t)$, see Section 3.2.1. Hence the asymptotic expansions, including the exponentially small terms originating from

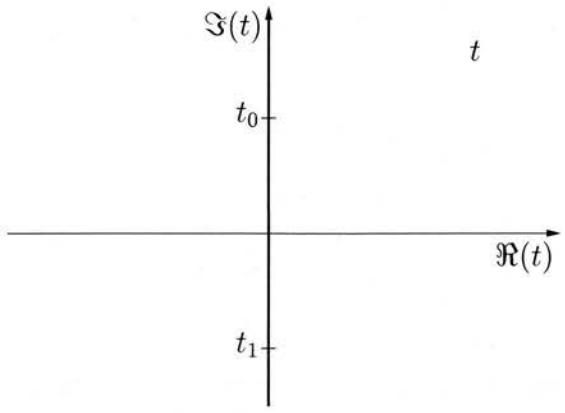

Figure 3.2: The double Stokes lines and the singular points of the coefficients in (3.5) in the complex t-plane

the dominant singularities t_j, are

$$
\begin{aligned}
u(t) &\sim \sum_{n=0}^{\infty} u_n(t)\varepsilon^n + \sum_{k=0}^{1} e^{f_{k(1-k)}(t)/\varepsilon} \sum_{s=0}^{\infty} g_{u,k,1-k,s}(t)\varepsilon^s, \\
v(t) &\sim \sum_{n=0}^{\infty} v_n(t)\varepsilon^n + \sum_{k=0}^{1} e^{f_{k(1-k)}(t)/\varepsilon} \sum_{s=0}^{\infty} g_{v,k,1-k,s}(t)\varepsilon^s, \\
w(t) &\sim \sum_{n=0}^{\infty} w_n(t)\varepsilon^n + \sum_{k=0}^{1} e^{f_{k(1-k)}(t)/\varepsilon} \sum_{s=0}^{\infty} g_{w,k,1-k,s}(t)\varepsilon^{s+1}, \\
x(t) &\sim \sum_{n=0}^{\infty} x_n(t)\varepsilon^n + \sum_{k=0}^{1} e^{f_{k(1-k)}(t)/\varepsilon} \sum_{s=0}^{\infty} g_{x,k,1-k,s}(t)\varepsilon^{s-2}, \\
y(t) &\sim \sum_{n=0}^{\infty} y_n(t)\varepsilon^n + \sum_{k=0}^{1} e^{f_{k(1-k)}(t)/\varepsilon} \sum_{s=0}^{\infty} g_{y,k,1-k,s}(t)\varepsilon^{s-2}.
\end{aligned}
$$

These expansions are valid in the complex t-plane on either side of the double Stokes-line depending on the choice of for which values of t we want the functions $u(t)$, $v(t)$, $w(t)$, $x(t)$ and $y(t)$ to be free of exponentially small oscillations.

The functions $u(t)$, $v(t)$, $w(t)$, $y(t)$ and $x(t)$ take real values for real t so the exponentially small terms that are switched on are complex conjugates. Hence using the expressions for the coefficients $g_{x,0,1,0}(t)$ and the coefficients (3.26) derived in last section, we find that the leading behaviour of the exponentially small

terms is

$$\begin{aligned}
u(t): &\quad -2\pi\kappa_0\beta\tanh(t)e^{-\pi/(2\varepsilon)}\cos(t/\varepsilon)\\
v(t): &\quad -2\pi\kappa_0\beta\,\mathrm{sech}(t)e^{-\pi/(2\varepsilon)}\cos(t/\varepsilon),\\
w(t): &\quad 2\pi\kappa_0\varepsilon\beta\left(\frac{1-\sinh^2(t)}{\cosh^2(t)}\right)e^{-\pi/(2\varepsilon)}\sin(t/\varepsilon),\\
x(t): &\quad -\frac{2\pi\kappa_0}{\varepsilon^2}e^{-\pi/(2\varepsilon)}\cos(t/\varepsilon),\\
y(t): &\quad -\frac{2\pi\kappa_0}{\varepsilon^2}e^{-\pi/(2\varepsilon)}\sin(t/\varepsilon).
\end{aligned} \tag{3.32}$$

We also know the expression for $g_{x,0,1,1}(t)$ and hence the corresponding coefficients in (3.27) for the other functions. We use this to give values for the second order term in ε in the asymptotic expansions of the exponentially small terms:

$$\begin{aligned}
u(t): &\quad -2\kappa_1\varepsilon e^{-\pi/(2\varepsilon)}\left(\frac{\beta\pi^2\tanh t}{2}\cos(t/\varepsilon)+\frac{\beta\pi\tanh t}{2}(2\tanh t-t)\sin(t/\varepsilon)\right)\\
v(t): &\quad -2\kappa_1\varepsilon e^{-\pi/(2\varepsilon)}\left(\frac{\beta\pi^2}{2\cosh t}\cos(t/\varepsilon)+\frac{\beta\pi}{2\cosh t}(2\tanh t-t)\sin(t/\varepsilon)\right)\\
w(t): &\ 2\kappa_1 e^{-\pi/(2\varepsilon)}\left[\left(\frac{4\pi}{\beta}\frac{\sinh t}{\cosh^3 t}+\pi\right)\sin(t/\varepsilon)+\frac{\beta}{2}\left(\frac{1-\sinh^2 t}{\cosh^2 t}\right)(2\tanh t-t)\cos(t/\varepsilon)\right]\\
x(t): &\quad -\frac{\pi\kappa_1}{\varepsilon}e^{-\pi/(2\varepsilon)}\left((2\tanh t-t)\sin(t/\varepsilon)+\pi\cos(t/\varepsilon)\right),\\
y(t): &\quad -\frac{\pi\kappa_1}{\varepsilon}e^{-\pi/(2\varepsilon)}\left((2\tanh t-t)\cos(t/\varepsilon)+\pi\sin(t/\varepsilon)\right).
\end{aligned}$$

We remark that the first order behaviour for $x(t)$ and $y(t)$ is in accordance with Vanneste (2004).

3.4 Discussion

We have found the first two terms in the asymptotic expansions for the exponentially small terms switched on as a function of β. These terms vanish for the same values of β and the number of such values seems to be infinite. Hence, for those values of β we can not determine the, if any, exponentially small terms being switched on from the analysis carried out in this chapter.

The possibility that there are no exponentially small terms being switched on seems unlikely as we are only considering the contribution from two of the infinitely many singular points and we are only considering the first two leading behaviours in a trans-series. Hence the small terms switched on could be doubly or more exponentially small. However, there is a possibility that all the power series in ε corresponding to each exponential factor in the trans-series (3.28) have the same structure such that for certain values of β, all the terms in all of these

power series vanish. Hence, in such case there would be no exponentially small terms and there would exist an invariant slow manifold.

For the values of β that the first Stokes multipliers accompanying the re-expansion of the second function in (3.28) are nonzero our calculations give an analytical expression of the first two order terms of the asymptotic behaviour of the inertia gravity waves. In particular, they confirm the exponential smallness of their amplitude and hence we confirm that there does not exist a slow manifold for this model to an accuracy beyond all orders. Hence, for such values of β it is not possible to reduce the Lorenz equation to a system of fewer variables without loss of information.

Chapter 4

Inertia-gravity wave generation for solutions of the Boussinesq equations

4.1 Introduction

It is known that the large-scale dynamics of the atmosphere and the oceans is characterised by a large frequency separation between high-energy slow motion and low-energy fast motion. Physically, the latter consists of inertia-gravity waves. The time-scale separation between slow motion and inertia-gravity waves originates in the fast rotation of the earth and it is reflected in the smallness of the Rossby number ε. This chapter provides an introduction to the next two chapters which deal with different aspects of a simple model that describes the spontaneous generation of fast inertia-gravity waves by a slow motion in a strongly stratified rotating fluid. The smallness of ε provides the basis for the asymptotic analysis that we carry out.

The model that we treat in what follows describes the evolution of a simple three-dimensional, horizontally sheared flow that is perturbed by a vortex. This vortex is defined by a choice of a potential vorticity distribution which we take to be gaussian. Our aim is to give a detailed description of how the perturbation progresses. As far as the potential vorticity is concerned, the evolution is the simple advection by the flow which sees the ellipsoidal distribution being elongated by the shear. The other fields, however, and in particular the vertical vorticity on which we focus, have a more complicated evolution, with the spontaneous appearance of inertia-gravity oscillation.

We consider the equations of motion in the hydrostatic limit and under the Boussinesq approximation which we refer to as the *Boussinesq equations*. These equations are a set of nonlinear partial differential equations in three spatial

dimensions. Our flow is a special linear solution of these equations of motion that is perturbed by a vortex. This choice of a solution is motivated by the work of Vanneste and Yavneh (2004) which examines particular solutions of the Boussinesq equations for a small ε; these solutions are the so called sheared disturbances representing a sheared plane wave. The sheared disturbances were originally discovered by Kelvin (Thomson, 1887).

The evolution of the sheared disturbances is governed by a simple ordinary differential equation which was solved numerically by McWilliams and Yavneh (1998) and asymptotically by Vanneste and Yavneh (2004). The gaussian vortex can be written as a superposition of independently evolving sheared disturbances. A first step in our analysis is to recover the ordinary differential equation that is a limiting case of the differential equation studied by Vanneste and Yavneh (2004) who did not use the hydrostatic approximations, see the book of Gill (1982) for informations on the equations of motion.

The ordinary differential equation already displays a type of inertia-gravity wave generation in the form of fast oscillations. This generation can be interpreted as a Stokes phenomenon for solutions of the differential equation. We continue the work of Vanneste and Yavneh (2004), who derived the leading behaviour of the spontaneously generated fast oscillation, and we derive the full asymptotic expansions of the solutions. Once we have obtained the asymptotics, we deduce the evolution of the gaussian vortex by integration over the three components of the wave-vector defining each sheared mode. We cannot evaluate this integral fully explicitly, hence the smallness of ε is needed to approximate the integral asymptotically. We are mainly interested in the generation of inertia-gravity waves that the Stokes phenomenon describes. We therefore choose an initial condition that is free of inertia-gravity waves at the initial time $t = 0$.

Our asymptotic results provide for the first time an explicit description of inertia-gravity wave generation in a realistic set-up. They go further than the earlier asymptotic results of Vanneste (2004) and Vanneste and Yavneh (2004) obtained with 'toy-models', notably because, to the opposite of their work, the perturbation that we consider is localised and has finite energy. Our results also complement recent work where inertia-gravity wave generation is examined through direct numerical simulations, see for example Viudez and Dritschel (2006), Plougonven and Snyder (2005), Zhang (2004) and O'Sullivan and Dunkerton (1995).

Finally, our result confirm that a motion that is initially balanced and free of fast oscillations generates exponentially small fast oscillations. This shows that there exists no invariant slow manifold as discussed in Section 3.1. In other words,

it is impossible to define a slow invariant manifold beyond all orders.

The rest of this chapter is devoted to a description of the model, including the representation of the vortex as a superposition of sheared modes, and the derivation of the aforementioned ordinary differential equation. The following two chapters describe the rest of the work discussed above in detail. In Chapter 5 we discuss the asymptotics of the solutions of the reduced differential equation. We take the analysis further than we need for the description of the vortex; we derive the full asympotic expansions of the solutions, thus extending the results of Vanneste and Yavneh (2004). The technique employed is different as it is based on resurgence relations of late coefficients. An interesting aspect of the asymptotic analysis is that the Stokes multipliers are functions of ε that can be represented by their Taylor series. Chapter 5 provides the results needed to proceed to estimate through a triple integral the vertical component of the vorticity corresponding to the full gaussian distribution of the potential vorticity. This estimate is discussed in Chapter 6. While the first integration can be carried out exactly, we use Bleistein's method to find the small-ε asymptotics of the second integral. The third integration is computed numerically. These calculations provide a three-dimensional structure of the inertia-gravity waves generated by the vortex.

4.2 Derivation of a differential equation

We wish to study the spontaneous generation of inertia-gravity waves by slow motion. Our set-up is a stratified fluid in an environment rotating with constant Coriolis frequency f. We do this, following Vanneste and Yavneh (2004), by considering the Boussinesq approximation of the equations of motion in the hydrostatic limit; we assume that the vertical change in pressure is a multiple of the gravitational acceleration g and the density-function in other words we assume that the vertical acceleration is negligible compared with the acceleration of gravity and the vertical pressure gradient.

The system of motion is

$$D_t U - fV = -\Phi_x, \tag{4.1}$$

$$D_t V + fU = -\Phi_y, \tag{4.2}$$

$$B = \Phi_z \tag{4.3}$$

together with the continuity equation

$$D_t \rho + W \rho_{0_z} = 0 \tag{4.4}$$

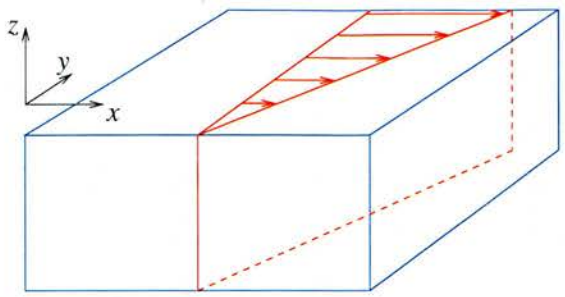

Figure 4.1: *Shear flow.* The arrows display the velocity which induces the shear in the flow. The vertical line is sheared as time evolves.

and the incompressibility equation

$$U_x + V_y + W_z = 0. \tag{4.5}$$

Here, $\boldsymbol{U} = (U, V, W)$ are the usual Cartesian velocity components, B is the buoyancy, $D_t = \partial_t + \boldsymbol{U} \cdot \nabla$ is the material derivative, $\rho_0(z) + \rho(x, y, z, t)$ is the fluid density with constant mean value $\bar{\rho}$, and $\Phi = P/\bar{\rho}$ is the geopotential where P is the pressure. The material derivative is a composition of a time derivative and a space derivative as a fluid in motion has properties depending both on spatial position and time; it follows the movments of an infinitely small particle, the material element, within the flow both in spatial location and time.

We consider solutions of this system which consists of two parts: a horizontal uniformed sheared flow with constant vorticity $-\Sigma$, and a perturbation. Figure 4.1 displays a shear flow. Considering such solutions of the form

$$\begin{aligned}(U, V, W, \Phi, B) = &\left[\Sigma y, 0, 0, -\frac{f\Sigma y^2}{2}, 0\right] \\ &+ [u(x, y, z, t), v(x, y, z, t), w(x, y, z, t), \varphi(x, y, z, t), b(x, y, z, t)],\end{aligned} \tag{4.6}$$

where we write the perturbation as a superposition of sheared disturbances, that is

$$\begin{aligned}
u(x, y, z, t) &= \int_{\mathbb{R}^3} \hat{u}(k, l, m, t) e^{i(kx + (l - k\Sigma t)y + mz)} dk dl dm, \\
v(x, y, z, t) &= \int_{\mathbb{R}^3} \hat{v}(k, l, m, t) e^{i(kx + (l - k\Sigma t)y + mz)} dk dl dm, \\
w(x, y, z, t) &= \int_{\mathbb{R}^3} \hat{w}(k, l, m, t) e^{i(kx + (l - k\Sigma t)y + mz)} dk dl dm, \\
\varphi(x, y, z, t) &= \int_{\mathbb{R}^3} \hat{\varphi}(k, l, m, t) e^{i(kx + (l - k\Sigma t)y + mz)} dk dl dm, \\
b(x, y, z, t) &= \int_{\mathbb{R}^3} \hat{b}(k, l, m, t) e^{i(kx + (l - k\Sigma t)y + mz)} dk dl dm,
\end{aligned} \tag{4.7}$$

allows us to reduce the system of partial differential equations to a single ordinary differential equation in time t. This approach differs from the one of Vanneste and Yavneh (2004) since we consider all real wave vectors $(k, l - k\Sigma t, m)$ whereas they only consider a single one.

Inserting (4.6) into (4.1)–(4.5), assuming that all nonlinear terms are negligible and noticing that equations (4.7) are essentially Fourier transforms of $\hat{u}$, $\hat{v}$, $\hat{w}$, $\hat{\varphi}$ and $\hat{b}$ leads to the following system of equations:

$$\hat{u}_t + (\Sigma - f)\hat{v} = -ik\hat{\varphi}, \tag{4.8}$$

$$\hat{v}_t + f\hat{u} = -i(l - \Sigma kt)\hat{\varphi}, \tag{4.9}$$

$$-\hat{b} = -im\hat{\varphi}, \tag{4.10}$$

$$\hat{b}_t + N_f^2\hat{w} = 0, \tag{4.11}$$

$$k\hat{u} + (l - \Sigma kt)\hat{v} + m\hat{w} = 0, \tag{4.12}$$

where $N_f^2 = -g/\bar{\rho}\frac{d\rho_0}{dz}$ is known as the squared buoyancy frequency. N_f is also known as the Brunt–Väisälä frequency and is here assumed to be a constant. The equations (4.8)–(4.12) can be reduced to one second order inhomogeneous differential equation for the function

$$\hat{\zeta} = ik\hat{v} - i(l - \Sigma kt)\hat{u},$$

which is related to the vertical component of the vorticity of the perturbation $\zeta_v(x, y, z, t)$ analogously to (4.7) by

$$\zeta_v(x, y, z, t) = \int_{\mathbb{R}^3} \hat{\zeta}(k, l, m, t)e^{i(kx+(l-k\Sigma t)y+mz)}dkdldm. \tag{4.13}$$

Let us show how we obtain this equation for $\hat{\zeta}$.

Defining $\hat{\mathcal{D}} = ik\hat{u} + i(l - \Sigma kt)\hat{v}$ we obtain by subtracting ik(4.9) from $i(l - \Sigma kt)$(4.8) the relation

$$\hat{\zeta}_t + (f - \Sigma)\hat{\mathcal{D}} = 0. \tag{4.14}$$

Adding ik(4.8) to $i(l - \Sigma kt)$(4.9) then results in

$$\hat{\mathcal{D}}_t + \frac{2\Sigma k(l - \Sigma kt)}{\lambda^2}\hat{\mathcal{D}} = \lambda^2\hat{\varphi} + \left(f - \frac{2k^2\Sigma}{\lambda^2}\right)\hat{\zeta}, \tag{4.15}$$

where we define $\lambda^2 = k^2 + (l - \Sigma kt)^2$.

We now introduce the Ertel potential vorticity anomaly (Gill, 1982, 240–243), a materially conserved quantity which is in the linear approximation given by

$$q = N_f^2\zeta_v + (f - \Sigma)b_z.$$

That is it has the conservation property

$$D_t q = 0.$$

Similarly to before we represent the function q by

$$q = \int_{\mathbb{R}^3} \hat{q}(k,l,m,t) e^{i(kx+(l-k\Sigma t)y+mz)} dk dl dm.$$

Combining the equations (4.11), (4.12) and (4.14) gives that

$$\hat{q}_t = 0.$$

This implies that the function $\hat{q}$ is the same for all times t given that the value of the triplet (k,l,m) is fixed. Hence we write

$$\hat{q}_0(k,l,m) = \hat{q}(k,l,m,t).$$

The linearisation amounts to the assumption that the balanced part of the vorticity ζ_v, say $\zeta_{\text{bal}} \approx q_0 N_f^{-1}$, has a much smaller magnitude than the shear. In other words $|\zeta_{\text{bal}}| << |\Sigma|$.

Our last step towards obtaining a single equation in $\hat{\zeta}$ is to eliminate $\hat{\varphi}$ from (4.15). We do this by using equation (4.10), the definitions of $\hat{\zeta}$ and $\hat{q}$, and relation (4.14) to find

$$\hat{\zeta}_{tt} + \frac{2\Sigma k(l-\Sigma kt)}{\lambda^2}\hat{\zeta}_t + \left[(f-\Sigma)\left(f - \frac{2k^2\Sigma}{\lambda^2}\right) + \frac{N_f^2\lambda^2}{m^2}\right]\hat{\zeta} = \frac{\lambda^2 \hat{q}_0}{m^2}. \tag{4.16}$$

We are interested in the regime where rotation dominates the effect of the shear. Then the Rossby number

$$\varepsilon = \frac{|\Sigma|}{f}$$

is a small parameter. A numerical estimate of ε would be 0.2 for the atmosphere and 0.002 for the oceans. We get this by noting that $\Sigma = U/L$ where U is the velocity scale and L is the horizontal length scale (Gill, 1982, 498). With $f = 10^{-4}s^{-1}$, we get the atmospheric result with $U \approx 10ms^{-1}$ and $L \approx 5 \cdot 10^5 m$ and the oceans result with $U \approx 2 \cdot 10^{-2}ms^{-1}$ and $L \approx 5 \cdot 10^4 m$.

There is only one other parameter remaining, namely

$$\beta = \frac{fm}{N_f k},$$

the ratio of the square-root of the Prandtl-ratio N_f^2/f^2 and the aspect ratio m/k. Here β is assumed to be $O(1)$. After rescaling the time according to $t \mapsto \frac{t}{|\Sigma|}$, equation (4.16) becomes

$$\varepsilon^2\left[\hat{\zeta}_{tt} + b(t-\sigma l/k)\hat{\zeta}_t\right] + c(t-\sigma l/k)\hat{\zeta} = \frac{(1+(t-\sigma l/k)^2)}{N_f^2\beta^2}\hat{q}_0 \tag{4.17}$$

where

$$b(t) = -\frac{2t}{(1+t^2)},$$
$$c(t) = (1-\sigma\varepsilon)\left(1 - \frac{2\sigma\varepsilon}{(1+t^2)}\right) + \frac{(1+t^2)}{\beta^2}.$$

Here, the value of $\sigma = \text{sign}(\Sigma)$ indicates whether the shear is anticyclonic ($\sigma = 1$) or if it is cyclonic ($\sigma = -1$).

Let us now revisit the function $\zeta(t)$, from (4.13).

4.3 $\zeta(t)$, the vertical vorticity of the perturbation

The vertical vorticity of the perturbation of the sheared perturbed solutions of the equations (4.1)–(4.5) is given by

$$\zeta_v(x,y,z,t) = \int_{\mathbb{R}^3} \hat{\zeta}(k,l,m,t) e^{i(kx+(l-k\Sigma t)y+mz)} dkdldm, \tag{4.18}$$

see equation (4.13), where $\hat{\zeta}$ is given by equation (4.17). In what follows we will focus on studying the function ζ_v as it contains all the information of the system (4.1)–(4.5).

The equation (4.17) for $\hat{\zeta}$ is a linear inhomogeneous equations. Hence, as $\hat{q}$ satisfies the property $\hat{q}_t = 0$ we find that $\hat{\zeta}$ is of the form

$$\hat{\zeta}(k,l,m,t) = \hat{q}_0(k,l,m)\zeta(t - \sigma l/k)$$

where we include the factor N_f^{-2} in the function $\hat{q}$, see Section 6.2.2, and the ζ-function on the right hand side satisfies the differential equation

$$\varepsilon^2\left(\frac{d^2\zeta}{dt^2} - \frac{2t}{1+t^2}\frac{d\zeta}{dt}\right) + \left((1-\sigma\varepsilon)\left(1 - \frac{2\sigma\varepsilon}{1+t^2}\right) + \frac{1+t^2}{\beta^2}\right)\zeta = \frac{1+t^2}{\beta^2}. \tag{4.19}$$

We can not evaluate the integral (4.18) explicitly. As the parameter ε is small we can evaluate it asymptotically in the limit as ε tends to zero. We do this by substituting for $\hat{\zeta}$ its leading behaviour found via the differential equation (4.19), see Chapter 5. After this substitution we successfully carry out the first of the three integrations in (4.18) analytically. The second integral we estimate asymptotically and we estimate the third numerically. We evaluate the integral in Chapter 6.

Chapter 5

Stokes-multiplier expansion in an inhomogeneous differential equation with a small parameter

5.1 Introduction

This chapter[1] is concerned with the small-ε asymptotics of solutions of the linear inhomogeneous differential equation

$$\varepsilon^2\left(\frac{\mathrm{d}^2\zeta}{\mathrm{d}t^2}-\frac{2t}{1+t^2}\frac{\mathrm{d}\zeta}{\mathrm{d}t}\right)+\left((1+\varepsilon)\left(1+\frac{2\varepsilon}{1+t^2}\right)+\frac{1+t^2}{\beta^2}\right)\zeta=\frac{1+t^2}{\beta^2}, \qquad (5.1)$$

where $\beta = O(1)$ is a fixed parameter, here assumed to be positive, and $\varepsilon > 0$ is the Rossby number. In particular we want to describe the spontaneous generation of fast oscillations by slow balanced motion. This equation is equation (4.19) for $\sigma = -1$. It is also a limiting case of that examined by McWilliams and Yavneh (1998) numerically, and analytically by Vanneste and Yavneh (2004).

The balanced motion is represented by a particular integral of (5.1) defined by its asymptotic expansion, while the fast oscillations are represented by the homogeneous solutions. The spontaneous generation of fast oscillations can then be identified as an instance of the Stokes phenomenon (e.g. Paris and Wood, 1995): the (subdominant) oscillations are switched on by the (dominant) balanced solution when t crosses a Stokes line, and their amplitude is exponentially small in ε. Estimating this amplitude thus amounts to the calculation of Stokes multipliers.

In their analysis of (5.1), Vanneste and Yavneh (2004) derived a leading-order approximation to the amplitude of the fast oscillations using the Kruskal–Segur technique of matched asymptotics in the complex t-plane (e.g. Hakim, 1998). In the present chapter, we revisit the problem and apply the somewhat more sophisticated technique of exponential asymptotics based on resurgence.

[1] This chapter is a part of the paper Ólafsdóttir, Olde Daalhuis and Vanneste (2005)

The upshot is a complete asymptotic expansion for the fast oscillations that are switched on; only a few terms in this expansion turn out to provide a remarkably accurate estimate for moderately small values of ε, as is confirmed by comparison with numerical solutions of (5.1).

In addition to its practical value, the asymptotic analysis of (5.1) has an interest from a more mathematical viewpoint, since it illustrates the structure of Stokes multipliers in problems with small parameters. The Stokes multipliers give the amplitude of the subdominant terms switched on by the Stokes phenomenon. In problems where the independent variable is the asymptotic parameters, these are simply constants; here, however, because the asymptotics is in terms of an independent parameter ε, the Stokes multipliers are functions of ε. What emerges from our analysis is that these functions can be conveniently computed as powers series.

The dependence of the Stokes multiplier on ε can be related to the fact that the (subdominant) homogeneous solutions are defined up to arbitrary ε-dependent factors. As a result, the coefficients in their power-series expansion in ε are defined up to arbitrary constants which appear as constants of integration (cf. Dingle, 1973). The choice of these constants affects the resurgence relation relating the expansions of the dominant and subdominant solutions. The appearance of an expansion for the Stokes multiplier does not seem to have been noted in earlier applications of exponential asymptotics to differential equations with small parameters.

Since this chapter discusses exponential asymptotics for an inhomogeneous linear differential equation, the results are related to the ones in Howls and Olde Daalhuis (2003), in which hyperasymptotic expansions are given for solutions of inhomogeneous linear differential equations with a singularity of rank one. As in that paper, the solutions of (5.1) that are switched on when Stokes lines are crossed are homogeneous solutions. We start our analysis of (5.1) by obtaining their small-ε asymptotics.

5.2 Homogeneous solutions

Homogeneous solutions of (5.1) satisfy

$$\varepsilon^2\left(\frac{\mathrm{d}^2\zeta}{\mathrm{d}t^2}-\frac{2t}{1+t^2}\frac{\mathrm{d}\zeta}{\mathrm{d}t}\right)+\left((1+\varepsilon)\left(1+\frac{2\varepsilon}{1+t^2}\right)+\frac{1+t^2}{\beta^2}\right)\zeta=0, \tag{5.2}$$

and have formal expansions of the form

$$\zeta_{\mathrm{h}}(t)\sim \mathrm{e}^{f(t)/\varepsilon}\sum_{n=0}^{\infty}b_n(t)\varepsilon^n, \tag{5.3}$$

where $f(t)$ satisfies the equation

$$f'(t)^2 + \frac{1+t^2+\beta^2}{\beta^2} = 0. \tag{5.4}$$

The coefficients $b_n(t)$ satisfy the recurrence relation

$$\begin{aligned} 2f'(t)b'_{n+1}(t) + \left(f''(t) - \frac{2t}{1+t^2}f'(t) + \frac{3+t^2}{1+t^2}\right) b_{n+1}(t) \\ = -b''_n(t) + \frac{2t}{1+t^2}b'_n(t) - \frac{2}{1+t^2}b_n(t), \end{aligned} \tag{5.5}$$

for $n \geq -1$, where we take $b_{-1}(t) = 0$. It is clear from (5.3)–(5.4) that the homogeneous solutions describe fast oscillations with $O(\varepsilon^{-1})$ frequency.

From (5.4) it follows that the differential equation has simple turning points at

$$t_p = \mathrm{i}\sqrt{1+\beta^2}, \qquad t_m = -\mathrm{i}\sqrt{1+\beta^2}.$$

It is convenient to define for $j = 1, 2$ and $k = p, m$ the functions

$$\begin{aligned} f_{jk}(t) &= (-1)^j \frac{\mathrm{i}}{\beta} \int_{t_k}^{t} \sqrt{1+\beta^2+\tau^2}\, d\tau \\ &= (-1)^j \frac{\mathrm{i}}{2\beta} \left(t\sqrt{1+\beta^2+t^2} + (1+\beta^2) \ln \left(\frac{t+\sqrt{1+\beta^2+t^2}}{t_k} \right) \right), \end{aligned} \tag{5.6}$$

which satisfy (5.4). These are multi-valued functions with branch points at the turning points. We take as the branch cuts the half lines $t = \pm r\mathrm{i}\sqrt{1+\beta^2}$, $r > 1$. Note that with these definitions we have the relations $f_{1p} = -f_{2p}$, $f_{1m} = -f_{2m}$, and for the principle branch of these functions

$$f_{jp}(t) = f_{jm}(t) + (-1)^j \frac{\pi(1+\beta^2)}{2\beta}, \qquad j = 1, 2.$$

With the particular choices $f(t) = f_{jk}(t)$, the recurrence relation (5.5) can be solved. Suitably normalised, the first term reads

$$b_{jk0}(t) = \left(\frac{t+\sqrt{1+\beta^2+t^2}}{t_k} \right)^{(-1)^j \mathrm{i}\beta/2} \frac{\sqrt{1+\beta^2+t^2} + (-1)^j \mathrm{i}\beta t}{(1+\beta^2+t^2)^{1/4}}. \tag{5.7}$$

The next terms are found by integration (5.5) and have the form

$$b_{jk,n+1}(t) = -b_{jk0}(t) \int^t \frac{b''_{jkn}(\tau) - \frac{2\tau}{1+\tau^2}b'_{jkn}(\tau) + \frac{2}{1+\tau^2}b_{jkn}(\tau)}{2f'_{jk}(\tau)b_{jk0}(\tau)}\, d\tau, \tag{5.8}$$

for $n = 0, 1, 2, \cdots$. Note that in these expressions we do not specify the constants of integration; changing these constants of integration amounts to multiplying the homogeneous solutions by an arbitrary function of ε (cf. Dingle, 1973).

With the notation introduced, we define four special solutions of (5.2) via their asymptotic expansions:

$$\zeta_{jk}(t) \sim \mathrm{e}^{f_{jk}(t)/\varepsilon} \sum_{n=0}^{\infty} b_{jkn}(t)\varepsilon^n, \qquad j = 1, 2 \text{ and } k = p, m, \tag{5.9}$$

as $\varepsilon \downarrow 0$. For real t, the functions $\zeta_{1p}(t)$ and $\zeta_{2m}(t)$ are the recessive solutions and uniquely determined by (5.9); the functions $\zeta_{1m}(t)$ and $\zeta_{2p}(t)$ are dominant but can be uniquely defined using the Borel–Laplace transform (e.g. Balser, 2000) or by insisting that (5.9) holds in a sufficiently large sector of the complex t-plane.

5.3 Particular integral

A particular integral of (5.1) that is free of fast oscillations can be defined by the formal asymptotic expansion

$$\zeta_{\mathrm{inh}}(t) \sim \sum_{n=0}^{\infty} a_n(t)\varepsilon^n, \tag{5.10}$$

as $\varepsilon \downarrow 0$. We define ζ_{inh} completely by requiring that (5.10) be the complete asymptotic expansion for $t < 0$; that is, ζ_{inh} does not contains exponentially small terms for $t < 0$. Equivalently, ζ_{inh} can be defined as the Borel–Laplace transform (e.g. Balser, 2000) on the right-hand side of (5.10).

Substituting the expansion (5.10) into (5.1), we obtain the recurrence relation

$$\begin{aligned} a_0(t) &= \frac{1+t^2}{1+\beta^2+t^2}, \qquad a_1(t) = \frac{-\beta^2(3+t^2)}{(1+\beta^2+t^2)^2}, \\ a_n(t) &= \frac{-\beta^2\left((1+t^2)a''_{n-2}(t) - 2ta'_{n-2}(t) + 2a_{n-2}(t) + (3+t^2)a_{n-1}(t)\right)}{(1+\beta^2+t^2)(1+t^2)}, \end{aligned} \tag{5.11}$$

$n \geq 2$, from which the $a_n(t)$ can be derived. Note that in contrast to the coefficients $b_{jkn}(t)$, these coefficients do not involve arbitrary constants of integration; they are uniquely determined by (5.11).

Remark: it might seem that the $a_n(t)$ have poles at $t = \pm\mathrm{i}$. However, a local analysis at these points shows that these are regular points of the differential equation (5.1), and also that all the $a_n(t)$ are regular there. That is, expanding the solution of (5.1), including the right-hand side, with in a Frobenius series in a neighbourhood of the points $t = \pm\mathrm{i}$ shows that the points $t = \pm\mathrm{i}$ are regular points of the differential equations. Re-expansion of this series in powers of ε, that is expanding the coefficients in a power series of ε, then implies that the $a_n(t)$ are regular at $t = \pm\mathrm{i}$. Hence, the only singularities of $a_n(t)$ are poles at the turning points t_k, $k = p, m$.

5.4 Stokes lines and Stokes multipliers

Through the Stokes phenomenon, the inhomogeneous solution (5.10) switches on homogeneous solutions of the form (5.3) when t crosses a Stokes line. To determine the Stokes lines, and to evaluate the corresponding Stokes multipliers, we now use the large-n asymptotics of the coefficients $a_n(t)$. Section 2.1.1 reviews the connection between the Stokes phenomenon and the growth of the coefficients in the divergent asymptotic expansions and further details can been seen in Chapter 2. For our purpose, it is sufficient to observe that when we substitute the ansatz

$$a_n(t) \sim K \sum_{s=0}^{\infty} \frac{\tilde{b}_s(t)\Gamma(n-s+\alpha)}{\left(-\tilde{f}(t)\right)^{n-s+\alpha}}, \tag{5.12}$$

as $n \to \infty$, into recurrence relation (5.11), then we find that $\tilde{f}(t)$ satisfies (5.4) and that the coefficients $\tilde{b}_s(t)$ satisfy recurrence relation (5.5). Equation (5.12) is a typical resurgence relation, which connects the late coefficients in the expansion of a particular solution to the coefficients of another solution.

From the remark following (5.11) we know that, in the complex t-plane, $a_n(t)$ has only singularities at the turning points t_p and t_m. On the other hand, according to (5.12), the singularities of $a_n(t)$ are located at the zeros of $\tilde{f}(t)$. It follows that the only candidates for $\tilde{f}(t)$ in (5.12) are the $f_{jp}(t)$ and $f_{jm}(t)$ defined above. The $\tilde{b}_s(t)$ also have the points t_m and t_p as singular points, but we will see below as we decide on the value of α that this only partly explains the singular nature of the $a_n(t)$ functions.

The connection between resurgence and the Stokes phenomenon indicates that the only homogeneous functions of the form (5.3) that can be switched on by $\zeta_{\text{inh}}(t)$ when a Stokes line is crossed behave like $\exp(\tilde{f}(t)/\varepsilon)$, where $\tilde{f}(t)$ is one of these four candidates. On a Stokes line these functions must be maximally subdominant; thus, the Stokes lines are

$$\{t \in \mathbb{C} \,|\, \Im f_{jk}(t) = 0\}, \qquad j = 1, 2 \text{ and } k = p, m,$$

and are illustrated in Figure 5.1. There are other Stokes lines corresponding to the non-relevant exponential scales and are thus not relevant to our analysis. These Stokes lines are given by

$$\{t \in \mathbb{C} \,:\, \Im(f_{jk} - f_{j'k'}) = 0\} \qquad \text{for } (j,k) \neq (j',k').$$

The $\tilde{b}_s(t)$ that correspond to $f_{jk}(t)$ are the $b_{jks}(t)$ defined in (5.8). These, however, are defined up to arbitrary constants of integrations. But, the asymptotic validity of (5.12) requires a suitable choice for these integration constants. This important point is discussed in details in Section 5.5.

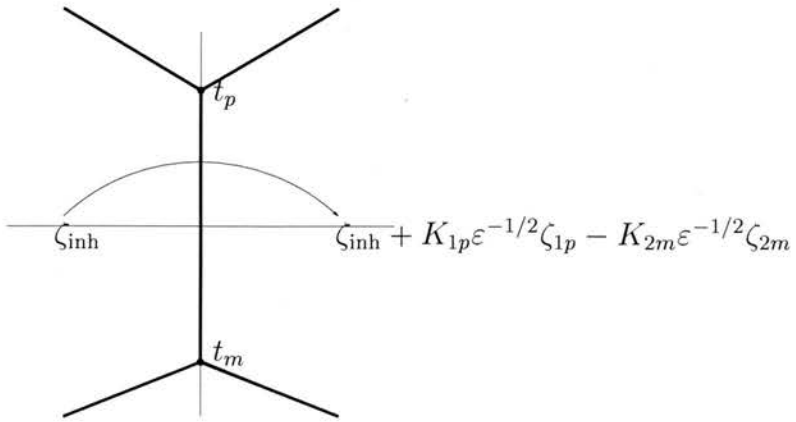

Figure 5.1: The Stokes lines and the Stokes phenomenon

Assuming that (5.12) holds, we determine the constants α and K by observing that as $t \to t_k$, $k = p, m$,

$$a_{2n}(t) \sim \frac{9\Gamma(3n)}{\Gamma(n)} \left(\frac{-\beta^2}{6t_k}\right)^{n+1} (t - t_k)^{-(3n+1)}, \tag{5.13}$$

$$a_{2n+1}(t) \sim (2 - \beta^2) \frac{3\Gamma(3n+2)}{2t_k\Gamma(n+1)} \left(\frac{-\beta^2}{6t_k}\right)^{n+1} (t - t_k)^{-(3n+2)}. \tag{5.14}$$

The reader can check this by substituting these relations in (5.11). Using (5.6), (5.7) and (5.13), we find that, for even n, both sides of (5.12) grow like $(t - t_k)^{-(3n/2+1)}$ as $t \to t_k$ provided that $\alpha = 1/2$. For odd n, the growth of the right-hand side with $\alpha = 1/2$ is apparently faster than the growth in $(t - t_k)^{-(3n+1)/2}$ expected from (5.14). This apparent mismatch is resolved by noting that the a_n are in fact obtained by summing four series of the form (5.12) (see (5.15) below), and that the dominant contributions cancel out for odd n, leading to a growth consistent with (5.14).

We summarise the results so far in

$$a_n(t) \sim \sum_{j=1,2} \sum_{k=p,m} \frac{K_{jk}}{2\pi\mathrm{i}} \sum_{s=0}^{\infty} \frac{b_{jks}(t)\Gamma(n - s + \frac{1}{2})}{(-f_{jk}(t))^{n-s+1/2}}, \tag{5.15}$$

as $n \to \infty$. Now we let $t \to t_k$ in (5.15) and compare the results with (5.13) and (5.14). The result is

$$K_{1p} = K_{2m} = \frac{-\mathrm{i}\sqrt{\beta\pi/2}}{(1 + \beta^2)^{3/4}}, \qquad K_{2p} = \mathrm{i}K_{1p}, \qquad K_{1m} = -\mathrm{i}K_{1p}. \tag{5.16}$$

For the moment we assume that we have taken the correct constants of integration in the $b_{jks}(t)$ for (5.15) to hold. We now analyse what happens when

t crosses the imaginary axis along the real axis. The part of the imaginary axis between the two turning points is a double Stokes line. When it is crossed, the two terms $K_{1p}\varepsilon^{-1/2}\zeta_{1p}(t)$ and $-K_{2m}\varepsilon^{-1/2}\zeta_{2m}(t)$ are switched on, with $\zeta_{1p}(t)$ and $\zeta_{2m}(t)$ exponentially small in ε, since $\Re f_{1p}(t) = \Re f_{2m}(t) = -\pi(1+\beta^2)/(4\beta) < 0$ for real t. (The opposite signs of the two terms switched on arise from the fact that t rotates around t_p and t_m in opposite senses as the Stokes lines are crossed.) In addition, since a double Stokes line is being crossed, there is also a switch on of an extra term that is exponentially smaller than (the already exponentially small) $K_{1p}\varepsilon^{-1/2}\zeta_{1p}(t) - K_{2m}\varepsilon^{-1/2}\zeta_{2m}(t)$; we will ignore this extra term. (For more details on double Stokes lines see for example Voros (1983)).

Let $\zeta(t)$ be a solution of the inhomogeneous differential equation (5.1) that has $\zeta_{\text{inh}}(t)$ as its complete asymptotic expansion for $t < 0$, then $\zeta(t)$ has $\zeta_{\text{inh}}(t) + K_{1p}\varepsilon^{-1/2}\zeta_{1p}(t) - K_{2m}\varepsilon^{-1/2}\zeta_{2m}(t)$ as its asymptotic expansion for $t > 0$ (cf. Section 2.1). The dominant part of $K_{1p}\varepsilon^{-1/2}\zeta_{1p}(t) - K_{2m}\varepsilon^{-1/2}\zeta_{2m}(t)$ is found from (5.3), (5.6), (5.7) and (5.16) to be given by[2]

$$-\sqrt{\frac{2\beta\pi}{\varepsilon}}\mathrm{e}^{-\pi(1+\beta^2+\beta^2\varepsilon)/(4\beta\varepsilon)}\frac{\sqrt{1+\beta^2+t^2}\sin R(t,\varepsilon) + \beta t\cos R(t,\varepsilon)}{(1+\beta^2+t^2)^{1/4}\,(1+\beta^2)^{3/4}}, \tag{5.17}$$

where

$$R(t,\varepsilon) = \frac{1}{2\beta\varepsilon}\left[t\sqrt{1+\beta^2+t^2} + (1+\beta^2)\ln\left(\frac{t+\sqrt{1+\beta^2+t^2}}{\sqrt{1+\beta^2}}\right)\right] + \frac{\beta}{2}\ln\left(\frac{t+\sqrt{1+\beta^2+t^2}}{\sqrt{1+\beta^2}}\right).$$

This dominant part depends only on the first coefficients b_{jk0}, which are entirely defined by (5.7) and is unaffected by the choice of constants of integrations for the b_{jks}, $s > 0$. To obtain higher-order corrections, however, it is necessary to determine the correct constants of integration in (5.8) which ensure that (5.15) is valid. This is considered in the next section.

As mentioned in the beginning of this chapter, equation (5.1) is the differential equation (4.19) in the case $\sigma = -1$. As σ takes only values in $\{-1, 1\}$ it acts as the sign of ε. Hence, the nth a-coefficient in (5.10) for $\sigma = 1$ is the same as for $\sigma = -1$ multiplied by $(-1)^n$. Hence, for either values of σ it is easy to see that the leading behaviour of the exponentially small terms being switched on by the particular integral (5.10) is given by

$$-\sqrt{\frac{2|\beta|\pi}{\varepsilon}}e^{-\pi(1+\beta^2-\sigma\beta^2\varepsilon)/(4|\beta|\varepsilon)}\frac{\sqrt{1+\beta^2+t^2}\sin R(t,\varepsilon) - \sigma|\beta|t\cos R(t,\varepsilon)}{(1+\beta^2+t^2)^{1/4}\,(1+\beta^2)^{3/4}},$$

[2]In the published paper there is a misprint in the exponent. The power of the second β should be two (as corrected here) instead of one. As all numerical calculations are done for $\beta = 1$ this did not affect other results in the paper.

where

$$R(t,\varepsilon)=\frac{1}{2|\beta|\varepsilon}\left(t\sqrt{1+\beta^2+t^2}+(1+\beta^2)\ln\left(\frac{t+\sqrt{1+\beta^2+t^2}}{\sqrt{1+\beta^2}}\right)\right)$$
$$-\frac{\sigma|\beta|}{2}\ln\left(\frac{t+\sqrt{1+\beta^2+t^2}}{\sqrt{1+\beta^2}}\right).$$

We will use this in Chapter 6.

5.5 The missing constants of integration

We first concentrate our analysis on the coefficient $b_{jk1}(t)$. Note that changing the constant of integration in (5.8) has the same effect as replacing $b_{jk1}(t)$ by $b_{jk1}(t)+\alpha_{jk1}b_{jk0}(t)$, where α_{jk1} is just a constant. Taking $b_{jk1}(t)+\alpha_{jk1}b_{jk0}(t)$ as the new $b_{jk1}(t)$ and determining all the other b-coefficients via recurrence relation (5.8) has the same effect as replacing each $b_{jk,s+1}(t)$ by $b_{jk,s+1}(t)+\alpha_{jk1}b_{jks}(t)$. The effect on (5.15) is

$$a_n(t)\sim\sum_{j=1,2}\sum_{k=p,m}\frac{K_{jk}}{2\pi\mathrm{i}}\left(\sum_{s=0}^{\infty}\frac{b_{jks}(t)\Gamma(n-s+\frac{1}{2})}{(-f_{jk}(t))^{n-s+(1/2)}}+\alpha_{jk1}\sum_{s=0}^{\infty}\frac{b_{jks}(t)\Gamma(n-s-\frac{1}{2})}{(-f_{jk}(t))^{n-s-(1/2)}}\right),$$

as $n\to\infty$.

The second step is the correction of $b_{jk2}(t)$ by $b_{jk2}(t)+\alpha_{jk2}b_{jk0}(t)$, where α_{jk2} is a constant. The effect is again that we replace all the higher $b_{jk,s+2}(t)$ by $b_{jk,s+2}(t)+\alpha_{jk2}b_{jks}(t)$. Continuing this process, we observe that adding the constants α_{jks} to $b_{jks}(t)$, $s=1,2,\cdots$ leads to the replacement of each $b_{jks}(t)$ by

$$\sum_{\ell=0}^{s}\alpha_{jk\ell}b_{jk,s-\ell},$$

where we have taken $\alpha_{jk0}=1$. The effect on the resurgence relation (5.15) is its replacement by

$$a_n(t)\sim\sum_{j=1,2}\sum_{k=p,m}\frac{K_{jk}}{2\pi\mathrm{i}}\sum_{\ell=0}^{\infty}\alpha_{jk\ell}\sum_{s=0}^{\infty}\frac{b_{jks}(t)\Gamma(n-s-\ell+\frac{1}{2})}{(-f_{jk}(t))^{n-s-\ell+(1/2)}},\tag{5.18}$$

as $n\to\infty$. Note that we can write (5.18) as

$$a_n(t)\sim\sum_{j=1,2}\sum_{k=p,m}\sum_{\ell=0}^{\infty}\frac{K_{jk\ell}}{2\pi\mathrm{i}}\sum_{s=0}^{\infty}\frac{b_{jks}(t)\Gamma(n-s-\ell+\frac{1}{2})}{(-f_{jk}(t))^{n-s-\ell+(1/2)}},\tag{5.19}$$

as $n\to\infty$, where we take $K_{jk\ell}=K_{jk}\alpha_{jk\ell}$. Hence, $K_{jk0}=K_{jk}$.

The analysis above shows that taking the correct constants of integration in (5.8) for (5.15) to be valid, is equivalent to taking the correct constants $K_{jk\ell}$,

$\ell = 1, 2, 3, \cdots$ in (5.19). Thus, instead of trying to determine the constants of integration in (5.8), we will restrict ourselves to determining the correct constants $K_{jk\ell}$ in (5.19); that is, we will fix the constants of integrations in the b_{jks} arbitrarily (so that (5.15) does not hold in general), and compute the $K_{jk\ell}$ for (5.19) to hold. Of course, once the $K_{jk\ell}$ are known, one can redefine a set of b_{jks} by

$$\frac{1}{K_{jk}} \sum_{\ell=0}^{s} K_{jk\ell} b_{jk,s-\ell}$$

so that (5.15) holds. In fact, a deeper analysis suggests that there is no alternative to the computation of the $K_{jk\ell}$; in particular, there is no obvious starting point for the integrals in (5.8) which would guarantee that (5.15) holds.

In this chapter we are in the fortunate situation that we were able, in the previous section, to determine the exact value of $K_{jk0} = K_{jk}$. We now show how one can determine all the missing constants. The method is very similar to the one discussed in Olde Daalhuis (1999). We use a truncated version of (5.19); to be more precise, we take L terms in the ℓ sum in (5.19). Suppose that we want to determine the constants $K_{jk\ell}$ for $j = 1, 2$, $k = p, m$ and $\ell = 0, 1, \cdots, L-1$ numerically. These are $4L$ unknowns. Note that for large n and bounded t the truncated version of (5.19) is an 'equation' in which the only unknowns are exactly these $K_{jk\ell}$. Thus by taking either $4L$ different values for n, or for t, we obtain $4L$ equations with $4L$ unknowns. Since we can take n as large as we want, we will be able to determine these $4L$ constants to any precision.

In the previous section we used (5.15) to determine the switching-on when the double Stokes line is crossed. Since the constants of integration had not yet been determined, we were only able to derive the switched-on terms to leading-order. We can now use (5.19) to calculate higher-order approximations to these terms. Using (2.5) and (2.6) from Section 2.1.1, we can write the terms switched on when the double Stokes line is crossed as $\tilde{K}_{1p}(\varepsilon)\zeta_{1p}(t) - \tilde{K}_{2m}(\varepsilon)\zeta_{2m}(t)$, where now the Stokes multipliers $\tilde{K}_{1p}(\varepsilon)$ and $\tilde{K}_{2m}(\varepsilon)$ are functions of ε:

$$\tilde{K}_{jk}(\varepsilon) = \sum_{\ell=0}^{\infty} K_{jk\ell} \varepsilon^{\ell-(1/2)}. \tag{5.20}$$

This expansion converges on a disk centred at zero with radius of convergence, $R_{K_{jk}} \in [0, \infty)$. Even if the series in (5.20) is divergent it can be used to approximate the Stokes-multipliers numerically.

The final result in the previous section is still the correct dominant term that is switched on when the double Stokes line is crossed. Why do we need all these extra terms in the expansion of the Stokes multipliers $\tilde{K}_{1p}(\varepsilon)$ and $\tilde{K}_{2m}(\varepsilon)$? We

illustrate in the next section that with these extra terms we can obtain results that are also valid when ε is not very small. In fact, one example shows good results for the case $\varepsilon = 1$.

In the previous section a careful analysis near the turning points was necessary to determine the exact values for the K_{jk0}. This required considering complex values of t. Here we note that when we are only interested in determining the $K_{jk\ell}$ numerically (to any precision) we can confine our calculations to the real t-axis. In fact, the numerical method given above works better when we take real t, because, for a given ℓ, the four terms in the $4L$ equations for the $K_{jk\ell}$ have similar order of magnitude.

5.6 A numerical illustration

In the numerical illustration we take $\beta = 1$. For the constant of integration in (5.8) we take $+\infty$ as one of the limits of integration. Thus the b-coefficients are now well defined. We define $\zeta_{\text{inh}}(t)$ as the solution of (5.1) that has (5.10) as its complete asymptotic expansion for $t < 0$. Hence, for $t < 0$ we can approximate this function via asymptotic expansion (5.10) in which we take the optimal number of terms. (See Olde Daalhuis (1998) for more detail on the optimal number of terms in asymptotic expansions.) From (5.19) it follows that the optimal number of terms in the approximation

$$\zeta_{\text{inh}}(t) \approx \sum_{n=0}^{N-1} a_n(t)\varepsilon^n, \tag{5.21}$$

is $N = [|f_{jk}(t)/\varepsilon|]$, where $[\cdot]$ denotes the integer part. Note that this N depends on t, but that for real t it does not depend on the choice of j and k. In practice, we take at least three terms, that is, we take

$$N = \max\left([|f_{jk}(t)/\varepsilon|], 3\right).$$

In this way the discontinuities in t of the approximant are less conspicuous.

For $t > 0$ we have to incorporate the Stokes phenomenon and approximate $\zeta_{\text{inh}}(t)$ by

$$\begin{aligned}\zeta_{\text{inh}}(t) \approx \sum_{n=0}^{N-1} a_n(t)\varepsilon^n &+ \mathrm{e}^{f_{1p}(t)/\varepsilon} \sum_{\ell=0}^{L-1} K_{1p\ell} \sum_{r=0}^{R-1} b_{1pr}(t)\varepsilon^{\ell+r-(1/2)} \\ &+ \mathrm{e}^{f_{2m}(t)/\varepsilon} \sum_{\ell=0}^{L-1} K_{2m\ell} \sum_{r=0}^{R-1} b_{2mr}(t)\varepsilon^{\ell+r-(1/2)},\end{aligned} \tag{5.22}$$

for some fixed values of L and R which we do not attempt to optimise. In the following numerical calculations we fixed the value of L and R by examining some choices.

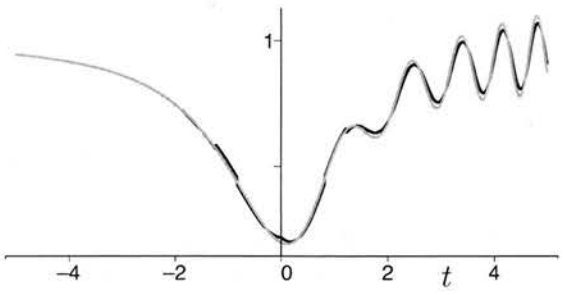

Figure 5.2: The exact (grey) and approximation (black) of a solution of equation (5.1) with $\varepsilon = 0.5$ and $L = R = 1$. The discontinuities are due to optimal truncation.

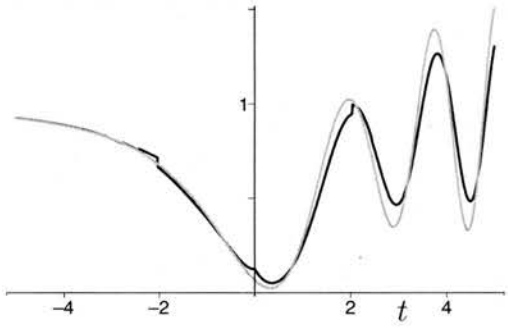

Figure 5.3: The exact (grey) and approximation (black) of a solution of equation (5.1) with $\varepsilon = 1$ and $L = R = 1$. The discontinuities are due to optimal truncation.

In our first illustrations we take only the leading-order Stokes multipliers and only the first b-coefficients, that is we set $L = R = 1$. We take $t = -5$ and $\varepsilon = 1/2$ and compute $\zeta_{\text{inh}}(t)$ and its derivative via (5.21). To compute the 'exact' $\zeta_{\text{inh}}(t)$ numerically we take these two values and integrate the differential equation (5.1) in the positive t direction. This gives the grey curve in Figure 5.2. The black curve in this Figure is (5.21) for $t < 0$ and (5.22) with $L = R = 1$ for $t > 0$. Note that the black curve has discontinuous jumps because that the optimal number of terms N changes with t. If we did not incorporate the Stokes phenomenon then the black curve would be symmetric in t, and there would be no oscillations on the right-hand side of Figure 5.2. Note that, in this first illustration, the small parameter $\varepsilon = 0.5$ is not very small; taking only the dominant terms of the parts that are switched on gives nonetheless a very good approximation for $t > 0$.

In the second illustration we take the even larger value $\varepsilon = 1$, and the result is given in Figure 5.3. This time, the leading-order approximation is not as good for $t > 0$. More terms in the expansion of the Stokes multipliers, and more b-

coefficients are needed to obtain a better approximation. We now fix $L = R = 5$. To compute the Stokes multipliers we use the approximation

$$a_n(t) \approx \sum_{j=1,2} \sum_{k=p,m} \sum_{\ell=0}^{4} \frac{K_{jk\ell}}{2\pi \mathrm{i}} \sum_{r=0}^{4} \frac{b_{jkr}(t)\Gamma(n-r-\ell+\frac{1}{2})}{(-f_{jk}(t))^{n-r-\ell+(1/2)}}. \tag{5.23}$$

In this equation, the $a_n(t)$ and $b_n(t)$ are calculated numerically from their recurrence relation, and the $K_{jk\ell}$ (including K_{jk0}) are regarded as unknowns. Hence, (5.23) is one equation with 20 unknowns. By taking $t = 1/2$ and for n the values $181, 182, \cdots, 200$, we obtain 20 equations and solve them. The result is

$$\begin{aligned}
K_{1p0} &= -0.7452250447\mathrm{i}, \\
K_{1p1} &= -0.3105104338 - 0.4657656523\mathrm{i}, \\
K_{1p2} &= -0.0232886541 + 0.3383269912\mathrm{i}, \\
K_{1p3} &= 0.1744022316 - 0.1406351894\mathrm{i}, \\
K_{1p4} &= -0.1578173268 - 0.0112755970\mathrm{i},
\end{aligned}$$

and $\mathrm{i}K_{1p\ell}$ and $\mathrm{i}K_{2m\ell}$ are complex conjugates, as can be expected from symmetry. Moreover, we see the convergence of the Stokes-multiplier K_{1p0} to the value K_{1p} with increased value of $L = R$. The next table shows this.

	K_{1p0}
$L = R = 0$	-0.7475692370i
$L = R = 1$	-0.7452543171i
$L = R = 2$	-0.7452252369i
$L = R = 3$	-0.7452250453i
$L = R = 4$	-0.7452250447i
$L = R = 5$	-0.7452250447i
K_{1p}	-0.7452250447i

We take the Stokes multipliers from above and use them in (5.22) with $L = R = 5$. The result is the black curve in Figure 5.4 which provides an excellent approximation to the exact solution.

5.7 Discussion

We have studied the exponential asymptotics of (1.1) using the resurgence relations which relate the late terms in the asymptotic expansion of its particular integral to the early terms in the expansion of its homogeneous solutions. Our approach, applicable to a wide class of problems with small parameters, highlights the relationship between (i) the constants of integrations that appear when constructing the homogeneous solutions, and (ii) the ε-dependence of the Stokes multipliers. The constants of integration can be chosen arbitrarily (reflecting the

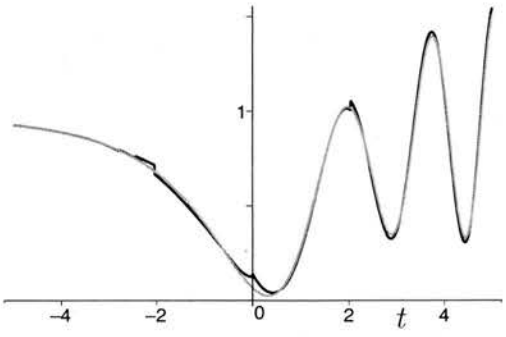

Figure 5.4: The exact (grey) and approximation (black) of a solution of equation (5.1) with $\varepsilon = 1$ and $L = R = 5$. The discontinuities are due to optimal truncation.

fact that the homogeneous solutions are defined up to an arbitrary function of ε). Different choices lead to different forms of the Stokes multipliers, so that the subdominant terms that are switched on are left invariant.

The particular equation studied in this chapter describes the spontaneous generation of inertia-gravity waves in a model of geophysical fluid. The results of Vanneste and Yavneh (2004) about the exponential smallness of this generation are recovered here using a different exponential-asymptotic technique. A useful extension is the computation of the switched-on terms describing the inertia-gravity waves to higher-order in ε: this makes it possible to estimate the wave amplitude with good accuracy for the values of the 'small' parameters as large as 1, that is, for values of the Rossby number ε large enough for the waves to have amplitudes similar to that of the balanced motion which generates them.

Chapter 6

Inertia-gravity-wave radiation by a sheared three-dimensional vortex

6.1 Introduction

In Chapter 4 we discussed special solutions of the Boussinesq equations that consists of a shear flow and a perturbation. We reduced this system of partial differential equations to an ordinary linear inhomogenous differential equation for the function $\hat{\zeta}(t)$ that is associated with the vertical component of the vorticity given by

$$\zeta_v(x,y,z,t) = \int_{\mathbb{R}^3} \hat{\zeta}(k,l,m,t) e^{i(kx+(l-k\sigma t)y+mz)} dkdldm. \tag{6.1}$$

We then in Chapter 5 discussed the asymptotic behaviour of $\hat{\zeta}(t)$ in the limit of the small Rossby number ε by translating the spontaneous generation of fast oscillation as a Stokes phenomenon and then employing the techniques of exponential asymptotics to derive the full asymptotic expansion of a particular integral.

The function $\zeta_v(t)$ governs the evolution of the slow motion, with $O(1)$ amplitude, and the generation of fast oscillation, with $O(\varepsilon^{-1})$ amplitude. We evaluate this functions asymptoticlly in the limit of small ε. We do this by manipulating the three integrals in (6.1) separately. We can only carry out the first integration explicitly. For the second integral, we use the the smallness of ε to estimate its behaviour asymptoically using Bleistein's method (Bleistein, 1966), and the last integral we carry out numerically. With these results we are able to provide a three-dimensional view of the evolution of the inertia-gravity waves for the first time.

6.2 Asymptotics of the function $\hat{\zeta}(t)$

As mentioned in the Section 4.3, the function $\hat{\zeta}(t)$ in (6.1) takes the form

$$\hat{\zeta}(k,l,m,t) = \hat{q}_0(k,l,m)\zeta(t-\sigma l/k) \tag{6.2}$$

where $\zeta(t)$ on the right hand side is a solution of the equation

$$\varepsilon^2\left(\frac{d^2\zeta}{dt^2} - \frac{2t}{1+t^2}\frac{d\zeta}{dt}\right) + \left((1+\sigma\varepsilon)\left(1+\frac{2\sigma\varepsilon}{1+t^2}\right) + \frac{1+t^2}{\beta^2}\right)\zeta = \frac{1+t^2}{\beta^2} \tag{6.3}$$

discussed in Chapter 5, and $\hat{q}_0(k,l,m)$ corresponds to the potential vorticity. In the notation of Chapter 5 we get two arbitrary multipliers for a fixed values of (k,l,m). Thus $\hat{\zeta}(t)$ becomes

$$\begin{aligned}\hat{\zeta}(k,l,m,t) = \hat{q}_0(k,l,m)\,[&\zeta_{inh}(t-\sigma l/k)\\ &+ K_{1p}(k,l,m)\zeta_{1p}(t-\sigma l/k) - K_{2m}(k,l,m)\zeta_{2m}(t-\sigma l/k)\\ &+C_1(k,l,m)\zeta_{1p}(t-\sigma l/k) + C_2(k,l,m)\zeta_{2m}(t-\sigma l/k)]\end{aligned}$$

where ζ_{inh} is a particular integral of (6.3) and ζ_{1p} and ζ_{2m} are solutions of the homogeneous part of (6.3).

We are interested in the generation of fast oscillation through a Stokes phenomenon. This fast oscillation is represented by the homogeneous solutions ζ_{1p} and ζ_{2m} that are switched on by the particular integral ζ_{inh} as the Stokes line $t = \sigma l/k$ is crossed. We choose as initial condition that the function ζ_v, (6.1), is free of oscillation for the time $t = 0$. We therefore restrict our analysis to positive values of time. We want to choose the values of the $C_1(k,l,m)$ and $C_2(k,l,m)$ to be corresponding to this choice of initial conditions.

The Stokes multipliers are not constant functions; they are continuous functions of the variables (k,l,m) that takes the value zero for $t < \sigma l/k$ and approximately the value given with (5.16) for $t > \sigma k/l$. This transition from zero to a nonzero value is continuous, see for example Berry (1989). On the other hand, the transition in the Stokes multipliers from zero to a nonzero value is very steep; it occurs on a $\varepsilon^{1/2}$ timescale. Thus, we can approximate the Stokes multipliers with the Heaviside function and treat them and the C_i-functions as constants.

Demanding that $\hat{\zeta}(k,l,m,\sigma l/k)$ has no oscillation and approximating the Stokes multipliers with Heaviside functions gives

$$\begin{aligned} C_1 &= -K_{1p}, \quad C_2 = K_{1p} \quad \text{if } \sigma l/k < 0,\\ C_1 &= C_2 = 0, \qquad\qquad\ \ \text{if } \sigma l/k \geq 0.\end{aligned}$$

For a later convenience and simpler notation let us define the function

$$\zeta_{\text{osc}}(t-\sigma l/k) = K_{1p}(k,l,m)\zeta_{1p}(t-\sigma l/k) - K_{2m}(k,l,m)\zeta_{2m}(t-\sigma l/k) \tag{6.4}$$

representing the fast oscillations. Then

$$\hat{\zeta}(k,l,m,t) = \hat{q}_0(k,l,m) \cdot \begin{cases} \zeta_{\text{inh}}(t-\sigma l/k) & \text{if } \sigma l/k < 0; \\ \zeta_{\text{inh}}(t-\sigma l/k) & \\ \quad +H(t-\sigma l/k)\zeta_{\text{osc}}(t-\sigma l/k) & \text{if } \sigma l/k \geq 0. \end{cases} \tag{6.5}$$

Having represented $\hat{\zeta}(t)$ by known functions, the asymptotic behaviour of $\zeta_v(t)$ can now be found using the integral representation (6.1).

6.2.1 Manipulation of the integral $\zeta_v(t)$

Before we find the asymptotic behaviour of the function $\zeta_v(t)$, (6.1), we note that with the notation (6.5) $\zeta_v(t)$ becomes

$$\begin{aligned} \zeta_v(x,y,z,t) = &\int_{\mathbb{R}^3} \hat{q}_0(k,l,m)\zeta_{\text{inh}}(t-\sigma l/k)e^{i(kx+(l-k\sigma t)y+mz)}dkdldm \\ &+\sigma\int_{-\infty}^{\infty}\left(\int_{-\sigma\infty}^{0}\int_{-\infty}^{0}+\int_{0}^{\sigma\infty}\int_{0}^{\infty}\right)H(t-\sigma l/k) \\ &\cdot \hat{q}_0(k,l,m)\zeta_{\text{osc}}(t-\sigma l/k)e^{ik(x+(l-\sigma kt)y+\beta z)}dkdldm \end{aligned}$$

where the σ multiplying the second triple integral and σ in the integration limits for the l-integral is due to the requirement that $\sigma l/k \geq 0$. Then

$$\begin{aligned} \zeta_v(x,y,z,t) &= \int_{\mathbb{R}^3} \hat{q}_0(k,l,m)\zeta_{\text{inh}}(t-\sigma l/k)e^{i(kx+(l-\sigma kt)y+mz)}dkdldm \\ &\quad +\sigma\int_{-\infty}^{\infty}\left(\int_{-\infty}^{0}\int_{\sigma kt}^{0}+\int_{0}^{\infty}\int_{0}^{\sigma kt}\right)\hat{q}_0(k,l,m) \\ &\quad \cdot \zeta_{\text{osc}}(t-\sigma l/k)e^{ik(x+(l-\sigma kt)y+\beta z)}dldkdm \\ &= I_1(x,y,z,t) + I_2(x,y,z,t) \end{aligned}$$

where we have defined

$$I_1(x,y,z,t) = \int_{\mathbb{R}^3} \hat{q}_0(k,l,m)\zeta_{\text{inh}}(t-\sigma l/k)e^{i(kx+(l-\sigma kt)y+mz)}dkdldm$$

and

$$\begin{aligned} I_2(x,y,z,t) = \sigma\int_{-\infty}^{\infty}&\left(\int_{-\infty}^{0}\int_{\sigma kt}^{0}+\int_{0}^{\infty}\int_{0}^{\sigma kt}\right)\hat{q}_0(k,l,m) \\ &\cdot \zeta_{\text{osc}}(t-\sigma l/k)e^{ik(x+(l-\sigma kt)y+\beta z)}dldkdm \end{aligned}$$

By looking at the last integral representation of the function $\zeta_v(x,y,z,t)$ we see that there appear two different kind of dynamics. A slow motion represented by the first integral I_1, and a fast oscillation represented by the second integral I_2. Recall that we took as an initial condition that the function ζ_v is free of

oscillations for $t = 0$ and note that $I_2(z, y, z, 0) = 0$. It is the fast motion that interests us, so from here on we focus on the integral I_2.

Let us change the variables of integration in I_2 from (k, l, m) to (k, τ, β) with $\tau = t - \sigma l/k$, and with $\beta = mf/(kN)$ as we also rescale z by the square-root of the Prandlt ratio N^2/f^2. Then, the modulus of the Jacobian is $k^2 f/N$, giving

$$I_2(x, y, z, t) = \frac{f}{N} \int_{-\infty}^{\infty} \int_0^t \int_{-\infty}^{\infty} k^2 \hat{q}_0(k, -\sigma k(\tau - t), k\beta) \zeta_{\text{osc}}(\tau) e^{ik(x - \sigma\tau y + \beta z)} dk d\tau d\beta.$$

We now consider a particlar initial potential-vorticity distribution $q_0(x, y, z)$. Evaluating I_2 then gives an approximation to the waves generated spontaneously when the shear rearranges the potential-vorticity distribution.

6.2.2 Exponential elliptic potential vorticity

Our choice of the initial potential vorticity is the ellipsoidal distribution

$$q_0(x, y, z) = \frac{\pi^{3/2}}{\alpha_1 \alpha_2 \alpha_3} \frac{N^3}{f} \exp\left(- \left[\frac{(x + \sigma T y)^2}{4\alpha_1^2} + \frac{y^2}{4\alpha^2} + \frac{z^2}{4\alpha^2} \right] \right)$$

for some constants α_i, $i = 1, 2, 3$. The parameter T is introduced to control the initial tilt of the ellipsoid against the shear. Taking advantage of the linearity of the problem, we have introduced the constant $\pi^{3/2} N^3/(\alpha_1 \alpha_2 \alpha_3 f)$ for later convenience. This implies that the potential vorticity at later time is

$$q(x, y, z, t) = \frac{\pi^{3/2}}{2^{3/2} \alpha_1 \alpha_2 \alpha_3} \frac{N^3}{f} e^{-\left[\frac{(x + \sigma(T-t)y)^2}{\alpha_1^2} + \frac{y^2}{\alpha_2^2} + \frac{z^2}{\alpha_3^2} \right]}. \tag{6.6}$$

Using the inverse Fourier transform, this gives

$$\begin{aligned} \hat{q}_0(k, l, m) &= \frac{1}{(2\pi)^3} \int_{\mathbb{R}^3} q_0(x, y, z) e^{i(kx + ly + mz)} dx dy dz \\ &= \frac{N^3}{f} e^{-(\alpha_1^2 k^2 + \alpha_2^2 (l - k\sigma T)^2 + \alpha_3^2 m^2)}. \end{aligned} \tag{6.7}$$

By taking the parameter T positive and large, we can reduce the radiation of wave at positive times close to $t = 0$, delaying the maximum emission until the later time $t = T$. Note that we assumed that $t \geq 0$ in Section 6.2. Also, at time $t = T$ the potential vorticity is spherically symmetric, see Figure 6.1.

We now evaluate the integral I_2 with (6.7).

6.2.3 The fast motion, evaluation of the integral I_2

We write

$$I_2(x, y, z, t) = \int_{-\infty}^{\infty} \int_0^t \int_{-\infty}^{\infty} \zeta_{\text{osc}}(\tau) I_{\text{gr}}(k, \tau, \beta, t) dk d\tau d\beta.$$

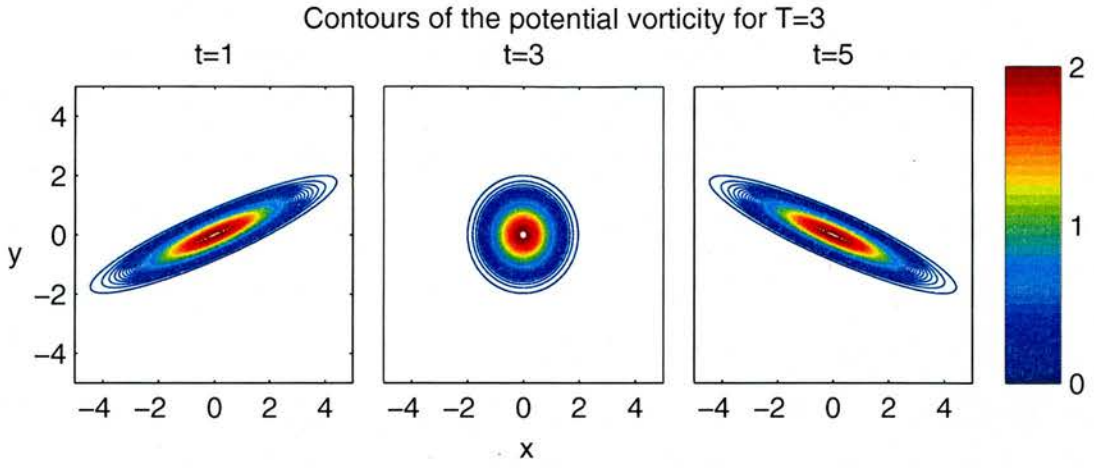

Figure 6.1: Contour lines for $q(x, y, z, t)$ for $z = 0$, $T = 3$, $\alpha_1 = \alpha_2 = \alpha_3 = 1$ and $t = 1$, $t = 3$ and $t = 5$ respectively from left to right. Here $\sigma = -1$; the flow is cyclonic and hence the ellipses are tilted to the left and the contour lines are circles for $t = T = 3$. The maximum emission of oscillations occurs at $t = T$.

where

$$\begin{aligned} I_{gr}(k, \tau, \beta, t) &= k^2 \hat{q}_0(k, -\sigma k(\tau - t), k\beta) e^{ik(x - \sigma\tau y + \beta z)} \\ &= k^2 e^{-k^2(\alpha_1^2 + \alpha_2^2(\tau - t + T)^2 + \alpha_3^2\beta^2)} e^{ik(x - \sigma\tau y + \beta z)} \end{aligned}$$

and we have substituted $\hat{q}_0$ by (6.7). Noting that

$$I_{gr}(-k, \tau, \beta, t) + I_{gr}(k, \tau, \beta, t) = 2k^2 e^{-A(\tau,\beta)k^2} \cos(B(\tau, \beta)k),$$

where we define

$$\begin{aligned} A(\tau, \beta) &= \alpha_1^2 + \alpha_2^2(\tau - t + T)^2 + \alpha_3^2\beta^2, \\ B(\tau, \beta) &= x - \sigma\tau y + \beta z, \end{aligned} \tag{6.8}$$

we have

$$\begin{aligned} I_2(x, y, z, t) &= \int_{-\infty}^{\infty} \int_0^t \zeta_{\text{osc}}(\tau) \int_0^{\infty} \left[I_{gr}(-k, \tau, \beta, t) + I_{gr}(k, \tau, \beta, t) \right] dk d\tau d\beta \\ &= \int_{-\infty}^{\infty} \int_0^t \zeta_{\text{osc}}(\tau) \int_0^{\infty} 2k^2 e^{-A(\tau,\beta)k^2} \cos(B(\tau, \beta)k) dk d\tau d\beta. \end{aligned}$$

Because ζ_{osc} is independent of k we can carry out the integration with regard to k explicitly to find that

$$\begin{aligned} I_2(x, y, z, t) = \sqrt{\pi} \int_{-\infty}^{\infty} \int_0^t \zeta_{\text{osc}}(\tau, \beta) e^{-B^2(\tau,\beta)/(4A(\tau,\beta))} \\ \cdot \left(\frac{1}{2A^{3/2}(\tau, \beta)} - \frac{B^2(\tau, \beta)}{4A^{5/2}(\tau, \beta)} \right) d\tau d\beta. \end{aligned}$$

Because ζ_{osc} depends on τ and β in a complicated manner, it is not possible to carry out further integrations explicitly. We can however take advantage of the smallness of ε to approximate I_2. In the next section we find an approximation to the integral with regard to τ, say I_β. The remaining integral with regard to β will then be computed numerically.

6.2.4 Asymptotics of the integral I_β

We now focus on the asymptotic behaviour of

$$I_\beta(x,y,z,t) = \sqrt{\pi}\int_0^t \zeta_{\text{osc}}(\tau,\beta)e^{-B^2(\tau,\beta)/(4A(\tau,\beta))}\left(\frac{1}{2A^{3/2}(\tau,\beta)} - \frac{B^2(\tau,\beta)}{4A^{5/2}(\tau,\beta)}\right)d\tau.$$

In Chapter 5 we derived the small-ε asymptotic behaviour of what we now call the function $\zeta_{\text{osc}}(t)$, (6.4). For convenience we reproduce the results. That is

$$\zeta_{\text{osc}}(t) \sim -\sqrt{\frac{2|\beta|\pi}{\varepsilon}}e^{-\pi(1+\beta^2-\sigma\beta^2\varepsilon)/(4|\beta|\varepsilon)}\frac{\sqrt{1+\beta^2+t^2}\sin R(t,\varepsilon) - \sigma|\beta|t\cos R(t,\varepsilon)}{(1+\beta^2+t^2)^{1/4}(1+\beta^2)^{3/4}},$$

where

$$R(t,\varepsilon) = \frac{1}{2|\beta|\varepsilon}\left(t\sqrt{1+\beta^2+t^2} + (1+\beta^2)\ln\left(\frac{t+\sqrt{1+\beta^2+t^2}}{\sqrt{1+\beta^2}}\right)\right) - \frac{\sigma|\beta|}{2}\ln\left(\frac{t+\sqrt{1+\beta^2+t^2}}{\sqrt{1+\beta^2}}\right).$$

To simplify our calculations we use that

$$\sqrt{1+\beta^2+\tau^2}\sin R(\tau,\varepsilon) - \sigma|\beta|\tau\cos R(\tau,\varepsilon) = \sqrt{1+\beta^2}\sqrt{1+\tau^2}\sin\left(R(\tau,\varepsilon) - \sigma S(\tau)\right)$$

where

$$S(\tau) = \arcsin\left(\frac{|\beta|\tau}{\sqrt{1+\beta^2}\sqrt{1+\tau^2}}\right).$$

Thus

$$I_\beta(x,y,z,t) \sim \Im\int_0^t g(\tau,\beta,\varepsilon)e^{-h_2(\tau,\beta)}e^{-f(\tau,\beta)/\varepsilon}d\tau. \tag{6.9}$$

where

$$f(\tau,\beta) = \frac{\pi}{4}\left(\frac{1}{|\beta|} + |\beta|\right) + \frac{i}{2|\beta|}\left(\tau\sqrt{1+\beta^2+\tau^2} + (1+\beta^2)\ln\left(\frac{\tau+\sqrt{1+\beta^2+\tau^2}}{\sqrt{1+\beta^2}}\right)\right),$$

$$g(\tau,\beta,\varepsilon) = -\pi\sqrt{\frac{2|\beta|}{\varepsilon}}\frac{\sqrt{1+\tau^2}}{(1+\beta^2+\tau^2)^{1/4}(1+\beta^2)^{1/4}} \cdot\left(\frac{1}{2A(\beta,\tau)} - \frac{B^2(\beta,\tau)}{4A^{5/2}(\beta,\tau)}\right)e^{-h_1(\beta,\tau)}$$

and,

$$h_1(\tau,\beta) = -\sigma\left(\frac{\pi|\beta|}{4} + \frac{i|\beta|}{2}\ln\left(\frac{\tau+\sqrt{1+\beta^2+\tau^2}}{\sqrt{1+\beta^2}}\right) + i\arcsin\left(\frac{|\beta|\tau}{\sqrt{1+\beta^2}\sqrt{1+\tau^2}}\right)\right)$$

and

$$h_2(\tau,\beta) = \frac{B^2(\tau,\beta)}{4A(\tau,\beta)}.$$

The functions $A(\tau,\beta)$ and $B(\tau,\beta)$ are given by (6.8).

When ε tends to zero it is clear that the exponential function $\exp(-f(\tau,\beta)/\varepsilon)$ governs the integral (6.9) and so does $\exp(-h_2(\beta,\tau))$ for certain values of x, y and z. Hence, we need to identify range of x, y and z. Thus, before we go any further we introduce a scaling of the variables x, y and z.

6.2.4.1 Scaling of x, y and z

The behaviour of the integral and I_β is governed by an exponential function whose exponent includes the factor ε^{-1}. An asymptotic estimate holding for as large a range of x, y and z as possible can be obtained by ensuring that the function h_2 appears at the same level as the function f. Recalling (6.8), we use that this is achieved if x, y, and z are $O(\varepsilon^{-1/2})$. Thus, we introduce the scaling

$$\begin{aligned} x &= \frac{x_n}{\sqrt{\varepsilon}}, \\ y &= \frac{y_n}{\sqrt{\varepsilon}}, \\ z &= \frac{z_n}{\sqrt{\varepsilon}} \end{aligned}$$

and assume that x_n, y_n and z_n are of order one. In accordance with this, we define

$$\begin{aligned} B_n(\beta,\tau) &= \varepsilon B(\beta,\tau), \\ f_n(\beta,\tau) &= f(\beta,\tau) + \varepsilon h_2(\beta,\tau). \end{aligned} \tag{6.10}$$

Then (6.9) takes the standard form

$$I_\beta(x,y,z,t) \sim \Im\int_0^t g(\tau,\beta,\varepsilon)e^{-f_n(\tau,\beta)/\varepsilon}d\tau. \tag{6.11}$$

6.2.4.2 The leading asymptotic behaviour of the integral I_β

Methods for the asymptotic evaluation of integrals of the form (6.11), such as Laplace's method or the method of steepest descent, assume that either an end-point or a saddle point of the f_n-function is the main contributer to the integral. Here the situation is more complicated.

The main contribution to the integral I_β comes either from a saddle point of f_n or an endpoint of the integration interval, or simultaneously from a saddle point of f_n and an endpoint of the integration interval. We examine the change in the behaviour of the integrand as x_n changes, fixing all other parameters, namely y_n, z_n and β.

We know that the constant-phase contours of f_n are steepest contours and that these contours are perpendicular to the constant contours of the real part of f_n. The Figures 6.2 display the constant-phase contour for $\Im f_n$ going through the saddle point τ_s, and contour lines of $\Re f_n$ in the complex τ-plane. In these figures we have fixed the values $y_n = -15$, $z_n = z = T = 0$ and $\beta = t = 1$, and we have $x_n = 0$, $x_n = 8$ and $x_n = 15$ respectively from the top down. For the value $x_n = 8$, the second figure, the saddle point dominates the integral but for $x_n = 0$, the first figure, the saddle point and the endpoint $\tau_e = 0$ dominate the integral simultaneously and similarly for $x_n = 15$, the last figure, the saddle point and the endpoint $\tau_e = t$ dominate the integral. This behaviour is not unique for these particular values of the parameters. In general the zero-endpoint and the saddle dominate the integral in regions where $x_n + \beta z_n$ is close to zero, and the t-endpoint and the saddle point dominate the integral in regions where $x_n + \beta z_n$ take values close to $\sigma t y_n$. Hence in these regions we need a method that uniformly combines these two contributions.

We use the somewhat more sophisticated method of Bleistein, (Bleistein, 1966), to find the leading behaviour of I_β. This method uniformly combines the contributions from the saddle point of f_n and an endpoint of the integration interval $[0, t]$ as the saddle point collides with the endpoint in such a way that both contributions are of significance to the integral. In regions where only the saddle point or the endpoint dominate the integral Bleistein's method gives as good approximation as methods only relaying on the endpoint and saddle point contributions. Also, it turns out that there does not exist an analytical expression of the saddle point. Hence, we use Bleistein's method to approximate the integral I_β for all values of the parameters.

We explain the details of Bleistein's method in Appendix B. There we show that for $\tau_e = 0$ we have

$$I_\beta(x, y, z, t) \sim \Im\left\{ e^{-(b-\frac{a^2}{2})/\varepsilon} \left[\sqrt{\frac{\pi}{2}} \left(1 + \operatorname{erf}\left(\frac{a}{\sqrt{2\varepsilon}} \right) \right) (\alpha_0 + \alpha_1 \varepsilon)\, \varepsilon^{1/2} + (\beta_0 + \beta_1 \varepsilon)\, \varepsilon \right] \right\}$$

where a and b satisfy

$$f_n(\tau_e) = b,$$
$$f_n(\tau_s) = b - \frac{a^2}{2}$$

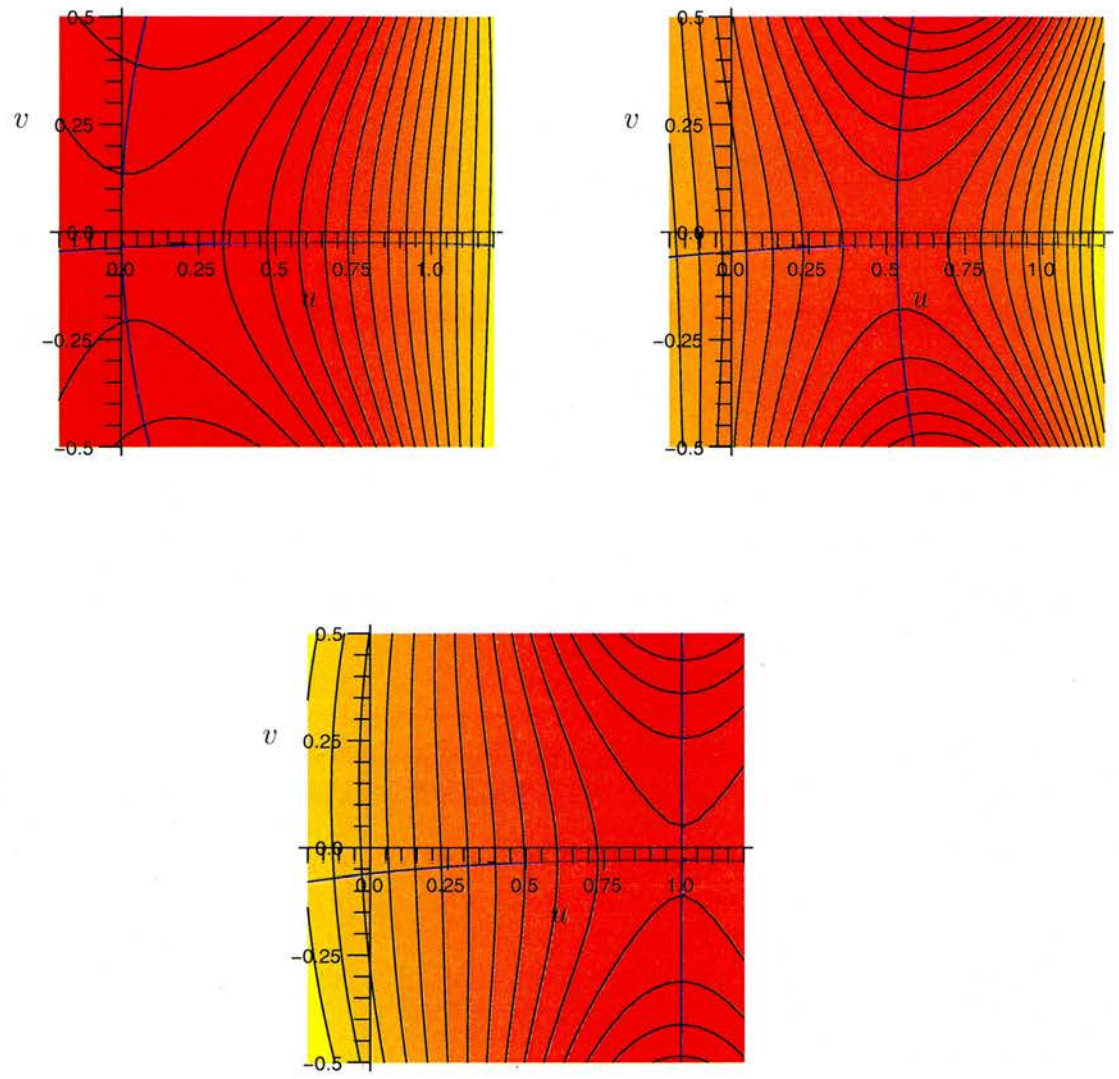

Figure 6.2: The figures show the contour $\Im f_n(t) = \Im f_n(\tau_s)$ where τ_s is a saddle point of f_n (in blue) plotted on top of the contour lines of the real part of $f_n(t)$ in the complex $\tau = u + iv$-plane. The colorcoding is from yellow (minimum) to red (maximum). Here we have fixed the value $y_n = -15$, $z_n = z = T = 0$ and $\beta = t = 1$ and x_n takes the values $x_n = 0$, $x_n = 8$ and $x_n = 15$ respectively from the top. These figures imply that the steepest descent contours, which we know to be perpendicular to the constant contours of $\Re f_n$, lie close to the real axis and they show how the saddle point moves from a vicinity of the zero-endpoint to a vicinity of the t-endpoint with the value of x_n. We will see later, Section C.2.1, that the real part of the saddle point is proportional to $\sigma(x_n + \beta z_n)/y_n$.

and

$$\alpha_0 = \frac{g(\tau_s)}{\sqrt{f_n''(\tau_s)}}, \qquad \beta_0 = \frac{\frac{g(\tau_s)}{\sqrt{f_n''(\tau_s)}} + \frac{ag(\tau_e)}{f_n'(\tau_e)}}{a},$$
$$\alpha_1 = \frac{1}{2}h_0''(a), \qquad \beta_1 = \frac{a\alpha_1 - \beta_0 + h_0'(0)}{a^2}$$

where

$$h_0'(0) = a^2\frac{g'(0)f_n'(0) - g(0)f_n''(0)}{f_n'(0)^3} + \frac{g(0)}{f_n'(0)}$$
$$h_0''(a) = \frac{\left(12g''(\tau_s)f_n''(\tau_s)^2 - 12g'(\tau_s)f_n''(\tau_s)f_n'''(\tau_s) - 3g(\tau_s)f_n''(\tau_s)f_n^{(4)}(\tau_s) + 5g(\tau_s)f'''(\tau_s)^2\right)}{12f_n''(\tau_s)^{7/2}}.$$

The case $\tau_e = t$ is similar and the difference is explained in the Appendix B.

We now verify our asymptotic approximation by comparing it with numerical evaluation of I_β.

6.3 Results

6.3.1 Introduction

Let us start the discussion of our numerical results by considering the integral I_β. The Figures 6.3 display numerics of the integral I_β for cyclonic flow ($\sigma = -1$) in the $x_n y_n$-plane for $z_n = 0$, $\beta = 1$, $\alpha_1 = \alpha_2 = \alpha_3 = 1$ and $\varepsilon = 0.1$. The first figure is for $t = 1$ and the second is for $t = 5$. These figures indicate that the fast oscillation is restricted to the region between the ray $(x_n + \beta z_n) = 0$ and $(x_n + \beta z_n) = \sigma t y_n$. Note that for the integral I_β the factor βz_n can be considered as a shift in x_n, compare to (6.8). Also, we see that the flow is sheared in time as the ray $x_n = \sigma t y_n$ rotates.

We can show analytically that the symmetries

$$I_\beta(x, -y, z, \beta, t) = I_\beta(-x, y, -z, \beta, t),$$
$$I_\beta(x, y, -z, \beta, t) = I_\beta(x, y, z, -\beta, t)$$

hold. Hence, we get the very useful symmetries:

$$\begin{aligned} I_2(x, -y, z, t) &= I_2(-x, y, -z, t), \\ I_2(x, y, -z, t) &= I_2(x, y, z, t). \end{aligned} \tag{6.12}$$

Hence we can restrict our analysis to the upper or lower-half plane. Hereafter we only look at numerics in the lower-half plane and we only consider positive values of z and thus positive values of z_n. The figures 6.3 indicate that we can limit our calculations further to the fourth quadrant for $\sigma = -1$ and the third for $\sigma = 1$.

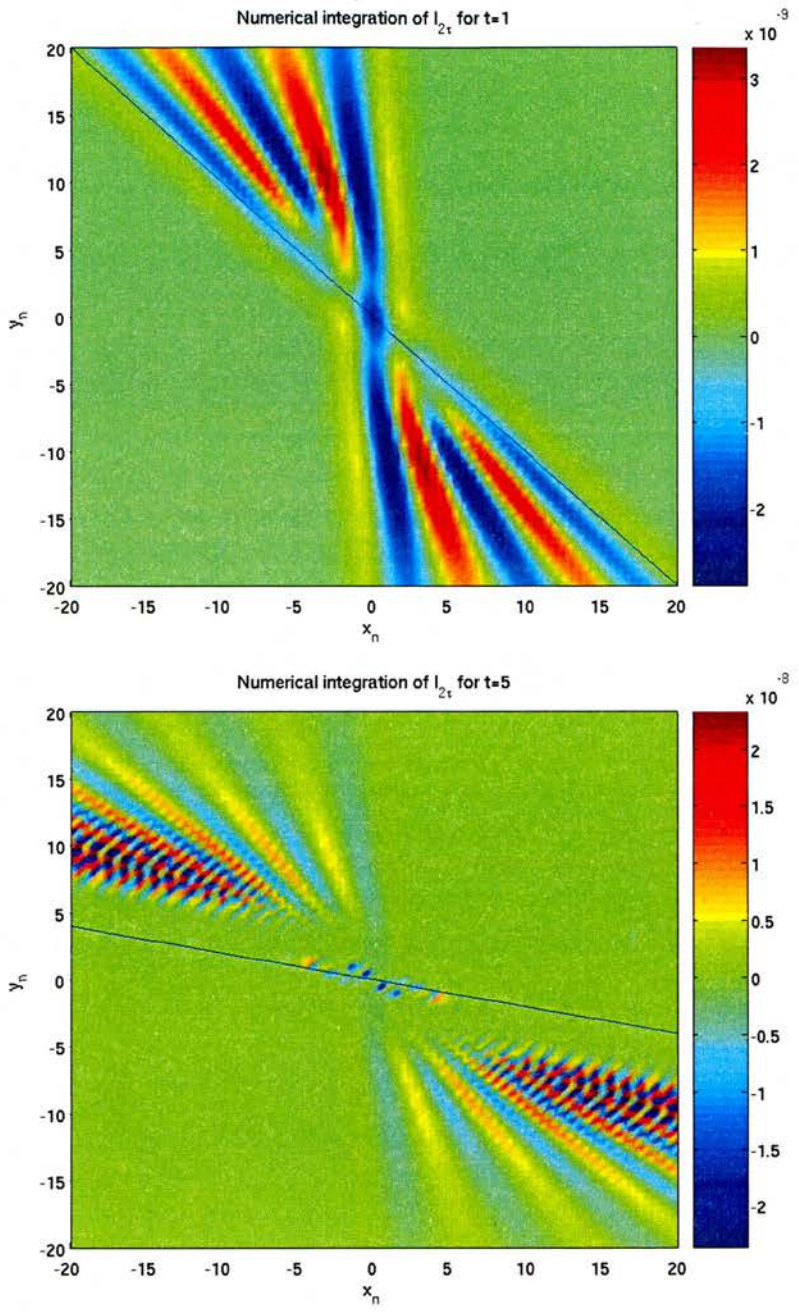

Figure 6.3: Numerical integration of I_β in the x_n-y_n plane and the lines $x_n = -ty_n$. Here we have fixed $T = 3$, $\beta = 1$, $\varepsilon = 0.1$ and $z = z_n = 0$. On the first figure $t = 1$ and on the second figure $t = 5$. We make these figures by using numerical integration methods in MATLAB with a low tolerance. Although these figures give a clear view of the nature of I_β, the accuracy is not very good. For example, what seems to be peaks around zero in the latter figure is due to numerical errors in the integration procedure. Also, what seems to be an oscillation along some of the rays is due to the resolution.

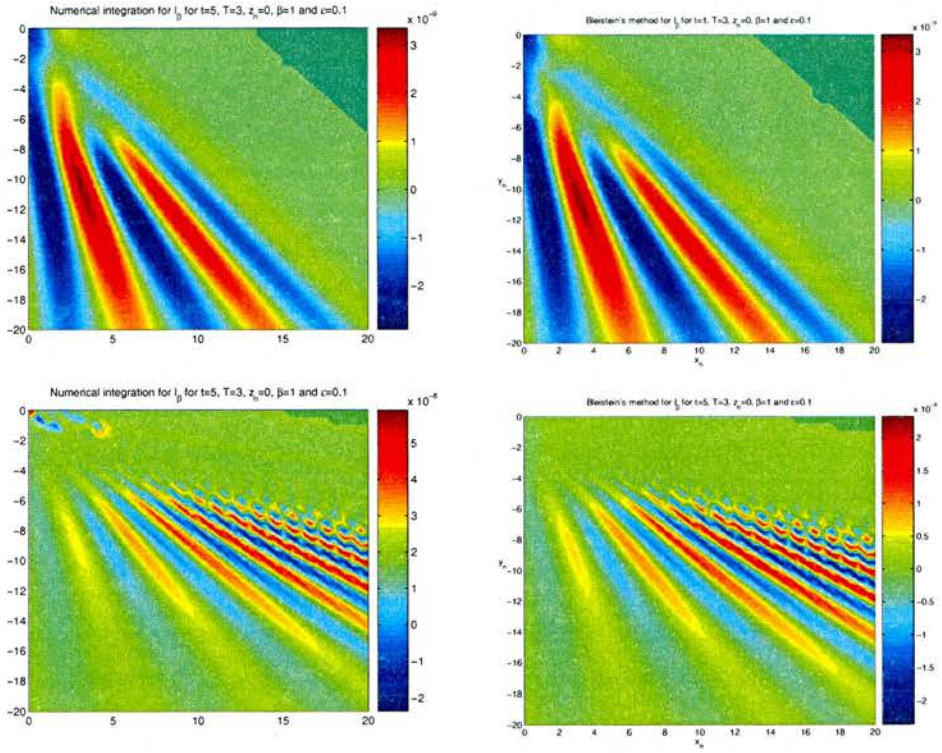

Figure 6.4: The figures to the left are the fourth quadrants of Figures 6.3 and the figures on the right are numerical approximations of I_β using Bleistein's method. These figures are plotted in the x_n-y_n plane where we have fixed $T = 3$, $\beta = 1$, $\varepsilon = 0.1$ and $z = z_n = 0$. On the figures in the first column we have $t = 1$ and on the figures in the second column we have $t = 5$. On the figures in the first column there are some peaks near to the origin that are due to numerical errors and on the figures for $t = 5$ there seems to be an oscillation along some of the rays. This is due to the resolution. It is clear from these figures that Bleistein's method gives a good approximation of the integral I_β.

We approximate the integral I_β numerically in the fourth quadrant using Bleistein's method. Figures 6.4 show approximations of I_β for the same values of the parameters as in Figure 6.3. We see that Bleistein's method gives a very good approximation to the integral I_β, see also Figure C.2. Hence, we estimate the full integral I_2 by integrating Bleistein's approximation of I_β numerically.

Next we discuss numerical results for the integral I_2 after having integrated numerically over β.

6.3.2 Numerical results for I_2

We are now in a position to compute an approximation of $I_2(x, y, z, t)$, which gives the waves generated spontaneously when a vortex with vorticity (6.6) evolves in a shear flow. We proceed as follows: for fixed x, y, z and t we find the saddle numerically for each value of β and then we compute an approximation to I_β using Bleistein's method. We use either $\tau_e = 0$ or $\tau_e = t$ as the endpoint for Bleistein's method, depending on which is closer to the saddle. Integrating the approximated values of I_β numerically gives an approximation of I_2. We remark that the amplitudes of these integrals are of course exponentially small. The details of the numerical implementation are given in Appendix C, the details of Bleistein's method are given in Appendix B. We take advantage of the fact that the symmetries (6.12) hold for the integral I_2 and we assume that $\sigma = -1$ in all our numerical examples.

We now report results obtained for $T = 3$. Because of our choice of an ellipsoidal potential vorticity with $\alpha_1 = \alpha_2 = \alpha_3 = 1$, see Section 6.2.2, this means that for time $t = T = 3$ the potential vorticity is spherically symmetric and we can expect to see maximum wave generation. The Figures 6.5 show the evolution of the flow in the $x_n y_n$-plane for $z_n = 0$, $\varepsilon = 0.1$ and time from $t = 0.25$ to $t = 6$ with the time-step 0.25. Here $\varepsilon = 0.1$, so the flow simulates an atmospheric flow. The oscillations are more or less restricted to the area $0 < x_n < \sigma t y_n$ as previously discussed and the figures clearly show how the magnitude of the oscillation grows up to time $t = T = 3$ and then diminishes. We observe that the magnitude of I_2 diminishes with large $|y_n|$, see also Figures 6.6. In general, we also observe that the crests of the waves diminish with large z_n, see Figure 6.7,

Figures 6.5 also show that the maximum of the flow is clearly being sheared with time up to time t around $t = 3$. However, they do not show clearly how smaller oscillations are being sheared along with the rotation of the ray $x_n = \sigma t y_n$. This is due to the fixed color-axis. If examined more closely, oscillations of small amplitude can been seen being sheared with the flow for large times, $t > 3$. Figure

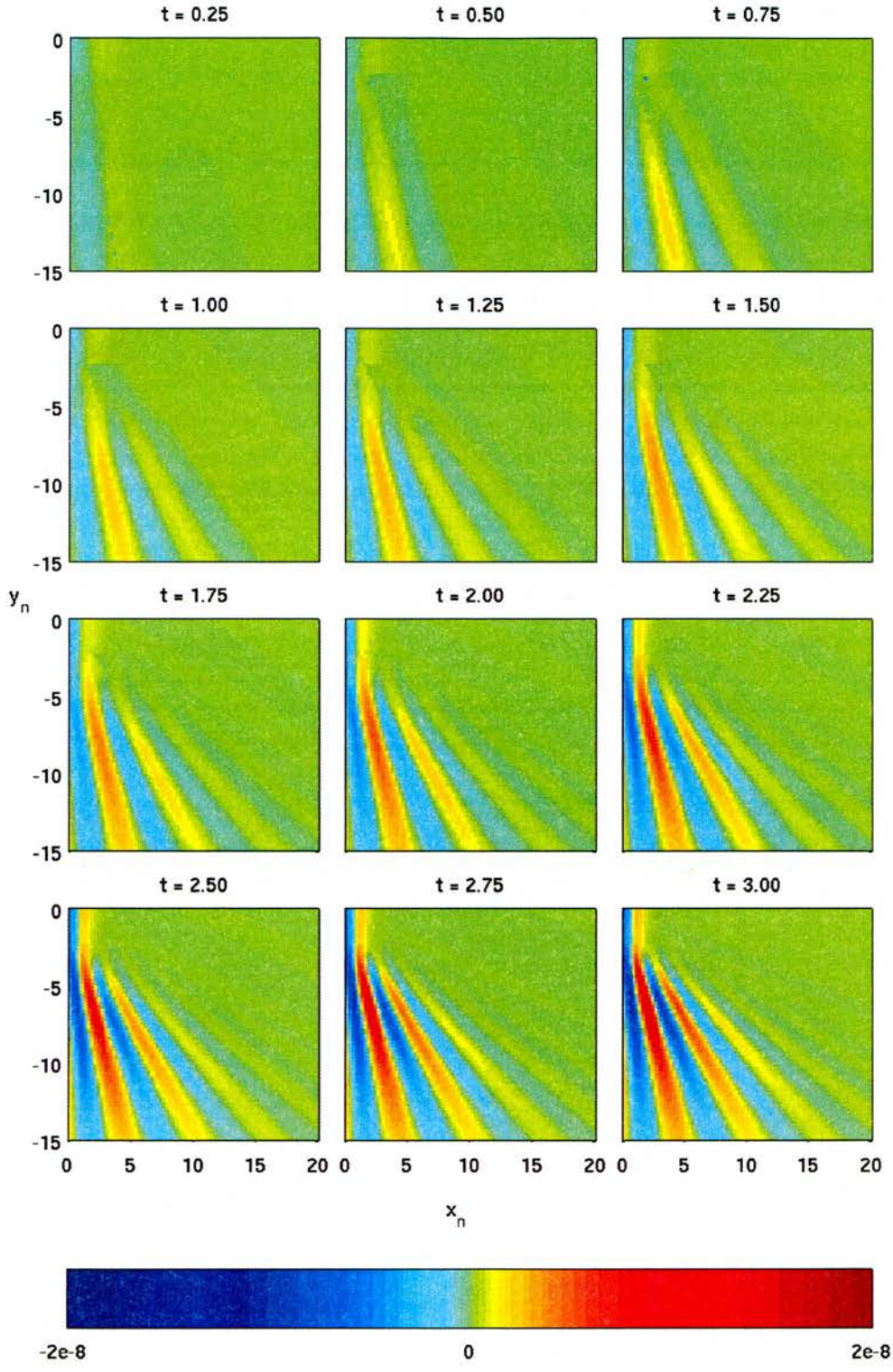

Figure 6.5: Numerics of the integral I_2 in the $x_n y_n$-plane for fixed $z_n = 0$, $T = 3$ and $\varepsilon = 0.1$. The time ranges from 0.25 to 6 by the step 0.25. Note how the oscillations grow up to time $t = T = 3$ and how the flow is sheared. *Continued on next page.*

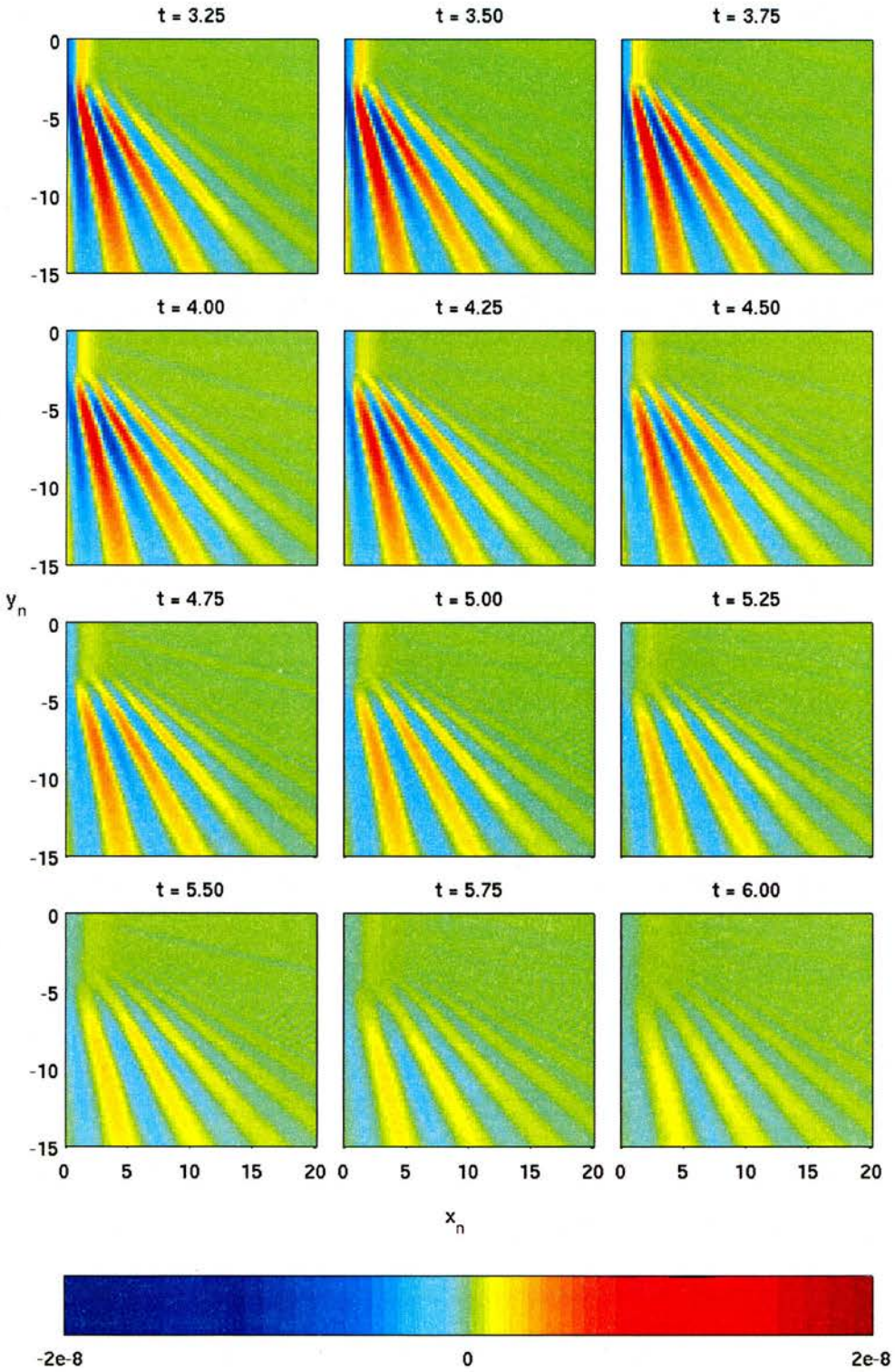

Figure 6.5: *Continued.*

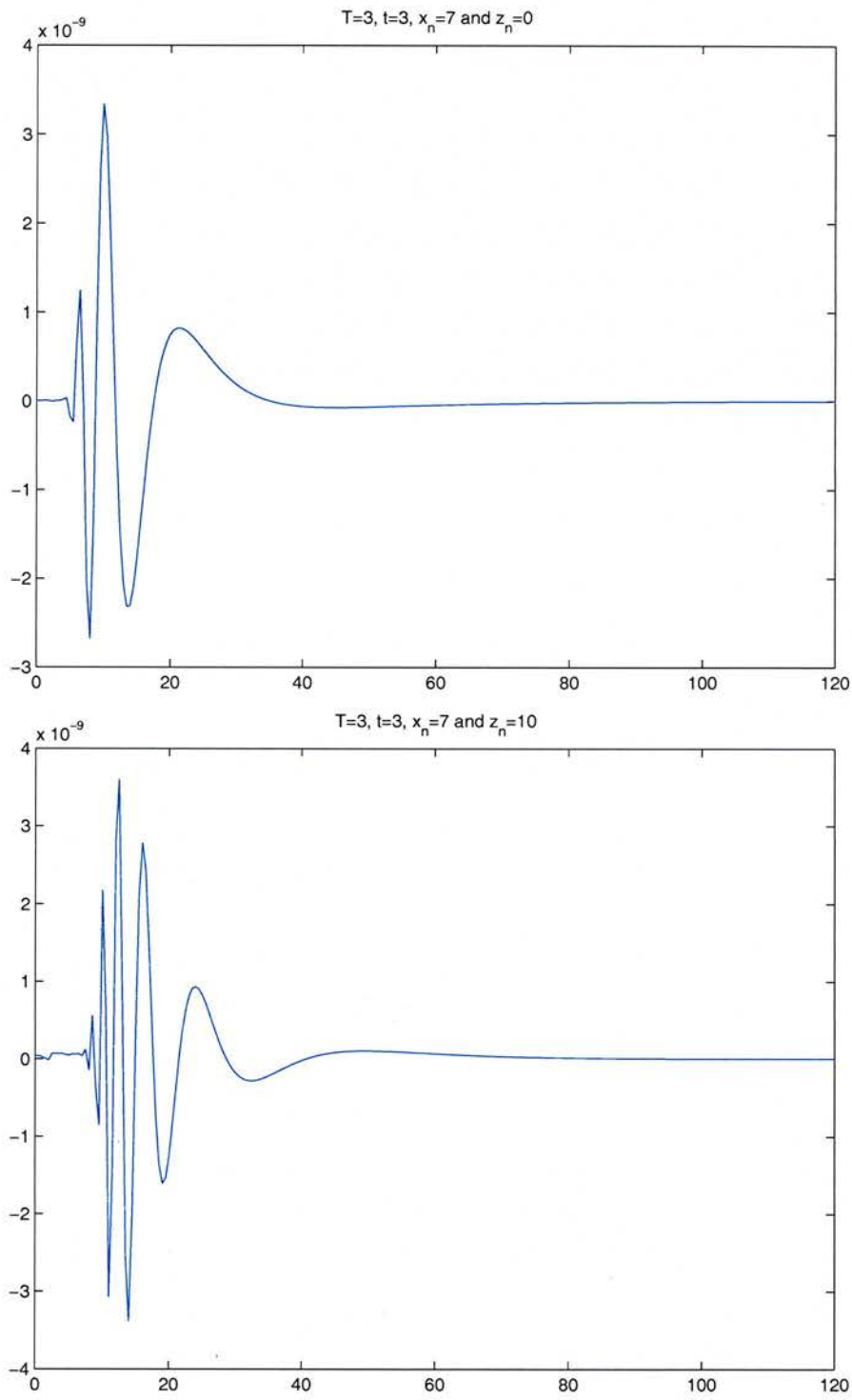

Figure 6.6: Here the integral I_2 is plotted as a function of $|y_n|$ for fixed $x_n = 7$, $t = T = 3$ and $\varepsilon = 0.1$. On the first figure we have $z_n = 0$ and on the second $z_n = 10$. These figures show how the integral is a diminishing function of $|y_n|$.

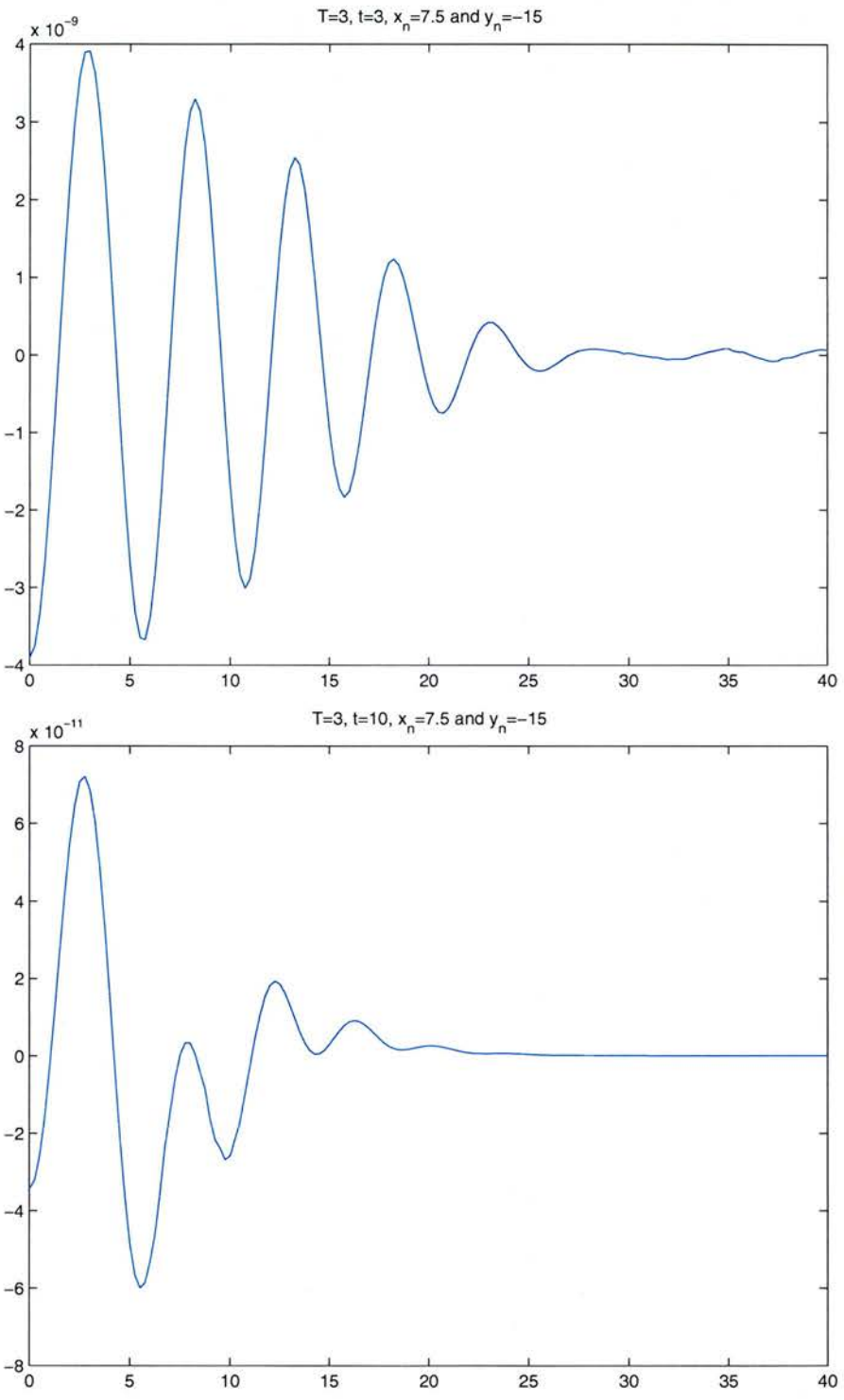

Figure 6.7: Here the integral I_2 is plotted as a function of z_n for fixed $x_n = 7.5$, $y_n = -15$, $\varepsilon = 0.1$ and $T = 3$ for the time $t = T = 3$ and $t = 10$. These figures show that the integral I_2 is a diminishing function of z_n.

6.8 gives a visualisation of the shear flow. The shear is displayed more clearly on

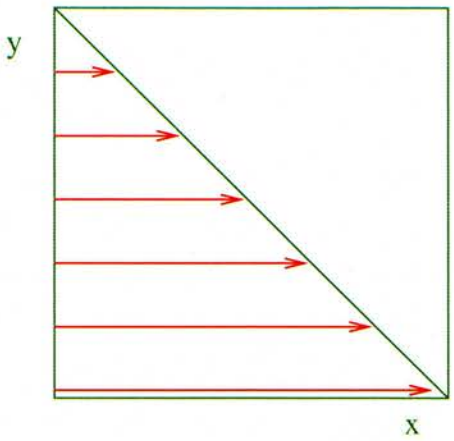

Figure 6.8: An example of the flow being sheared. The arrows represent the velocity field.

Figures 6.10, see discussion below.

There seems to be a discrepancy between Figure 6.4 of I_β for $t = 5$ and the figure for $t = 5$ in 6.5 as the former shows the maximum perturbation of the oscillation clearly being sheared whereas the latter does not. This is because of cancellations as we integrate over β, see figure 6.9.

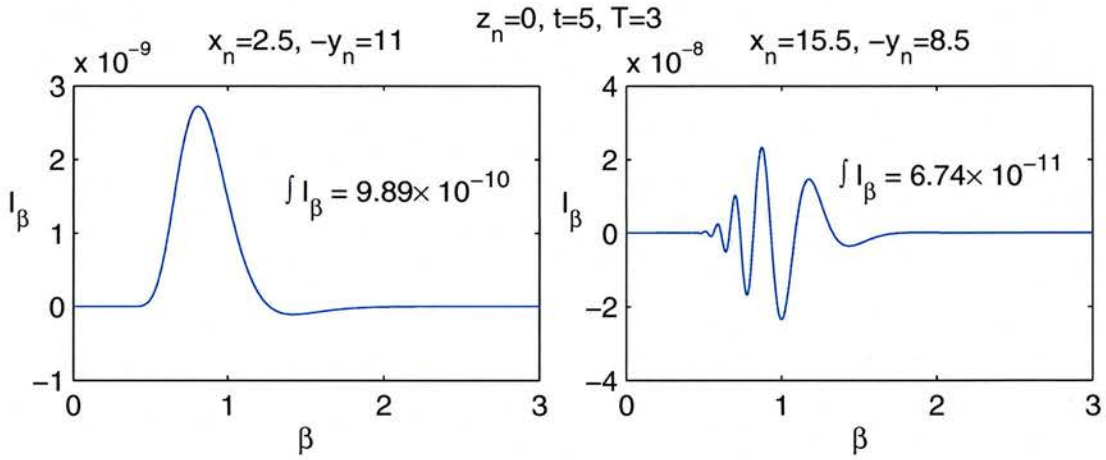

Figure 6.9: The integral I_β plotted as a function of β for $x_n = 2.5$ and $-y_n = 11$ on the left and, $x_n = 15.5$ and $-y_n = 8.5$ on the right. Here $z_n = 0$, $t = 5$, $T = 3$ and $\varepsilon = 0.1$. These figure show that as we integrate over β the integral takes on much smaller value on the right although the amplitude of the oscillation is much larger than on the figure on the left. Note that for $z_n = z = 0$, I_β is an even function of β.

The columns in Figure 6.10 show the numerics of the integral I_2 in the $x_n y_n$-plane for $\varepsilon = 0.1$ and time from $t = 1$ to $t = 7$. Here z_n takes the values

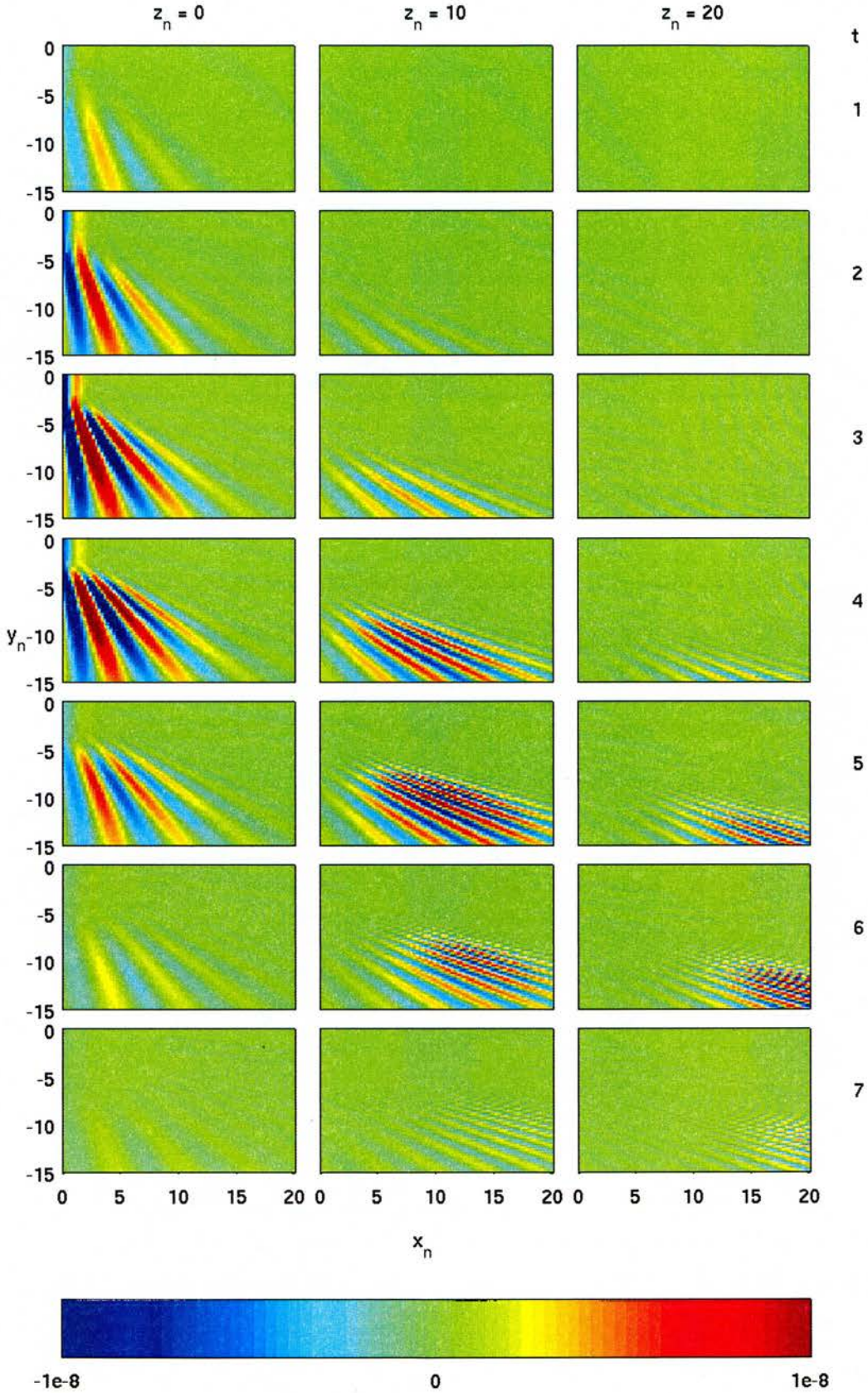

Figure 6.10: Numerics of the integral I_2 in the $x_n y_n$-plane for fixed $z_n = 0$, the first column, $z_n = 10$, the second column and $z_n = 20$, the third column. *Continued on next page.*

$z_n = 0$, $z_n = 10$ and $z_n = 20$ in the columns from left to right respectively. These figures display how the flow evolves in three dimensions. For $z_n = 0$ we see the oscillations grow up to time $t = T = 3$. The magnitude of the oscillations is still large at time $t = 4$ but then it diminishes for larger time. For $z_n = 10$, we see the oscillations appear at time $t = 3$ but their amplitude reaches a maximum between $t = 4$ and $t = 5$ and decreases thereafter. The oscillations for $z_n = 20$ reach their maximum even later in time than the ones for $z_n = 0$ and $z_n = 10$. We see their maximum at time $t = 6$ and it diminishes abruptly for later times. Figure 6.10 shows that the flow is being sheard in time, most clearly for $z_n = 10$ and we see the flow being sheared in z_n.

All our numerical demonstrations have been done for cyclonic flow, the case $\sigma = -1$. In general, we observe the same behaviour for the choice of anticyclonic flow, that is $\sigma = 1$. The only real difference is in the magnitude which is larger in the case $\sigma = 1$ than in the case $\sigma = -1$. This is because of the σ prefactor in the exponent-function $h_2(\tau, \beta)$ in the integrand of the integral (6.9).

6.4 Summary

We have, for the first time, given a rigorous analytical description of the spontaneous generation of inertia-gravity waves in a realistic setting by both using the technique of exponential asympotics for a ordinary differential equation and uniform asymptotics for a Laplace-type integral. This we use to give an visual example of the evolution of inertia-gravity waves generated by a three-dimensional vortex in a setting that approximates the dynamics of the atmosphere. The scale of the spontaneously generated inertia gravity waves is such that they are negligible compared to the slow motion. However in reality, these waves travel upwards in the atmosphere and simultaneously their amplitude increases such that they govern the dynamics in the upper troposphere and lower stratosphere. It is thus important to understand the nature of the generation of inertia gravity waves in order to understand the fundamental nature of the atmosphere.

Figure 6.10: *Continued*: Here $T = 3$ and $\varepsilon = 0.1$. The time ranges from $t = 1$ to $t = 7$ from the top figure down, with the time step one. We see how the effect of βz_n being a shift in x_n for the integral I_β. The maximum oscillation happens at time $t = T = 3$ for $z_n = 0$ whereas the oscillation start to appear according to the colour scale at $t = T$ for the other values of z_n. For the other values of z_n the magnitude is at maximum around $t = 5$ for $z_n = 10$ and $t = 6$ for $z_n = 20$. As mentioned above for previous figures, there seem to be semi-circular waves propagating for large times. These are only artifacts of our choice of grid and the resolution.

Appendix A

Recurrence relation for the g-coefficients

The recurrence relations below can be obtained by substituting (3.21) into the system (3.7). In that case we have to use the assumption that n is always greater than any fixed s and rewrite sums such as $\sum_{k=0}^{n} u_k v_{n-k}$ in the following way

$$\sum_{k=0}^{n} u_k v_{n-k} = \sum_{k=0}^{n/2} u_k v_{n-k} + \sum_{m=0}^{n/2} u_{n-m} v_m \tag{A.1}$$

and then we substitute (3.21) for the large indexed terms. Also, the recurrence relation can be obtained by substituting the series (3.30) into the linearised model (3.29). The latter gives

1.

$$\begin{aligned}\frac{[f'g_{u,0} - \beta v_0 g_{y,0}]}{\varepsilon} + \left[f'g_{u,1} + g'_{u,0} + g_{v,0}w_0 - \beta(v_0 g_{y,1} + v_1 g_{y,0})\right] \\ + \sum_{n=0}^{\infty}\left[f'g_{u,n+2} + g'_{u,n+1} + \sum_{k=0}^{n} v_k g_{w,n-k} + \sum_{k=0}^{n+1} g_{v,k} w_{n+1-k}\right. \\ \left. -\beta\left[\sum_{k=0}^{n+2} v_k g_{y,n+2-k} + \sum_{k=0}^{n} g_{v,k} y_{n-k}\right]\right]\varepsilon^{n+1} = 0\end{aligned}$$

Hence

$$\begin{aligned}&f'g_{u,0} = \beta v_0 g_{y,0},\\ &f'g_{u,1} + g'_{u,0} + g_{v,0}w_0 - \beta(v_0 g_{y,1} + v_1 g_{y,0}) = 0 \quad \text{and}\\ &f'g_{u,n+2} + g'_{u,n+1} + \sum_{k=0}^{n} v_k g_{w,n-k} + \sum_{k=0}^{n+1} g_{v,k} w_{n+1-k}\\ &\qquad - \beta\left[\sum_{k=0}^{n+2} v_k g_{y,n+2-k} + \sum_{k=0}^{n} g_{v,k} y_{n-k}\right] = 0.\end{aligned}$$

2.

$$\frac{[f'g_{v,0}+\beta u_0 g_{y,0}]}{\varepsilon}+\left[f'g_{v,1}+g'_{v,0}-g_{u,0}w_0+\beta(u_0g_{y,1}+u_1g_{y,0})\right]$$
$$+\sum_{n=0}^{\infty}\left[f'g_{v,n+2}+g'_{v,n+1}-\sum_{k=0}^{n}u_kg_{w,n-k}-\sum_{k=0}^{n+1}g_{u,k}w_{n+1-k}\right.$$
$$\left.+\beta\left[\sum_{k=0}^{n+2}u_kg_{y,n+2-k}+\sum_{k=0}^{n}g_{u,k}y_{n-k}\right]\right]\varepsilon^{n+1}=0.$$

Hence

$$f'g_{v,0}=-\beta u_0g_{y,0},$$
$$f'g_{v,1}+g'_{v,0}-g_{u,0}w_0+\beta(u_0g_{y,1}+u_1g_{y,0})=0 \quad \text{and}$$
$$f'g_{v,n+2}+g'_{v,n+1}-\sum_{k=0}^{n}u_kg_{w,n-k}-\sum_{k=0}^{n+1}g_{u,k}w_{n+1-k}$$
$$+\beta\left[\sum_{k=0}^{n+2}u_kg_{y,n+2-k}+\sum_{k=0}^{n}g_{u,k}y_{n-k}\right]=0.$$

3.

$$[f'g_{w,0}+u_0g_{v,0}+g_{u,0}v_0]$$
$$+\sum_{n=0}^{\infty}\left[f'g_{w,n+1}+g'_{w,n}+\sum_{k=0}^{n+1}[u_kg_{v,n+1-k}+g_{u,k}v_{n+1-k}]\right]\varepsilon^{n+1}=0.$$

Hence

$$f'g_{w,0}+u_0g_{v,0}+g_{u,0}v_0=0 \quad \text{and}$$
$$f'g_{w,n+1}+g'_{w,n}+\sum_{k=0}^{n+1}[u_kg_{v,n+1-k}+g_{u,k}v_{n+1-k}]=0.$$

4.

$$\frac{[f'g_{x,0}+g_{y,0}]}{\varepsilon^2}+\sum_{n=0}^{\infty}\left[f'g_{x,n+1}+g_{y,n+1}+g'_{x,n}\right]\varepsilon^{n-1}=0$$

Hence

$$g_{y,0}=-f'g_{x,0} \quad \text{and}$$
$$f'g_{x,n+1}+g_{y,n+1}+g'_{x,n}=0.$$

5.

$$\frac{[(f')^2+1]\,g_{x,0}}{\varepsilon^2}+\frac{\left[[(f')^2+1]\,g_{x,1}+f''g_{x,0}+2f'g'_{x,0}\right]}{\varepsilon}$$
$$+\sum_{n=0}^{\infty}\left[\left[1+(f')^2\right]g_{x,n+2}+f''g_{x,n+1}+2f'g'_{x,n+1}+g''_{x,n}\right.$$
$$\left.+\beta\sum_{k=0}^{n}[u_kg_{v,n-k}+g_{u,k}v_{n-k}]\right]\varepsilon^n=0$$

Hence,

$$(f'(t))^2 = -1,$$

$$g'_{x,0} = 0 \quad \text{and as } f'' = 0$$

$$2f'g'_{x,n+1} + g''_{x,n} + \beta \sum_{k=0}^{n} [u_k g_{v,n-k} + g_{u,k} v_{n-k}] = 0.$$

Appendix B

Bleistein's method

Bleistein's method (Bleistein, 1966) provides an asymptotic expansion of a Laplace-type integral whose main contribution comes from a saddle point of the exponent in the integrand and an endpoint of the integration range. This method uniformly combines the contributions from the saddle point and the endpoint, and is particularly useful when the saddle coalesces with an endpoint as a parameter changes. Let us use Bleistein's method to find the asymptotics of

$$I_\beta(x,y,z,t) = \Im \int_0^t g(\tau,\varepsilon) e^{-f_n(\tau)/\varepsilon} d\tau$$

where we do not write the β-dependency explicitly.

The idea of Bleistein's method is to write the integral I_β in the form

$$\int_0^\infty e^{-(w^2/2 - aw + b)/\varepsilon} g(w) dw$$

where ε is the small parameter, $w = a$ corresponds to the relevant saddle point τ_s of f_n, and $w = 0$ corresponds to the relevant endpoint, τ_e, of the integration range whose contribution is of same order as the contribution from the saddle point. Thus we write

$$f_n(\tau) = \frac{w^2}{2} - aw + b. \tag{B.1}$$

To begin with, let us assume that $\tau_\mathrm{e} = 0$. Then

$$\begin{aligned} f_n(\tau_\mathrm{e}) &= b, \\ f_n(\tau_\mathrm{s}) &= b - \frac{a^2}{2}. \end{aligned} \tag{B.2}$$

Hence

$$a = \pm\sqrt{2(f_n(\tau_\mathrm{e}) - f_n(\tau_\mathrm{s}))} \tag{B.3}$$

and can be considered as a measurement of the distance between the values of f_n at the saddle and the endpoint. We have to make sure that the topological order of the endpoints and the saddle is the same in the coordinates τ and w. Thus, we

choose the sign of a in order to keep this order right. Analytically, in our problem it is not clear which sign of a we want to choose as we can not find an expression for the saddle point. However, as we evaluate a numerically, we can keep track of the correct sign of a. This is discussed in Section C.2.3.

With this notation

$$\begin{aligned}\int_0^t g(\tau,\varepsilon)e^{-f_n(\tau)/\varepsilon}d\tau &= \int_0^{w(t)} e^{-(w^2/2-aw+b)/\varepsilon} g(\tau(w))\frac{d\tau}{dw}dw \\ &= \int_0^{w(t)} e^{-(w^2/2-aw+b)/\varepsilon} h_0(w)dw\end{aligned} \tag{B.4}$$

where $w(t)$ corresponds to the endpoint t and $h_0(w) = g(\tau(w))d\tau/dw$. Next, we expand $h_0(w)$ around the saddle point and the endpoint simultaneously by writing

$$h_0(w) = \alpha_0 + \beta_0(w-a) + w(w-a)k_0(w), \tag{B.5}$$

where the coefficient α_0 represents the expansion around $w = a$ and the coefficient β_0 represents the expansion around $w = 0$. Hence we take

$$\begin{aligned}\alpha_0 &= h_0(a), \\ \beta_0 &= \frac{h_0(a) - h_0(0)}{a}.\end{aligned}$$

Now by differentiating equation (B.1) with respect to w and noting the relation between $w = a$ and $\tau = \tau_s$ we get

$$\left.\frac{d\tau}{dw}\right|_{w=a} = \lim_{w\to a}\frac{(w-a)}{df_n/d\tau} = \lim_{w\to a}\frac{(w-a)}{f_n''(\tau_s)(\tau-\tau_s)} = \frac{1}{f_n''(\tau_s)\left.\frac{d\tau}{dw}\right|_{w=a}}$$

thus

$$\alpha_0 = h_0(a) = \frac{g(\tau_s)}{\sqrt{f_n''(\tau_s)}}.$$

Similarly we get

$$\beta_0 = \frac{h_0(a) - h_0(0)}{a} = \frac{\frac{g(\tau_s)}{\sqrt{f_n''(\tau_s)}} + \frac{ag(\tau_e)}{f_n'(\tau_e)}}{a}.$$

Now we can estimate the integral I_β.

Introducing (B.5) in (B.4) and extending the integration range to infinity we obtain after integration by parts

$$\begin{aligned}I_\beta(x,y,z,t) \sim \Im\Bigg(e^{-(b-\frac{a^2}{2})/\varepsilon}\left[\alpha_0\sqrt{\frac{\pi}{2}}\left(1+\operatorname{erf}\left(\frac{a}{\sqrt{2\varepsilon}}\right)\right)\varepsilon^{1/2} + \beta_0\varepsilon\right] \\ +\varepsilon\int_0^\infty e^{-(w^2/2-aw+b)/\varepsilon}\frac{d}{dw}\left(wk_0(w)\right)dw\Bigg).\end{aligned} \tag{B.6}$$

The remaining integral is $O(\varepsilon^{3/2})$ and hence in principle negligible. However, for our problem, we found that the accuracy of the first two terms was not sufficient

to provide reliable results with typical relevant values of ε. We therefore derive more terms in the asympotic expansion of the integral I_β.

To find the third term in the expansion we expand the function $h_1(w)$ in the same manner as before around $w = a$ and $w = 0$. That is we write

$$h_1(w) = \frac{d}{dw}\left(wk_0(w)\right) = \alpha_1 + \beta_1(w-a) + w(w-a)k_1(w) \tag{B.7}$$

where as before

$$\begin{aligned}\alpha_1 &= h_1(a),\\ \beta_1 &= \frac{h_1(a) - h_1(0)}{a}.\end{aligned}$$

In terms of the function $h_0(w)$ these coefficients are

$$\begin{aligned}\alpha_1 &= \frac{1}{2}h_0''(a),\\ \beta_1 &= \frac{\frac{a^2}{2}h_0''(a) - h_0(a) + h_0(0) + ah_0'(0)}{a^3} = \frac{a\alpha_1 - \beta_0 + h_0'(0)}{a^2}.\end{aligned}$$

where we calculate with similar methods as before

$$\begin{aligned}h_0'(0) &= a^2\frac{g'(0)f_n'(0) - g(0)f_n''(0)}{f_n'(0)^3} + \frac{g(0)}{f_n'(0)}\\ h_0''(a) &= \frac{\left(12g''(\tau_\mathrm{s})f_n''(\tau_\mathrm{s})^2 - 12g'(\tau_\mathrm{s})f_n''(\tau_\mathrm{s})f_n'''(\tau_\mathrm{s}) - 3g(\tau_\mathrm{s})f_n''(\tau_\mathrm{s})f_n^{(4)}(\tau_\mathrm{s}) + 5g(\tau_\mathrm{s})f'''(\tau_\mathrm{s})^2\right)}{12f_n''(\tau_\mathrm{s})^{7/2}}.\end{aligned}$$

Substituting $h_1(w)$ by its expansion (B.7) in (B.6) then gives

$$\begin{aligned}I_\beta(x,y,z,t) \sim \Im\Bigg(e^{-(b-\frac{a^2}{2})/\varepsilon}\Bigg[\sqrt{\frac{\pi}{2}}\left(1+\operatorname{erf}\left(\frac{a}{\sqrt{2\varepsilon}}\right)\right)(\alpha_0+\alpha_1\varepsilon)\,\varepsilon^{1/2} + (\beta_0+\beta_1\varepsilon)\,\varepsilon\Bigg]\\ +\varepsilon^2\int_0^\infty e^{-(w^2/2-aw+b)/\varepsilon}\frac{d}{dw}\left(wk_1(w)\right)dw\Bigg),\end{aligned}$$

where the remaining integral is now $O(\varepsilon^{5/2})$.

Further terms in the asmptotic expansion could be obtained by expanding succsessively the derivative of the k_n function. This is Bleistein's method, giving a recursive scheme to find an asymptotic expansion of the integral.

In what follows, we neglect the $O(\varepsilon^{5/2})$ terms and hence employ the approximation

$$\begin{aligned}&I_\beta(x,y,z,t) \sim\\ &\Im\left(e^{-(b-\frac{a^2}{2})/\varepsilon}\left[\sqrt{\frac{\pi}{2}}\left(1+\operatorname{erf}\left(\frac{a}{\sqrt{2\varepsilon}}\right)\right)(\alpha_0+\alpha_1\varepsilon)\,\varepsilon^{1/2} + (\beta_0+\beta_1\varepsilon)\,\varepsilon\right]\right)\end{aligned} \tag{B.8}$$

when the saddle point τ_s is close to the endpoint $\tau_\mathrm{e} = 0$.

When the saddle point τ_s is close to the other endpoint $\tau_e = t$ we derive an analogous approximation by substituting $(t - \tau)$ for τ in (B.4). This amounts to changing b from $b = f_n(\tau_e = 0)$ to $b = f_n(\tau_e = t)$, adjusting the value of a accordingly and, substituting $f_n^{(n)}(\tau_s)$ by $(-1)^n f_n^{(n)}(\tau_s)$ and $g^{(n)}(\tau_s)$ by $(-1)^n g^{(n)}(\tau_s)$ in the α_i and β_i-coefficients in equation (B.8).

As mentioned before in this section there does not exist an expression for the saddle τ_s. However, for a fixed value of the variables we can always find its value numerically and hence approximate the integral I_β.

Appendix C

Numerical implementation of I_2

C.1 Endpoint and saddle point contributions

Bleistein's method gives the asymptotic behaviour of the integral I_β as for all values of x_n, y_n and z_n by uniformly combining the contribution from a saddle point and an endpoint. Still there are values of x_n, y_n and z_n where the contribution from the endpoints gives as good approximation of the integral and a region where the saddle point contribution gives a good contribution.

Figures C.1 give an example of a region where the saddle point gives a good approximation and the first figure in C.2 gives an example of region where the endpoint method fails but the saddle point gives a good approximation for certain values of the parameters. As using Bleistein's method we need three terms in expansion provided by the saddle-point method, see Olver (1974, 127). As we need to find the saddle point numerically both in saddle-point method as in Bleistein's method there is no gain of using saddle-point methods in regions where it gives as good approximation as Bleistein's method. On the contrary it saves calculation time to use the endpoint contribution, found by partial-integration. Hence, in numerical implementations we approximate the integral I_β with the endpoint contribution for $|y_n| < 3$.

From figures C.1–C.2 we see that on a ray parallel to the real axis in the lower half of the $x_n y_n$-plane we start of having a single pulse merging from the endpoints, which then splits up to two separate ones which represent each of the endpoints. Then with larger σy_n, an additional oscillatory part appears in between the endpoints. This oscillatory part emerges from the saddle point. The pulse that corresponds to the zero-endpoint is static in a neighbourhood of $x_n = 0$ whereas the pulse corresponding to the t-endpoint is located at the $x_n = \sigma t y_n$. In general in a plane parallel to the $x_n y_n$-plane the pulse corresponding to the zero-endpoint is positioned around $x_n + \beta z_n = 0$ and the pulse corresponding to the t-endpoint is positioned in a neighbourhood of $x_n + \beta z_n = \sigma t y_n$.

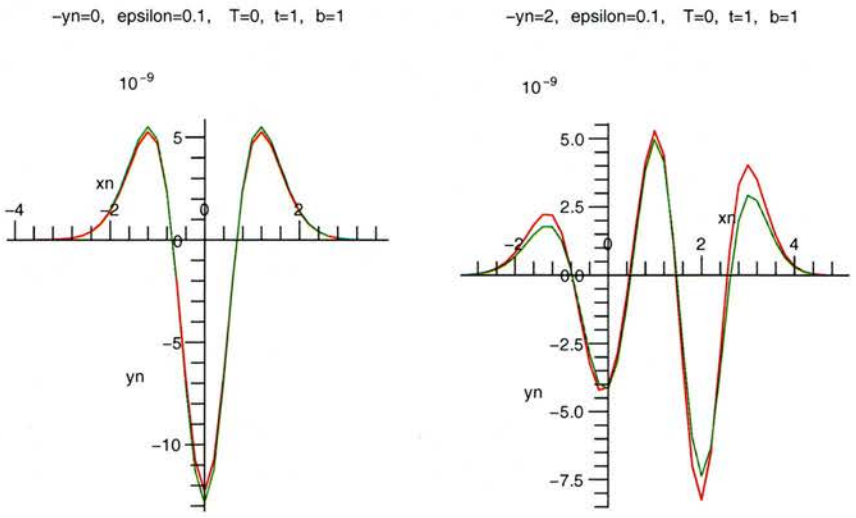

Figure C.1: For fixed $y_n = 0$, $z_n = 0$, $t = 1$ and $T = 0$ we plot I_β for different values of x_n for $\varepsilon = 0.1$ and $\beta = 1$. The red curve is numerical integration of I_β and the green one is the endpoint contribution.

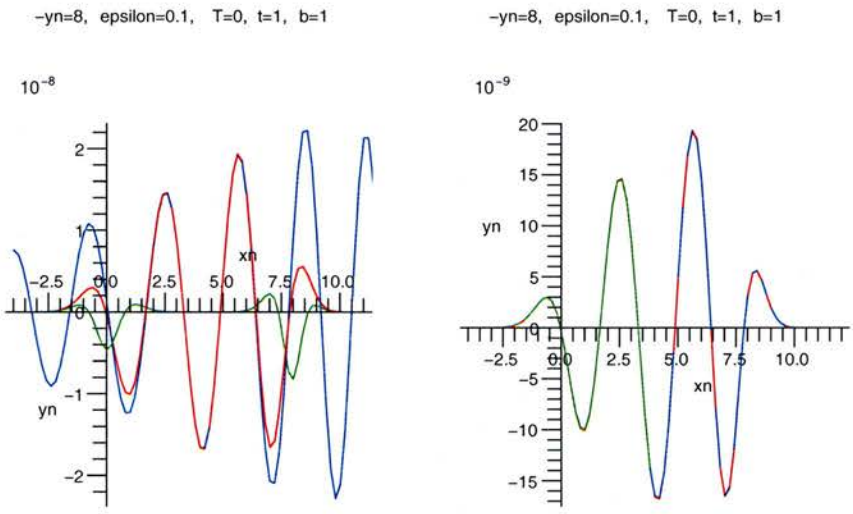

Figure C.2: For fixed $y_n = -8$, $z_n = 0$, $t = 1$ and $T = 0$ we plot I_β for different values of x_n for $\varepsilon = 0.1$ and $\beta = 1$. The red curve is numerical integration of I_β. On the figure to the left the green curve is the endpoint contribution and the blue curve is the saddle point contribution, using three terms in the expansion. On the figure to the right the green curve is Bleistein's method including the zero-endpoint and the blue curve is Bleistin's method including the t-endpoint.

For values of x_n, y_n and z_n where the endpoint method does not give a proper approximation we use the Bleistein's method. Let us look at its numerical implementation.

C.2 Numerical implementation of Bleistein's method

To obtain numerical approximations via Bleistein's method of the integral I_β there are three things that we have to consider when we have fixed the values of all the parameters. These things are:

1. how are we going to find the saddle point numerically since there does not exist an analytic expression for it.

2. when to switch between the two Bleistein's methods.

3. which sign of a in (B.3) we want to use. That is which one of the roots

$$a = \pm\sqrt{2\left(b - f_n(\tau_s, \beta)\right)} = \pm\sqrt{2\left(f_n(\tau_e, \beta) - f_n(\tau_s, \beta)\right)} \tag{C.1}$$

   do we want to use to reserve the topological order of the endpoint and the saddle point.

Let us resolve these problem in the same order as listed here.

C.2.1 Finding the saddle point numerically

We use the Newton-Raphson method (e.g. Kincaid and Cheney, 2001, 181-90) to find the saddle point numerically. The method is iterative and needs an initial guess of the root of the function f_n. We know that

$$\begin{aligned}\frac{df_n(\beta,\tau)}{d\tau} =& \frac{d}{d\tau}\left(f(\beta,\tau) + \frac{B_n(\beta,\tau)}{4A(\beta,\tau)}\right) \\ =& -\frac{i\sqrt{1+\beta^2}}{|\beta|} + \frac{\sigma\left(x_n - \sigma\tau y_n + \beta z_n\right) y_n}{2\left(\alpha_1^2 + \alpha_2^2(\tau - t + T)^2 + \alpha_3^2\beta^2\right)} \\ & - \frac{\left(x_n - \sigma\tau y_n + \beta z_n\right)^2 (\tau - t + T)}{2\left(\alpha_1^2 + \alpha_2^2(\tau - t + T)^2 + \alpha_3^2\beta^2\right)^2}.\end{aligned}$$

The later two term are zero for

$$\begin{aligned}\tau_1 &= \frac{\sigma(x_n + \beta z_n)}{y_n}, \\ \tau_2 &= \frac{\sigma y_n(\alpha_1^2 + \alpha_2^2(t-T)^2 + \alpha_3^2\beta^2) - \alpha_2^2(t-T)(x_n + \beta z_n)}{\alpha_2^2(\sigma y_n(t-T) - (x_n + \beta z_n))}.\end{aligned}$$

The function $B_n^2(\beta,\tau)/(4A(\beta,\tau))$ is also zero for the $\tau = \tau_1$, thus the exponential function governing the integrand takes a maximum for a value of τ which real

part is close to τ_1. Hence, as an initial guess, for large values of x_n, y_n and z_n we look for a saddle point close to τ_1.

It seems that the saddle function is a differentiable function. Since in our calculations there is only one parameter value changing at each time we guess that the saddle point lies on a line with the last two saddle points that we found by changing the value of this parameter. To be more precise, say we have all the parameters fixed except x_n, and we have found the saddles τ_0 corresponding to $x_n = x_0$ and τ_1 corresponding to $x_n = x_1$ and now we want to find the saddle τ_2 corresponding to a value $x_n = x_2$. Then we use as an initial guess in Newton-Raphson method $\tau_{\text{in}} = \tau_1 + (\tau_1 - \tau_0) = 2\tau_1 - \tau_0$. This gives better results in general than using only the previous saddle point as an initial guess. This is significantly better if our step size in x_n, y_n and z_n is rather large, like one, and when the value of $x_n + \beta z_n$ is larger than $|ty_n|$.

For a tolerance set to be 10^{-6} we usually find a relevant saddle in less than five iterations via the Newton-Raphson method. Still there are cases when we do not succeed to find the right saddle point or we do not find a saddle point at all. As f_n has more than one saddle point it may happens that we find a saddle but not the one we want to use. Although we do not have an expression for the saddle, observations have shown that the relevant saddle has negative imaginary part and it turns out that if we find an irrelevant saddle point its imaginary part is positive. In theses cases, which seem to happen mostly for small values of x_n, we make another attempt to find the saddle using the *fsolve* function from the *optimization toolbox* in MATLAB with the previous saddle as an initial guess. The *fsolve* solves for the real and imaginary part separately and takes far more time to find the saddle than our self implemented Newton-Raphson method.

The rare cases where we do not find the saddle point at all are related to the value of β being close to zero or even more seldom cases where β takes on large values. These cases are much less frequent when we use the interpolation between the saddles and when we decrease the stepsize in x_n, z_n and y_n. For both small and large values of β the value of the integrand is very small because of the nature of the real part of f_n, see (6.10). Therefore when this happens we fix the outcome to be zero.

C.2.2 The dominant endpoint

Bleistein's method as discussed in section B gives an asymptotic approximation of I_β when one of the endpoint and the saddle point govern the integral. Thus, we have two asymptotic approximations of the integral and we have to find where want to use each of them.

In section C.1 we observed how the contribution from the endpoints evolved from a single pulse to two separate pulses for large y_n representing each of the endpoints. When y_n becomes even larger the saddle point contribution appears as an oscillatory part between the pulses. As the saddle is governing the integral in the region in between the pulses both methods should give the same approximation to I_β. Thus, we use Bleistein's method with the zero endpoint if $x_n + \beta z_n$ is close to zero and Bleistein's method with the t endpoint if $x_n + \beta z_n$ is close to $\sigma t y_n$. And we change between methods when $x_n + \beta z_n \approx \sigma t y_n/2$.

Having decided on when to use each of the two Bleistein's methods, we have to decide on the sign of the root in a from each of them.

C.2.3 The sign of a

We choose the sign in

$$a = \pm\sqrt{2(f_n(\tau_e, \beta) - f_n(\tau_s, \beta))}$$

such that the topological order of the saddle point and the endpoint is preserved in the complex τ-plane. As we do not know the expression for the saddle it is hard to decide this analytically but observations show that in Bleistein's method including the zero endpoint we choose

$$a = \begin{cases} -\sqrt{2(b - f_n(\tau_s, \beta))} & \text{if } x_n + \beta z_n = 0 \text{ and } \sigma t \leq \sigma T, \\ \sqrt{2(b - f_n(\tau_s, \beta))} & \text{if } x_n + \beta z_n = 0 \text{ and } \sigma t > \sigma T, \\ -\sigma \operatorname{sign}(x_n + \beta z_n)\sqrt{2(b - f_n(\tau_s, \beta))} & \text{else} \end{cases}$$

and in Bleistein's method including the t endpoint we choose

$$a = \begin{cases} \sqrt{2(b - f_n(\tau_s, \beta))} & \text{if } (x_n + \beta z_n) = \sigma t y_n, \\ -\sigma \operatorname{sign}(\sigma t y_n - (x_n + \beta z_n))\sqrt{2(b - f_n(\tau_s, \beta))} & \text{else} \end{cases}$$

where we assume that $\operatorname{sign}(0) = 1$.

C.2.4 Numerical integration of I_β

We calculate the integral numerically for x_n between 0 and 20, y_n between 0 and 15 and for the three values of z_n in $\{0, 10, 20\}$. For the numerical integration in β we use Simpson's method, see for example Kincaid and Cheney (2001, 483-484) and we have noted that the main contribution comes from β in the two regions around $\beta = -1$ and $\beta = 1$. Hence, restricting the β-integration to the interval $[-3, 3]$ results in an error of less than 1%. We find this percentage by increasing the integration interval and varying the stepsize.

We choose the stepsize for β to be $1/30$. We arrived at this choice by examining the case $t = 7$ for stepsize in β at $1/10$, $1/30$ and $1/100$. We examined this special

value of t as we observed unexpected oscillation for high values of the time t for stepsize 1/10. We noted that passing from 1/30 to 1/100 results in a correction of the integral by less than 1% and therefore the increase in calculation time in passing from 1/30 to 1/100 does not make the result better.

The integral, as a function of x_n and y_n, has the appearance of a wave. To be able to see this from the numerical results we need to choose the grid sufficiently tight so that the crests of the waves appear clearly. For $z_n = 0$ it is enough to take the size of the x_n and y_n steps as 0.5 but for $z_n = 10$ and $z_n = 20$ it becomes necessary to take the stepsize 0.25. Hence all the figures in this thesis have the stepsize 0.25.

Bibliography

Airy, G. B. (1838), 'On the intensity of light in the neighbourhood of a caustic', *Camb. Phil. Trans.* **VI**, 397–403.

Balser, W. (2000), *Formal power series and linear systems of meromorphic ordinary differential equations*, New York: Universitext, Springer.

Berry, M. V. (1989), 'Uniform asymptotic smoothing of Stokes's discontinuities', *Proc. Roy. Soc. London Ser. A* **422**(1862), 7–21.

Bleistein, N. (1966), 'Uniform asymptotic expansions of integrals with stationary point near algebraic singularity', *Comm. Pure Appl. Math.* **19**, 353–370.

Bokhove, O. and Shepherd, T. G. (1996), 'On Hamiltonian balanced dynamics and the slowest invariant manifold', *J. Atmospheric Sci.* **53**(2), 276–297.

Camassa, R. (1995), 'On the geometry of an atmospheric slow manifold', *Phys. D* **84**(3-4), 357–397.

Dingle, R. B. (1973), *Asymptotic expansions: their derivation and interpretation*, New York: Academic Press.

Gill, A. E. (1982), *Atmosphere-ocean dynamics*, Academic Press.

Hakim, V. (1998), Asymptotic techniques in nonlinear problems: some illustrative examples, *in* C. Godrèche and P. Manneville, eds, 'Hydrodynamics and nonlinear instabilities', Cambridge University Press, chapter 3, pp. 295–386.

Howls, C. J. and Olde Daalhuis, A. B. (2003), 'Hyperasymptotic solutions of inhomogeneous linear differential equations with a singularity of rank one', *R. Soc. Lond. Proc. Ser. A Math. Phys. Eng. Sci.* **459**(2038), 2599–2612.

Kincaid, D. and Cheney, W. (2001), *Numerical analysis*, third edn, Brooks/Cole Publishing Co., Pacific Grove, CA. Mathematics of scientific computing.

Lorenz, E. N. (1986), 'On the existence of a slow manifold', *J. Atmos. Sci.* **43**(15), 1547–1557.

Lorenz, E. N. and Krishnamurthy, V. (1987), 'On the nonexistence of a slow manifold', *J. Atmos. Sci.* **44**, 2940–2950.

MacKay, R. S. (2004), Slow manifolds, *in* 'Energy Localisation and Transfer', Vol. 22 of *Advanced Series in Nonlinear Dynamics*, World Scientific Publishing, Singapore, pp. 149–192.

McWilliams, J. C. and Yavneh, I. (1998), 'Fluctuation growth and instability associated with a singularity of the balance equations', *Phys. Fluids* **10**(10), 2587–2596.

Ólafsdóttir, E. I., Olde Daalhuis, A. B. and Vanneste, J. (2005), 'Stokes-multiplier expansion in an inhomogeneous differential equation with a small parameter', *Proc. R. Soc. Lond.* **461**, 2243–2256.

Olde Daalhuis, A. B. (1998), 'Hyperasymptotic solutions of higher order linear differential equations with a singularity of rank one', *R. Soc. Lond. Proc. Ser. A Math. Phys. Eng. Sci.* **454**(1968), 1–29.

Olde Daalhuis, A. B. (1999), 'On the computation of Stokes multipliers via hyperasymptotics', *Sūrikaisekikenkyūsho Kōkyūroku* **1088**, 68–78. Resurgent functions and convolution integral equations (Japanese) (Kyoto, 1998).

Olde Daalhuis, A. B. and Olver, F. W. J. (1994), 'Exponentially improved asymptotic solutions of ordinary differential equations. II. Irregular singularities of rank one', *Proc. Roy. Soc. London Ser. A* **445**(1923), 39–56.

Olver, F. W. J. (1974), *Asymptotics and special functions*, Academic Press [A subsidiary of Harcourt Brace Jovanovich, Publishers], New York-London. Computer Science and Applied Mathematics.

O'Sullivan, D. and Dunkerton, T. J. (1995), 'Generation of inertia-gravity waves in a simulated life cycle of baroclinic instability', *J. Atmos. Sci.* **52**(21), 3695–3716.

Paris, R. B. and Wood, A. D. (1995), 'Stokes phenomenon demystified', *Bull. Inst. Math. Appl.* **31**(1-2), 21–28.

Plougonven, R. and Snyder, C. (2005), 'Gravity waves excited by jets: propagation versus generation', *Geophys. Res. Lett.* **32**, 107–117.

Scorer, R. S. (1950), 'Numerical evaluation of integrals of the form $I = \int_{x_1}^{x_2} f(x)e^{i\phi(x)}dx$ and the tabulation of the function $\mathrm{Gi}(z) = (1/\pi)\int_0^\infty \sin(uz + \frac{1}{3}u^3)du$', *Quart. J. Mech. Appl. Math.* **3**, 107–112.

Stokes, G. G. (1850), 'On the numerical calculation of a class of definite integrals and infinite series', *Trans. Camb. Phil. Soc.* **IX**.

Stokes, G. G. (1857), 'On the discontinuity of arbitrary constants which appear in divergent developments', *Trans. Camb. Phil. Soc.* **X**, 106–128.

Temme, N. M. (1996), *Special functions: an introduction to the classical functions of mathematical physics*, John Wiley and Sons, New York Chichester Brisbane Toronto Singapore.

Thomson, W. (1887), 'Stability of fluid motion–rectilinear motion of viscous fluid between two parallel planes', *Philos. Mag.* **24**, 188–196.

Vanneste, J. (2004), 'Inertia-gravity wave generation by balanced motion: Revisiting the lorenz-krishnamurthy model', *J. Atmos. Sci.* **61**, 224–234.

Vanneste, J. and Yavneh, I. (2004), 'Exponentially small inertia-gravity waves and the breakdown of quasi-geostrophic balance', *J. Atmos. Sci.* **61**, 211–223.

Viudez, A. and Dritschel, D. G. (2006), 'Spontaneous generation of inertia-gravity wave packets by balanced geophysical flows', *J. Fluid Mech.* **553**, 107–117.

Voros, A. (1983), 'The return of the quartic oscillator: the complex WKB method', *Ann. Inst. H. Poincaré Sect. A (N.S.)* **39**(3), 211–338.

Zhang, F. (2004), 'Generation of mesoscale gravity waves in upper-tropospheric jet-front systems', *J. Atmos. Sci.* **61**(4), 440–457.